Prepared for:

Rijkswaterstaat RIZA

Voorspelinstrument duurzame vaarweg

Calibration of the multi-domain model

Report

April 2008

WL | delft hydraulics

Q4357.20

Prepared for:

Rijkswaterstaat RIZA

Voorspelinstrument duurzame vaarweg

Calibration of the multi-domain model

Mohamed Yossef, Chris Stolker, Sanjay Giri, Anke Hauschild and Saskia van Vuren

Report

April 2008

WL | delft hydraulics

Client:	Rijkswaterstaat RIZA
Title:	Voorspelinstrument duurzame vaarweg

Abstract:

The DVR programme calls for a prediction tool to evaluate the proposed intervention measures. Accordingly, WL | Delft Hydraulics was commissioned the task of developing an advanced 2-D morphodynamic model of the Rhine system in the Netherlands (Van Vuren et al., 2006). The model contains several innovative, recently developed aspects (Yossef et al., 2006). We refer to this model as "DVR model". However, the earlier developed model had a significant downside; that is the model had different sediment transport formulations for each branch. Moreover, the calibration of the model was not properly carried out. Thus, linking the entire model in its previous state would have been impossible.

In this study we develop the model further such that the model is operational in its entirety. This study includes the following:

- Analysis, choice, implementation and testing of an overall sediment transport formula that is suitable for all branches in the model. This is motivated by the need to run the model in its entirety. The overall formula had to be able to represent the morphological behaviour of the Bovenrijn, where the Meyer-Peter & Müller formula is most suitable, as well as the morphological behaviour of the lower Waal where the Engelund & Hansen formula is the most suitable. We concluded from this study that the formula of Van Rijn (1984a; b) is the most suitable. Additional functionality has been implemented in Delft3D and it was used successfully in the calibration of the model.
- Hydrodynamic calibration of the OLR conditions. The OLR defines the reference level for navigability as well as dredging activities. The calibration is carried out as a first step to guarantee a correct reproduction of dredging activities.
- Global morphological calibration of the model using the new transport formula. The calibration covered the Bovnrijn, Waal and Pannerdensch Kanaal.
- Morphological calibration for the dredging activities in the Waal River. A calibration for the Waal is carried out focusing on correct reproduction of the dredging activities.

References:	RI-4737 "Vervolg Bouw morfologisch model DVR"

Ver	Author	Date	Remarks	Review	Approved by
1.0	dr. Mohamed Yossef	04 December 2007		dr. ir. E. Mosselman	dr. A.G. Segeren
1.1	dr. Mohamed Yossef	17 December 2007		dr. ir. E. Mosselman	dr. A.G. Segeren
2.0	dr. Mohamed Yossef	18 January 2008		dr. ir. E. Mosselman	dr. A.G. Segeren
3.0	dr. Mohamed Yossef	25 April 2008		dr. ir. E. Mosselman	dr. A.G. Segeren

Project number:	Q4357.20
Keywords:	River morphology, model calibration, sediment transport, numerical modelling
Number of pages:	120
Classification:	Confidential until January 2010
Status:	Final

wL | delft hydraulics

Clant:	Rijkswaterstaat RIZA
Title:	Voorspelinstrument duurzame vaarweg – calibration of the multi domian model

Samenvatting:

Het DVR-programma vraagt om een voorspelinstrument om de voorgestelde maatregelen te evalueren. WL | Delft Hydraulics had de opdracht om een geavanceerd 2D morfodynamisch model te ontwikkelen van het systeem van de Rijn in Nederland (Van Vuren e.a., 2006). Het model bevat verscheidene innovatieve, recent ontwikkelde aspecten (Yossef e.a., 2006). We duiden dit model aan als "DVR-model". Het eerder ontwikkelde model had een significante tekortkoming; dwz het model had verschillende transport formuleringen voor de verschillende riviertakken. Verder had er slechts een beperkte calibratie van het model plaats gevonden. Hierdoor was het onmogelijk om de afzonderlijke riviertakken aan elkaar te koppelen. In deze studie ontwikkelen wij het model verder zodanig dat het totale model operationeel is. De studie omvat het volgende:

- Analyse, keuze, implementatie en toetsen van een sediment transportformule die past bij alle riviertakken in het model. De motivatie hiervoor is het rekenen met het complete model. De nieuw gekozen sedimenttransport formule moet het morfologische gedrag in de Bovenrijn (waar de transportformule van Meyer-Peter en Müller het beste past) combineren met het mofologische gedrag van het benedenstroomse deel van de Waal (waar de Engelund & Hansen formule beter past). De conclusie uit de studie is een sedimenttransportformule gebaseerd op Van Rijn (1984a; b) het beste bij de eisen past. Hiervoor is extra functionaliteit toegevoegd aan Delft3D en deze is succesvol gebruikt in de calibratie van het complete model.
- Hydrodynamische calibratie van de OLR (Overeengekomen Lage Rivierstand) Het OLR definieert een referentieniveua voor bevaarbaarheid en baggerwerkzaamheden. De calibratie is uitgevoerd als een eerste stap om de juiste baggerwerkzaamheden te reproduceren.
- Een globale morfologische calibratie van het DVR model gebruikmakend van de nieuwe transport formule. De calibratie bevatte de Boven Rijn, Waal en het Pannerdensch Kanaal. .

Morfologische calibratie voor baggerwerkzaameheden in de Waal. Een calibratie voor de Waal is uitgevoerd waarbij de nadruk is gelegd op het reproduceren van de baggerwerkzaamheden.

References:	RI-4737 "Vervolg Bouw morfologisch model DVR"

Ver	Author	Date	Remarks	Review	Approved by
1.0	dr. Mohamed Yossef	04 December 2007		dr. ir. E. Mosselman	dr. A.G. Segeren
1.1	dr. Mohamed Yossef	17 December 2007		dr. ir. E. Mosselman	dr. A.G. Segeren
2.0	dr. Mohamed Yossef	18 January 2008		dr. ir. E. Mosselman	dr. A.G. Segeren
3.0	dr. Mohamed Yossef	25 April 2008		dr. ir. E. Mosselman	dr. A.G. Segeren

Project number:	Q4357.20
Keywords:	River morphology, model calibration, sediment transport, numerical modelling
Number of pages:	120
Classification:	Confidential until January 2010
Status:	Final

Contents

Appendices

1 Introduction

1.1 Background

The Rhine is the most navigated inland waterway in Western Europe. Due to its advantageous location in the Rhine delta, the inland waterways in the Netherlands form a natural access to the continent of Europe. As a consequence of climate change and morphological changes in the Rhine system an increasing number of nautical bottlenecks are expected in the coming years. In order to meet the demands for navigation also in the future, Directorate for Public Works and Water Management introduced the programme Duurzame Vaardiepte Rijndelta (DVR) (Sustainable Navigation Depth for the Rhine Delta). Within the DVR programme, river intervention measures will be defined and evaluated to maintain and improve the navigability of the Rhine.

The DVR programme calls for a prediction tool to evaluate the proposed intervention measures. Accordingly, WL | Delft Hydraulics was commissioned the task of developing an advanced 2-D morphodynamic model of the Rhine system in the Netherlands (Van Vuren et al., 2006). The model contains all kinds of innovative, recently developed aspects, amongst which domain decomposition, sediment transport over non-erodible layers and functionality for sediment management to assess dredging and dumping strategies (Yossef et al., 2006). In this report, we refer to this model as “DVR model”.

The advanced DVR model can be used to assess the long-term large-scale evolution of the Rhine system (scale of longitudinal profile evolution of river reaches, e.g. in response to training works). As the model incorporates also complex time-dependent multi-dimensional phenomena, such as curvature-induced bar-pool patterns in bends, assessment is also possible at the intermediate spatial scale (scale of alternate bars and cross-sectional profile evolution). For a detailed description of the model, reference is made to Van Vuren et al. (2006), Yossef et al. (2006), and Mosselman et al. (2007).

However, the earlier developed model had a significant downside; that is the model had different sediment transport formulations for each branch. Moreover, the calibration of the model was not carried out properly. Thus, linking the entire model in its previous state would have been impossible. In this report we develop the model further such that the model is operational in its entirety.

1.2 Assignment

This project includes four primary tasks:

1- Reducing the computational time.
2- Improving the model (*this report*).
3- Case study of fixed layer and nourishment in the Bovenrijn.
4- Improving the model’s physical concepts.

The objective of the study presented in this report is to improve the DVR model that was constructed earlier. The model has been used to conduct some case studies in relation to the DVR project (Mosselman et al. 2007). The recommendation from that study was to conduct a thorough morphological calibration of the DVR model. Accordingly in this study the following activities are carried out:

- Chapter 2: Analysis, choice, implementation and testing of an overall sediment transport formula that is suitable for all branches in the model.
- Chapter 3: Hydrodynamic calibration of the OLR conditions.
- Chapter 4: Global morphological calibration of the entire model using the transport formula reached in Chapter 2.
- Chapter 5: Detailed morphological calibration for the Waal River, including dredging activities.

The work has been carried out within the agreement RI-4737 "Vervolg Bouw morfologisch model DVR", (in English: Continued construction of morphological model for DVR). The project is known in WL | Delft Hydraulics as Q4357.00.

1.3 Organisation

This report is the second in a series of three within this project. The team contributing to the project consisted of: Chris Stolker, Anke Hauschild, Sanjay Giri, Willem Ottevanger, Saskia van Vuren, Kees Sloff, Erik Mosselman, Bert Jagers, Frans van der Knaap and Mohamed Yossef. The later was the project leader and the editor of this report. Arjan Sieben managed the project on behalf of Rijkswaterstaat RIZA.

2 An overall sediment transport formula

2.1 Background

The established practice in the Netherlands is that different sediment transport formulas are applied to different reaches of the Dutch Rhine branches. The MPM (Meyer-Peter & Müller, 1948) formula suits the upper Rhine branches best, whereas the EH (Engelund & Hansen, 1967) formula is the most suitable predictor for the lower Rhine branches and the tidal rivers of the Delta. The current development of morphological models covering both upper and lower Rhine branches, however, calls for a single overall formulation. This formulation should tend to the MPM formula in the upper branches and to the EH formula in the lower branches.

We follow two avenues to find a suitable formulation. First of all, the Van Rijn (1984a; b) formula is considered because in principle, it should be suitable for both upper and lower branches. However, it has the disadvantage of being rather complex. Therefore, the second avenue of finding a simple overall predictor would be attractive, because it would allow theoretical analyses that are needed to diagnose model errors and to determine whether unexpected model results are a manifestation of an error or essential behaviour of the system.

2.2 Method

2.2.1 Criteria for choice

The following criteria have been defined for the choice of a sediment transport formula that is suitable for the entire Rhine branches:

1. The formula should have a similar behaviour as the MPM formula (Eq. 2.1) for Shields parameter values below 0.09, which corresponds to the conditions in the Bovenrijn.

$$\begin{aligned} S_{MPM} &= \alpha_{MPM}\, m_{MPM} \left(\mu\theta - \theta_{cr}\right)^{3/2} \\ m_{MPM} &= 8\sqrt{\Delta\, g\, D_{50}^{3}} \end{aligned} \tag{2.1}$$

where:

S_{MPM}	sediment transport rate based on the formula of MPM
α_{MPM}	calibration coefficient for the formula of MPM
μ	ripple factor or efficiency factor
θ	Shields mobility parameter
θ_{cr}	critical Shields parameter (conventianl value = 0.047)
D_{50}	median sediment diameter
Δ	relative density $(\rho_s - \rho_w) / \rho_w$
g	acceleration of gravity (9.81 m/s^2)

2. The formula should have a similar behaviour as the EH formula (Eq. 2.2) for Shields parameter values above 0.3, which corresponds to the conditions in the Midden-Waal and the Beneden-Waal.

$$S_{EH} = \alpha_{EH}\, m_{EH}\, u^5$$
$$m_{EH} = \frac{0.05}{\sqrt{g}\, C^3 \Delta^2 D_{50}} \tag{2.2}$$

where:

S_{EH}	sediment transport rate based on the formula of EH
α_{EH}	calibration coefficient for EH formula
C	Chézy friction coefficient
u	magnitude of flow velocity

3. If a simple predictor according to the second avenue is used, it should be kept simple, with at most only one additional calibration parameter. Otherwise the main advantage over the Van Rijn formula would disappear.
4. For physical reasons, the degree of nonlinearity n in the general sediment transport formula $S = m\,\theta^{\frac{n}{2}}$, should always be larger than 3 (Mosselman, 2005). This can be seen from the following general sediment transport formula

$$\frac{S}{\sqrt{\Delta\, g\, D^3}} = \alpha\,\theta^{\frac{n}{2}} = \alpha\left(\frac{u^2}{C^2 \Delta\, D}\right) \xrightarrow{\text{hence}} S \propto D^{\left(\frac{3-n}{2}\right)} \tag{2.3}$$

   the common observation that sediment transport rate decreases as sediment grain size increases implies that n should be greater than 3.

5. Preferably, the degree of nonlinearity should decrease monotonously as the Shields parameter increases.
6. The degree of nonlinearity should be about 4 or 5 for large Shields parameter values. The value of 5 complies with the EH predictor, but studies on sand-bed rivers show that a value of 4 may occur as well (Grishanin, 1990). Van Rijn's formula also yields a value around 4.

2.2.2 Alternative formulations

As indicated earlier we compare between the formula of van Rijn (1984a; b) and alternative formulation that is a combination of MPM and EH. The Van Rijn (1984) sediment transport formula is considered to be one of the most accurate and commonly used formulations. It has the advantage of having two separate expressions for bed load and suspended load. The formula of Van Rijn is presented in Appendix A. The alternative formula (combined formula) is based on Sieben (1998).

Sieben (1998) has proposed a combination formula that has been evaluated subsequently by Sloff & Mosselman (1998). The present analysis extends the previous work in the following ways:

a) Sieben (1998) based his combination formula on a weighting factor α_p defined in Eq. (2.4). The weighting factor takes values from 1 at initiation of sediment motion ($\theta = \theta_{cr}$) to 0 at high sediment mobility ($\theta >> \theta_{cr}$). If the tuning parameter $P < 1$, the combination formula with this weighting function moves away rapidly from EH and tends smoothly to MPM. If $P > 1$, the formula moves away rapidly from MPM and tends smoothly to EH; a value of $P = 1.5$ has been recommended earlier. An S-shaped or sigmoid weighting function would have a smooth transition to both MPM and EH at the same time. Several possibilities for such a weighting function have been investigated.

$$\alpha_P = \left(\frac{\theta_{cr}}{\mu\theta} \right)^P \tag{2.4}$$

In this way, the combined sediment transport formula can be written in the form:

$$S_{AS_a} = \underbrace{\left(\alpha_{MPM}\, m_{MPM}\right)^{\alpha_P} \left(\mu\theta - \theta_{cr}\right)^{\alpha_P \cdot 3/2}}_{MPM} \cdot \underbrace{\left(\alpha_{EH}\, m_{EH}\right)^{1-\alpha_P} \cdot \left(C^2\, \Delta\, D_{50}\right)^{(1-\alpha_P)\cdot 5/2}\, \theta^{(1-\alpha_P)\cdot 5/2}}_{EH} \tag{2.5}$$

b) Sieben (1998) placed weighting functions in the exponents of his combination formula. A simpler formula arises when the weighting functions are used as multiplication factors:

$$S_{AS_b} = \underbrace{\alpha_P \cdot S_{MPM}}_{MPM} + \underbrace{\left(1-\alpha_P\right) \cdot S_{EH}}_{EH} \tag{2.6}$$

2.2.3 Analysis of behaviour

With the aim of choosing one of the three alternative sediment transport formulae given in the previous section, five sediment transport formulae are analysed in this section. These are:

- Meyer-Peter & Mueller (MPM, given in Eq. 2.1),
- Engelund & Hansen (EH, given in Eq. 2.2),
- Original Sieben (AS_a, given in Eq. 2.5),
- Variant of Sieben formula (AS_b, given in Eq. 2.6), and
- Van Rijn 1984 (VR, given in Appendix A)

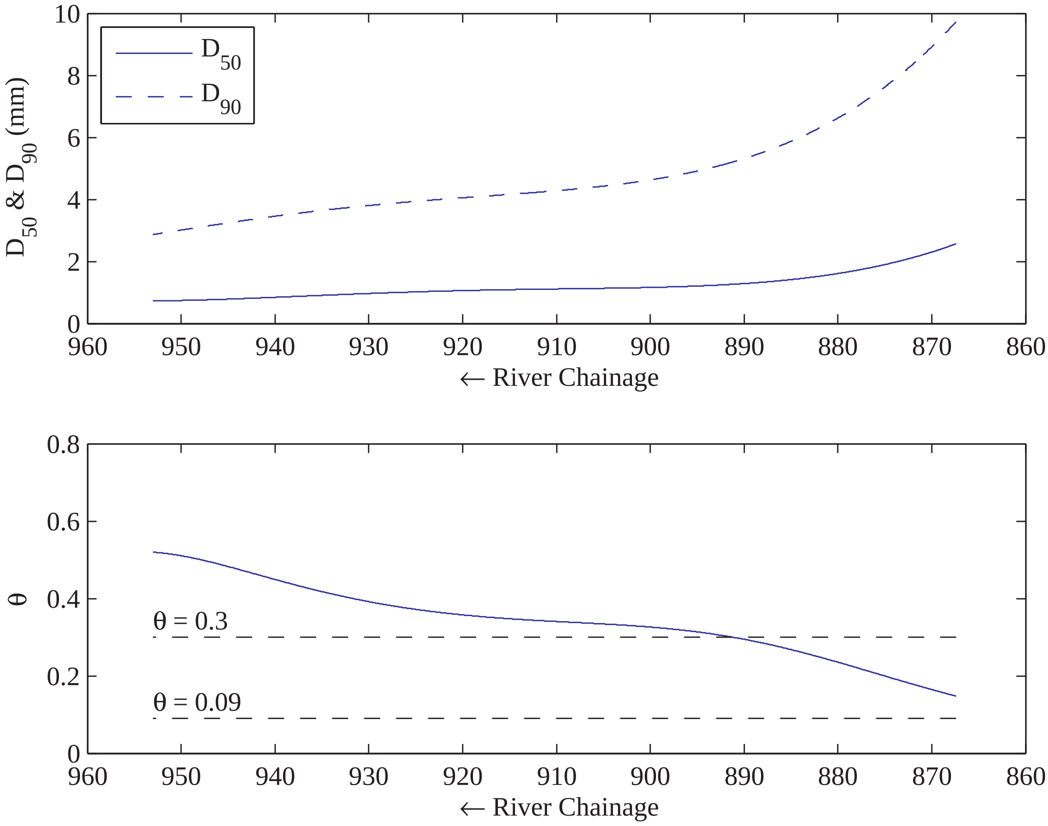

Figure 2.1 Sediment size and Shields parameter as deduced from the model's initial boundary conditions; upper panel: sediment size, and lower panel: Shields parameters.

The MPM formula is presented as it was used in the previous case studies (Mosselman et. al. 2007). The EH formula is given for comparison and to evaluate whether the desired effect defined in criteria № 2 is satisfied.

Based on the sediment sizes that are used in the model (see Figure 2.1), the analysis was carried out for a slightly wider range of D_{50} (from 0.1 to 6.0 mm); $D_{90} = 4 \times D_{50}$. An average flow depth of 6.0 m, flow velocity of 1.1 m/s, and a Chézy coefficient of 45 $m^{1/2}/s$ were used in the analysis given herein.

Three parameters are used to compare the different formulae, viz. the transport rate S, the dimensionless sediment transport rate ϕ defined in Eq. 2.7, and the degree of nonlinearity n defined in Eq. 2.3.

$$\phi = \frac{S}{\sqrt{\Delta g D_{50}^3}} \tag{2.7}$$

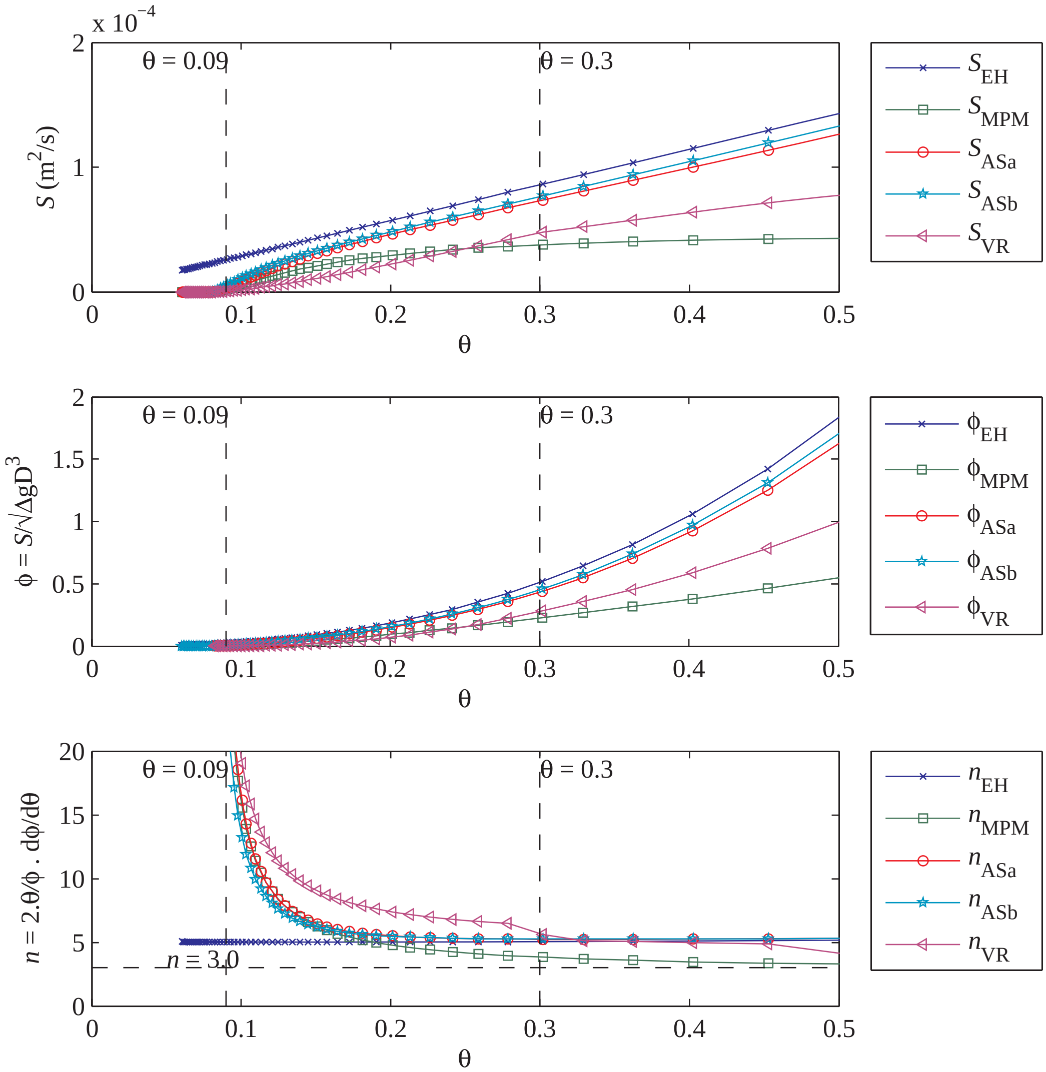

Figure 2.2 Behaviour of different sediment transport formulae, upper panel: transport rate; middle panel: dimensionless transport rate; lower panel: degree of nonlinearity. Original formulations with transient parameter P = 1.5 and calibration parameters set to unity.

Figure 2.2 gives an overview of the behaviour of the different sediment transport formulae. In this figure, calibration parameters were set to unity for all formulae. The transport formula of Van Rijn was evaluated based on the current implementation in Delft3D, i.e. using a user specified constant fall velocity. The following can be noted:

- The total transport rates calculated based on EH, MPM, and VR differs significantly from one another.
- Both Sieben formulae AS_a, and AS_b have a similar behaviour. They give the desired behaviour of being similar to MPM at low Shields number and change into EH at high Shields number (see Figure 2.2 lower panel). Nevertheless, due to the large difference between the transport rates calculated using MPM and EH, the AS formulae converges to EH at a relatively high Shields parameter (see Figure 2.2 upper and middle panels). When using proper calibration parameter (α_{EH} affecting the formulae: EH, AS_a and AS_b), that reduce the transport rate of the EH formula, the agreement takes place at lower Shields parameter better (see Figure 2.3).

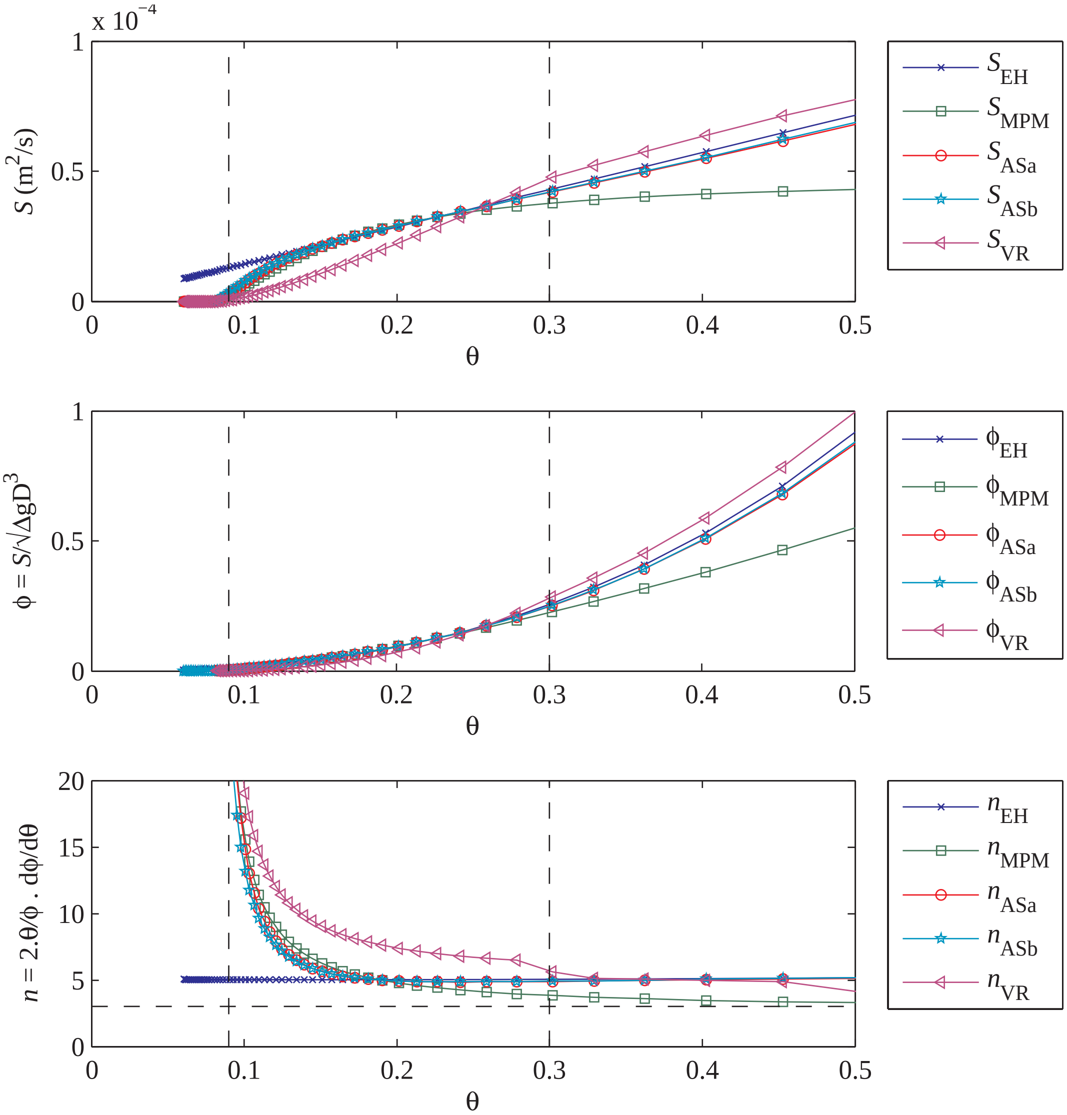

Figure 2.3 Behaviour of different sediment transport formulae, upper panel: transport rate; middle panel: dimensionless transport rate; lower panel: degree of nonlinearity. Changes in EH formula using a calibration parameter $\alpha_{EH} = 0.5$.

- The sediment transport formula of van Rijn as currently implemented in Delft3D deviates from MPM for low values of the Shields parameter (see Figure 2.2 and Figure 2.3). Moreover, there is an abrupt change in the degree of nonlinearity n (at T = 3.0, as given in Eq. A.3, around θ = 0.3 in this case); this is due to the way in which the bed load component is calculated (see Eq. A.2). By reducing the bed load transport formula to Eq 2.8, and using calibration parameters $\alpha_{BED} = 1.5$, and $\alpha_{SUS} = 0.5$, the behaviour of the van Rijn formula is now similar to that of MPM at low Shields values and similar to that of EH at high Shields values (see Figure 2.4).

$$S_b = \alpha_{BED} \cdot 0.1\sqrt{\Delta\, g\, D_{50}^3}\, D_*^{-0.3} T^{1.5} \qquad (2.8)$$

with α_{BED} calibration parameter for bed load transport component.

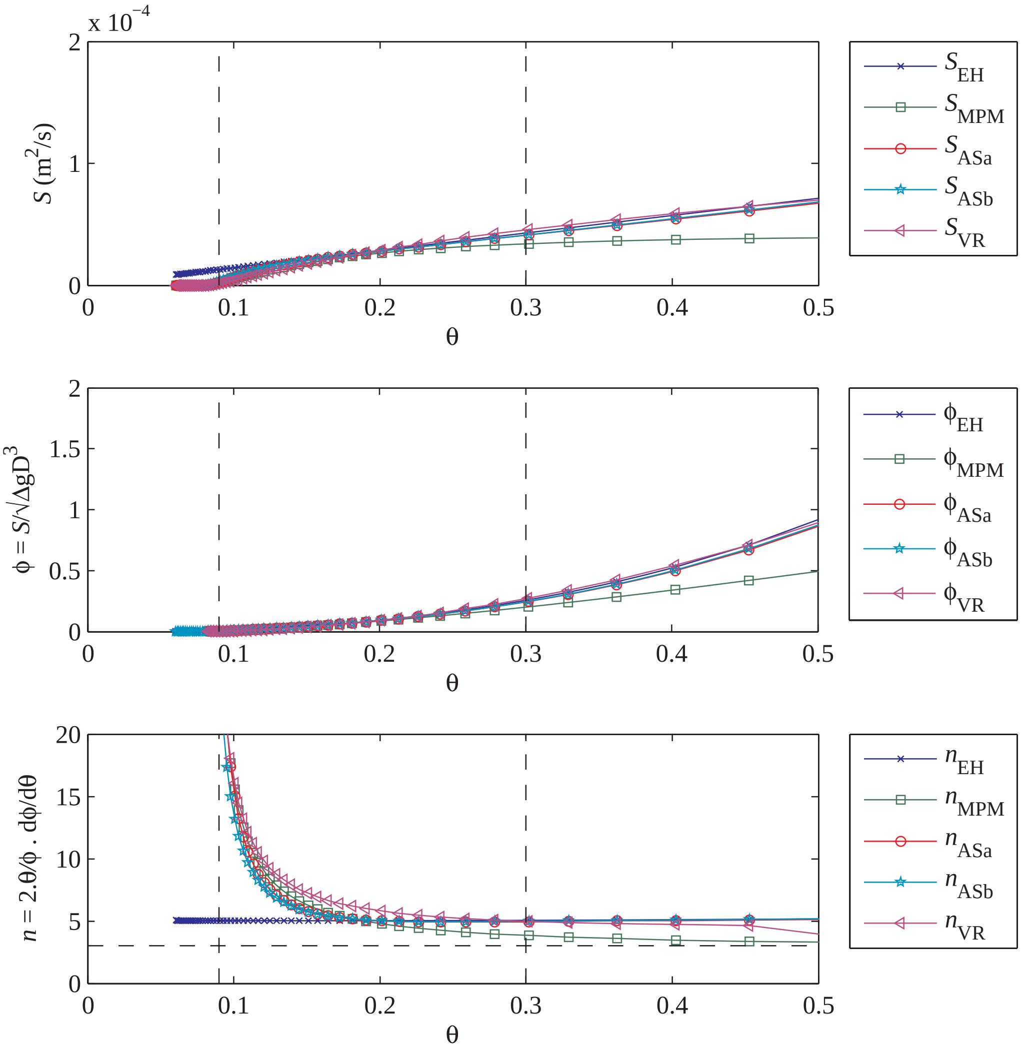

Figure 2.4 Behaviour of different sediment transport formulae, upper panel: transport rate; middle panel: dimensionless transport rate; lower panel: degree of nonlinearity. Changes in EH formula: using a calibration parameter $\alpha_{EH} = 0.5$; Changes in VR formula: using reduced van Rijn equation with $w_s = f(d_{50})$, $\alpha_{SUS} = 0.3$, $\alpha_{BED} = 1.5$.

2.2.4 Choice of a sediment transport formula

The plots of the two Sieben formulae given in Eqs. 2.5 & 2.6 show that they have a similar behaviour. For both AS_a and AS_b, as well as combinations thereof, a large range of intermediate Shields parameter values is found where the combination formula complies with neither MPM nor EH, irrespective of the calibration parameter, α_P. This gives rise to the following problems:

- It is not possible to calibrate the combination formula properly (unambiguously) for an important range of conditions occurring in the Rhine branches;
- A better compliance with MPM or EH at the intermediate Shields parameter values might be obtained by introducing a second calibration parameter. However, this would increase the under-determination and would render proper calibration even more

difficult. It would be in conflict with the third criterion that the new predictor should be kept truly simple.

Based on these findings, and given the behaviour of the Van Rijn formula which complies with the specified criteria given earlier, we favour the Van Rijn formula. Its complexity is a disadvantage; however it has the following advantages:

- it is more physicals-based than the Sieben formulae,
- it is more generally accepted by the scientific community,
- it can be extended more easily to more complex hydrodynamic conditions, such as waves,
- it is possible as well to use separate predictions for suspended load which can be used later as a first step towards including wash load, and
- by having two separate calibration parameters for bed load and suspended load it is possible to influence, independently, the degree of nonlinearity *n* or the total transport capacity.

Accordingly, the sediment transport formula of Van Rijn, with some modification from the current implementation in Delft3D is selected. It is tested in Section 2.3.

2.2.5 Implementation

In accordance with the analysis given earlier, a new sediment transport formula has been implemented in Delft3D (IFORM#77). The new formula is based on the current implementation of van Rijn (1984a; b) with some additional options that allow for the following:

- possibility to calibrate the bed load transport and the suspended load transport separately using two different calibration coefficients (α_{BED} and α_{SUS}),
- possibility to choose a constant fall velocity or calculated fall velocity based on three different fall velocity formulations,
- possibility to opt for a reduced formula for bed load transport as given in Eq 2.8, and finally
- additional possibility to control the critical Shields parameter for the initiation of motion.

2.3 Results

The implemented Van Rijn formula has been tested using the Waal domain of the DVR model. The result was compared with that of the model using the MPM formula that has been used in the previous study (Mosselman et al. 2006). Figure 2.5 gives a comparison between the yearly sediment transport rates using the two different transport formulae. It is clear that the formula of van Rijn yields a higher transport in the lower Waal where the Shields parameter is higher than 0.3 (cf. Figure 2.1 & Figure 2.3). We need to note that only

minor calibration has been performed to yield a result comparable to the MPM formula. The actual model calibration is conducted in Chapter 4.
Here we present a quick comparison between the bedform celerity and the 2D behaviour based on the two formulas.

The bedform celerity is evaluated by tracking a trench migration. Three trenches were introduced into the model near km 870, km 890, and km 920. Figure 2.6 and Figure 2.7 show that the model when using the VR equation yields a similar bed celerity to the one of the model when using the MPM. They both yield a trench migration speed close to 1.0 km/year.

The 2D behaviour is evaluated by comparing the left bank and right bank profiles. The results show that the 2D behaviour compares well between the two different transport formulae see Figure 2.8 to Figure 2.10 where comparisons between the bed level of the left and right banks for the two models are given. The results show that the two transport formulations yield nearly the same result.

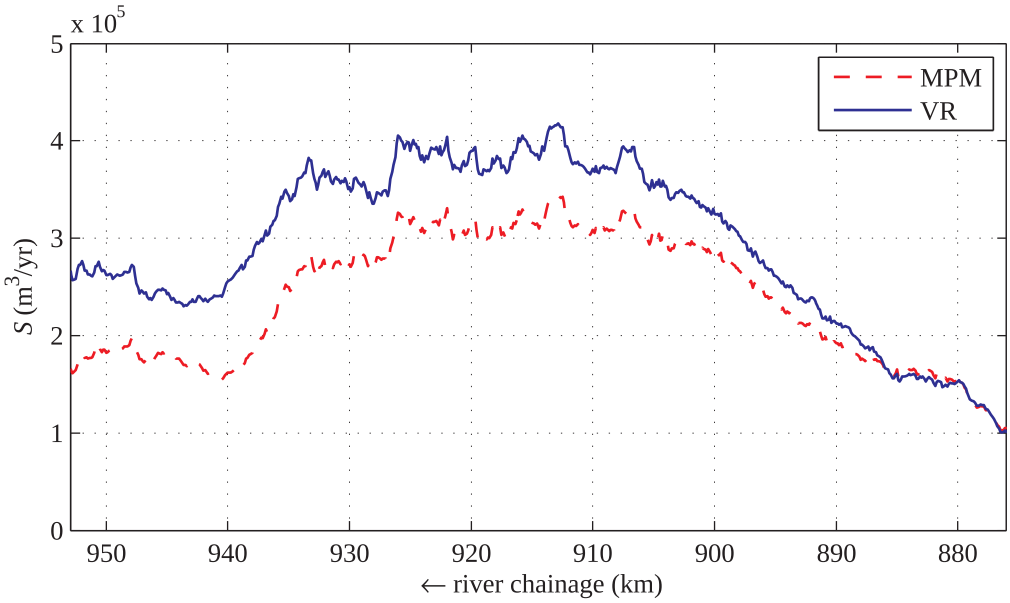

Figure 2.5 Yearly sediment transport, including pores, in the Waal; comparison between the model using MPM and that using VR.

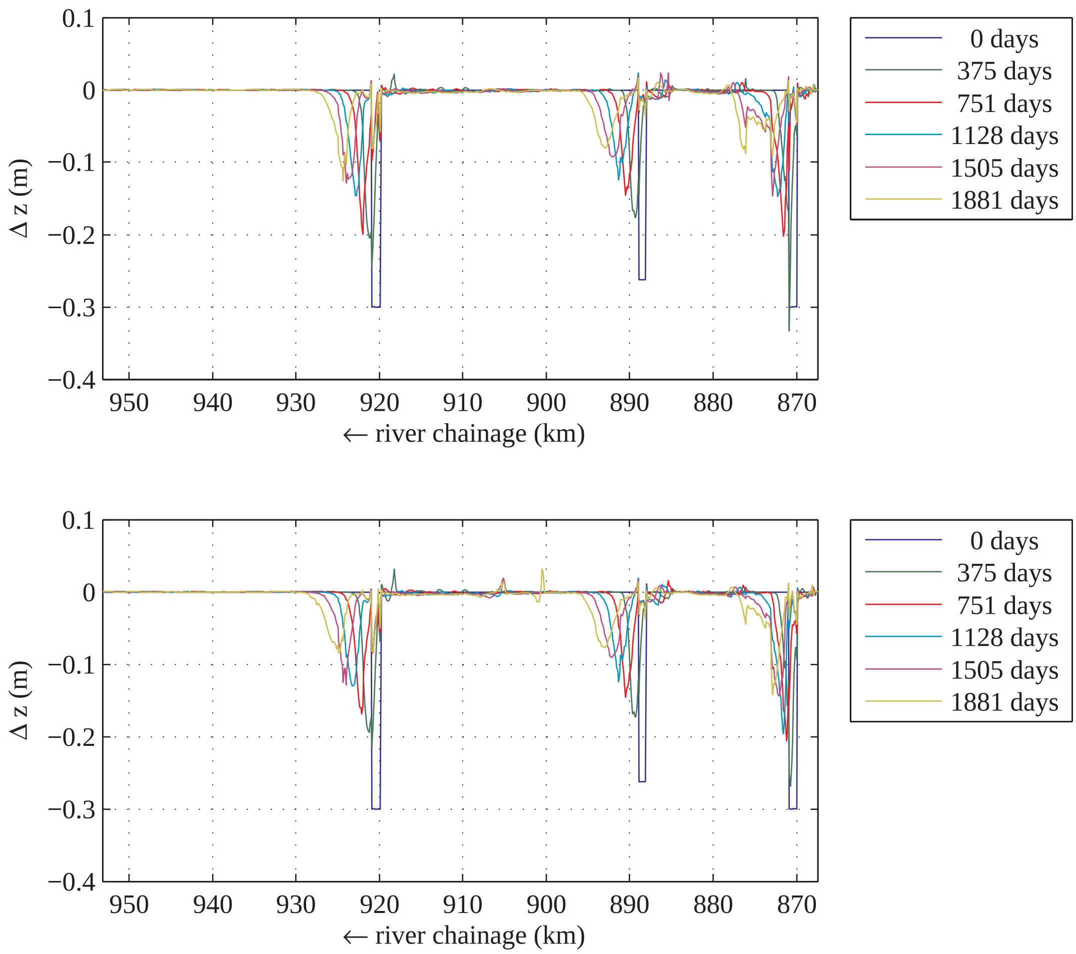

Figure 2.6 Cross-section averaged bed level changes; comparison between the temporal developments of three trenches using MPM (upper panel) and VR (lower panel).

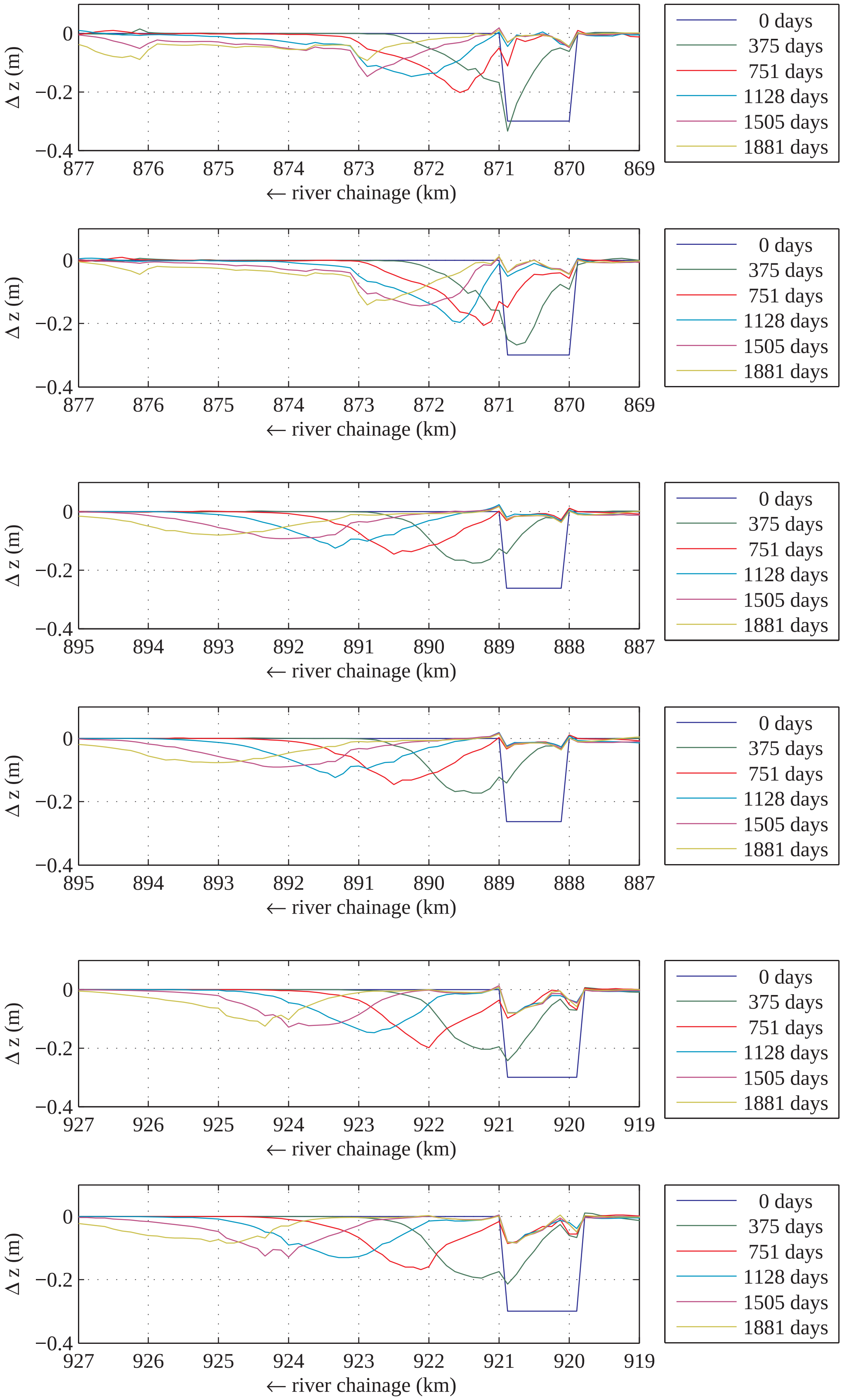

Figure 2.7 Cross-section averaged bed level changes; detailed comparison between the temporal developments of three trenches using MPM (upper panels) and VR (lower panels).

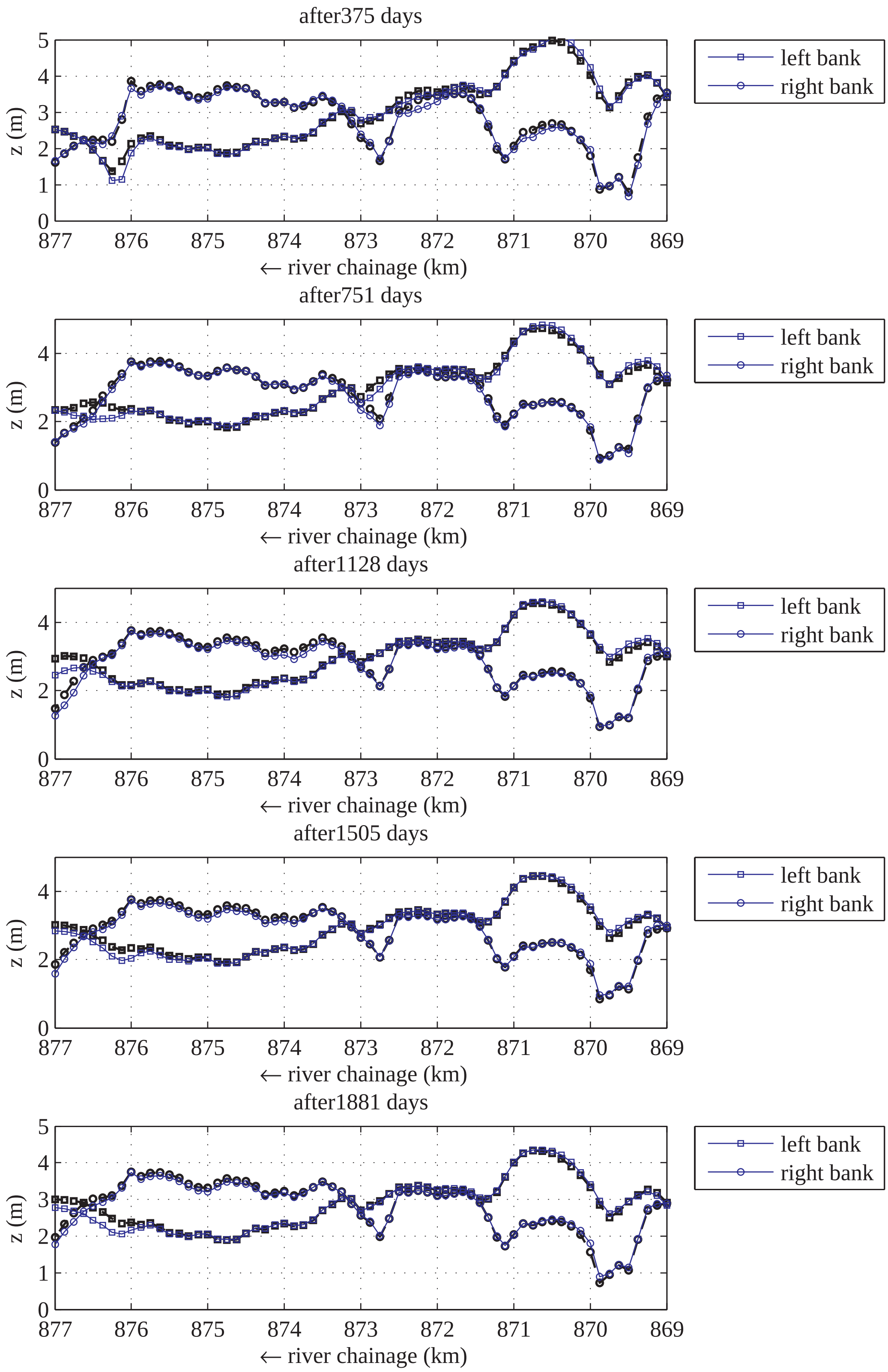

Figure 2.8 Comparison between the MPM model and the VR model at different time steps; black: MPM model, blue: VR model – Upper Waal.

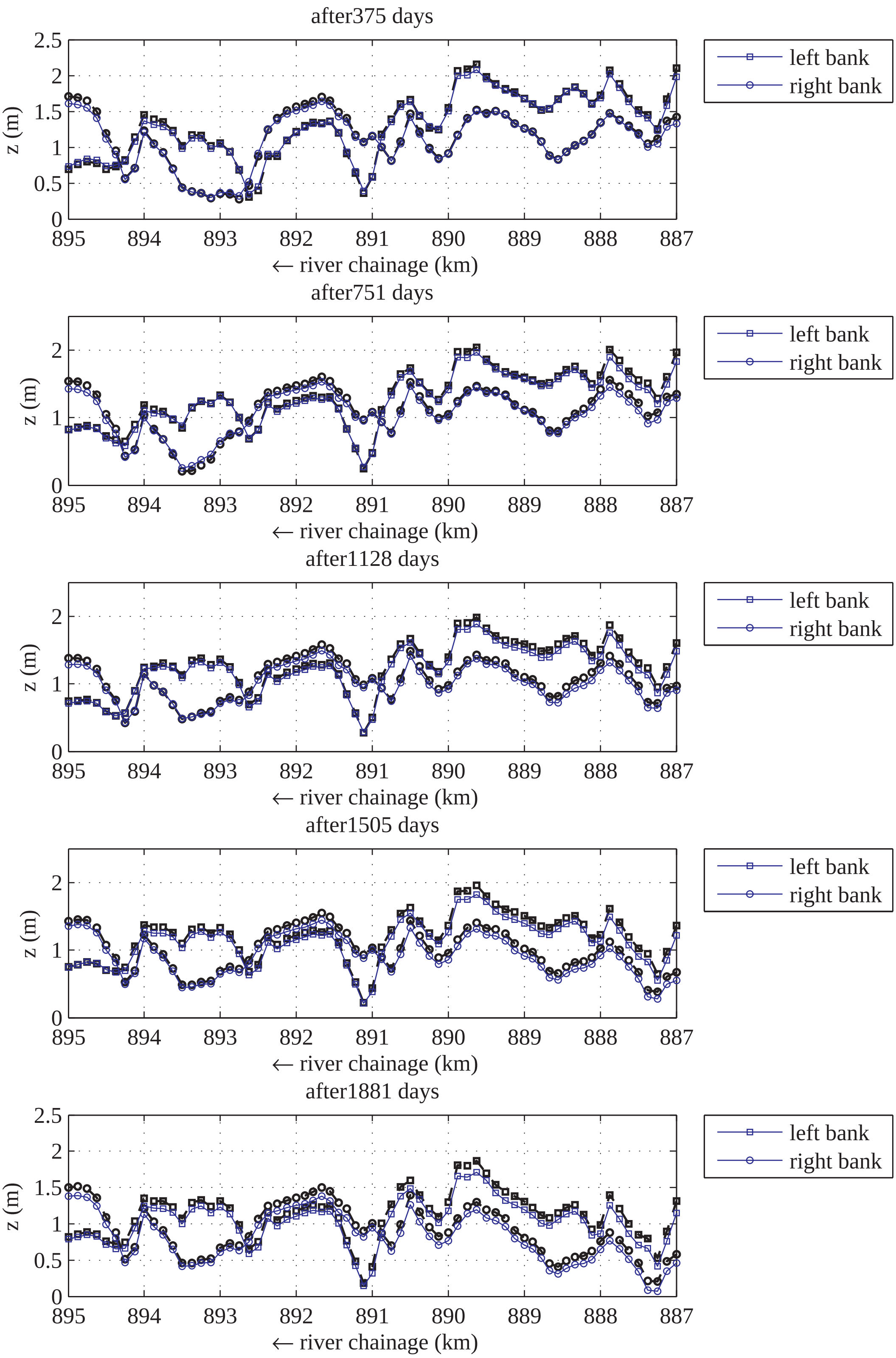

Figure 2.9 Comparison between the MPM model and the VR model at different time steps; black: MPM model, blue: VR model – Middle Waal.

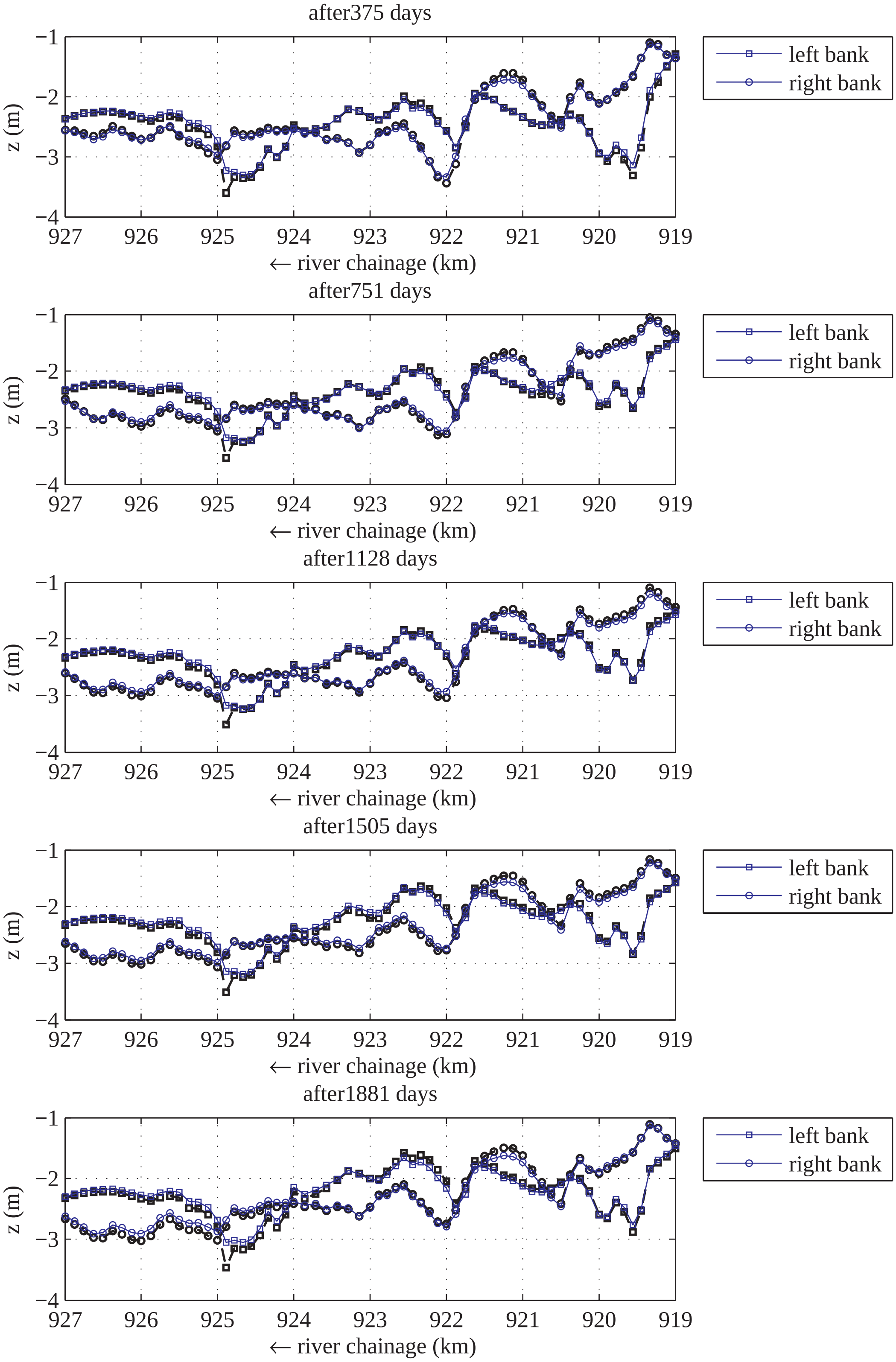

Figure 2.10 Comparison between the MPM model and the VR model at different time steps; black: MPM model, blue: VR model – Lower Waal.

2.4 Conclusion

In this chapter a new sediment transport formula has been analytically evaluated, implemented and tested for the use in the DVR model. The starting point was the need for a single overall sediment transport formula that tend to the MPM formula in the upper branches and to the EH formula in the lower branches. The aim is to be able to model the entire Rhine system using this formula.

From the evaluation of the behaviour of some selected formulations we reached the conclusion that the sediment transport formula of van Rijn (1984a; b) is the most suitable. Some additional options were introduced to the formula and accordingly implemented in Delft3D; these include

- Possibility to use a reduced version of the equation of bed load transport (Eq. A.2) to as given in Eq. A.19
- Possibility to use different calibration parameters for the bed load and suspended load. Both calibration parameters are user specified inputs.
- Use a variable fall velocity (w_s) that is internally calculated based on the sediment size rather than using a user specified input value.
- Introduce the possibility to specify a user defined critical Shields parameter θ_{cr}. This option is introduced inline with the experience from modelling the Bovenrijn, where a rather law critical Shields parameter is needed to reproduce its morphological behaviour correctly.

The formula was tested successfully to behave as intended. What remains to be carried out is a detailed calibration of the parameters of the formula for the specific needs of the morphological calibration. This will be carried out in Chapter 4.

3 Hydrodynamic calibration

3.1 Background

Mosselman et al. (2007) carried out a number of case studies, including an evaluation of the dredging activities on the Waal River was carried out. The dredging option was triggered when the depth of the navigation channel (150 m or 170 m wide) is less than 2.50 m measured from the OLR reference level. In that model, however, the calculated OLR overestimated the OLR of 2002 with more than 25 cm. As a possible reason Mosselman et al. (2007) mention that the model was not calibrated on OLR conditions.

Therefore, and as part of improving the current model, a hydrodynamic calibration on low discharge situations is carried out. This chapter presents the method and the results of this calibration.

The calibration was carried out using the low discharge data of 3 September 2003. For that day a laser altimetry measurement of the 2D water level of the Waal River is available. According to Donar database, the average discharge on the Bovenrijn during that day was 989 m^3/s, and the discharge of the Waal at Tiel was 772 m^3/s. It was decided not to calibrate the model based on the OLR levels as it is a deduced water level that does not necessarily match any measured situation. Calibration of the model on low discharges, however, has some limitations. The uncertainty in the actual discharge is large due to temporary variations as a result of for instance weir operation and lateral inflow. Nevertheless, these uncertainties are accepted.

3.2 Method

3.2.1 Water level data

RIZA delivered spatially averaged values of the laser altimetry measurement of the water level; viz. all laser altimetry values in grid cells of 500 m long and 50 m wide of a river axis oriented grid were averaged, leading to 6 points in every transverse cross-section within the main channel, cross-sections were 500 m apart. Cross-section-averaged water levels were determined along the river for use in the comparison between the measured and calculated water levels. With respect to the accuracy of the laser altimetry measurements the following is noticed:

- It appears that when all six transverse water level measurements are averaged, the standard deviation increases to around 0.6 m (Figure 3.1). Yet, when neglecting the two outer points, which deviate seriously with respect to the four inner points in the cross-section, the standard deviation decreases significantly to a value of approx. 2 to 3 cm. Therefore, only the inner four points in each transverse section are averaged. With respect to the large standard deviation, it may be possible that the outer grid cells used to average the laser altimetry measurements are overlapping with groynes.

- Figure 3.1 also shows that the provided laser altimetry values contain three sections at which data are missing.

- Along the longitudinal profile some irregularities are observed, e.g. sometimes the water level rises in downstream direction. The largest water level rise of approximately 10 cm is noticed in the vicinity of the downstream boundary.

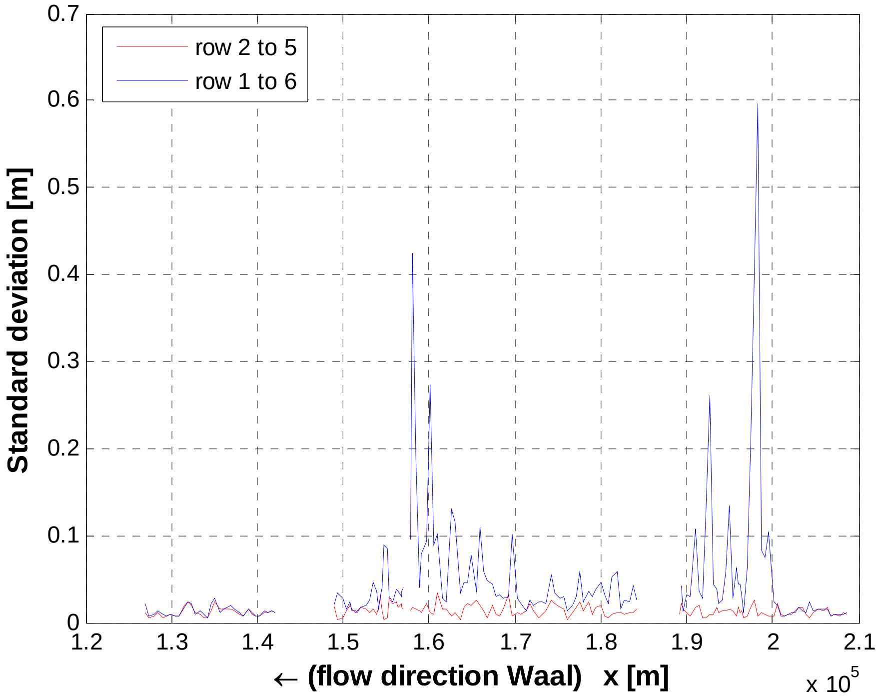

Figure 3.1 Standard deviation of the total six transverse laser altimetry water levels (blue) and inner four points (red).

3.2.2 Bed level data

RIZA provided the multi-beam measurement of the main channel bed of 2003 that was measured during the period 7 March till 12 April. The multi-beam data were projected on the Delft3D model grid and subsequently combined with the floodplain of the previously developed DVR model (Van Vuren et al., 2006).

Compared with the bed level of the DVR model (Van Vuren et al. 2006), which was based on the main channel bed level of 1997, the average bed level in the entire Waal is lowered by some 0.50 m. This is shown in Figure 3.2 which presents the cross-section averaged bed level of both 2003 and 1997, and in Figure 3.3 that presents the difference in bed level. These plots were determined based on the coarse DVR grid. One important reason for this difference is the morphological change after 1997, while the other reason is the fact that after the year 2000 the summer bed of the Rhine branches has been measured using multi-beam techniques whereas before this date it was done using single-beam instruments. Due to the systematic difference between the two techniques, the bed level in the Waal can be at least 0.20 m lower when measured using multi-beam instruments. This difference can be attributed to several causes, among which is the ability of multi-beam instruments to determine the bed level of the troughs of the dunes better.

Note that the outer grid cells in the main channel have not been taken into account in the previous comparison. The deviation along these grid cells is even larger, although the additional difference can probably be explained. The schematisation of the original DVR model, and thus of the main channel bed, was done using Baseline (version 3.2). In this version the shallower banks were included in the interpolation and determination of the bed level of the outer parts of the main channel. Due to new insights, in the new version of Baseline (version 4.02), this approach has been abandoned, leading to lower bed levels in the outer parts of the main channel. Although the laser altimetry bed of 2003 was not prepared using Baseline 4.02, it was processed in accordance with the new methodology. With respect to the previous DVR model it can be concluded that the main channel was probably too restricted, leading to higher flow velocities and larger sediment transport. It is therefore recommended to use Baseline version 4.02 in future.

The remainder of the DVR model (Mosselman et.al., 2007) has remained unaltered. This for instance means that the roughness values etc of the floodplain are still based on the Baseline/WAQUA model that was used for the PKB study. Furthermore, the alluvial roughness in the Delft3D model is based on the Van Rijn roughness predictor.

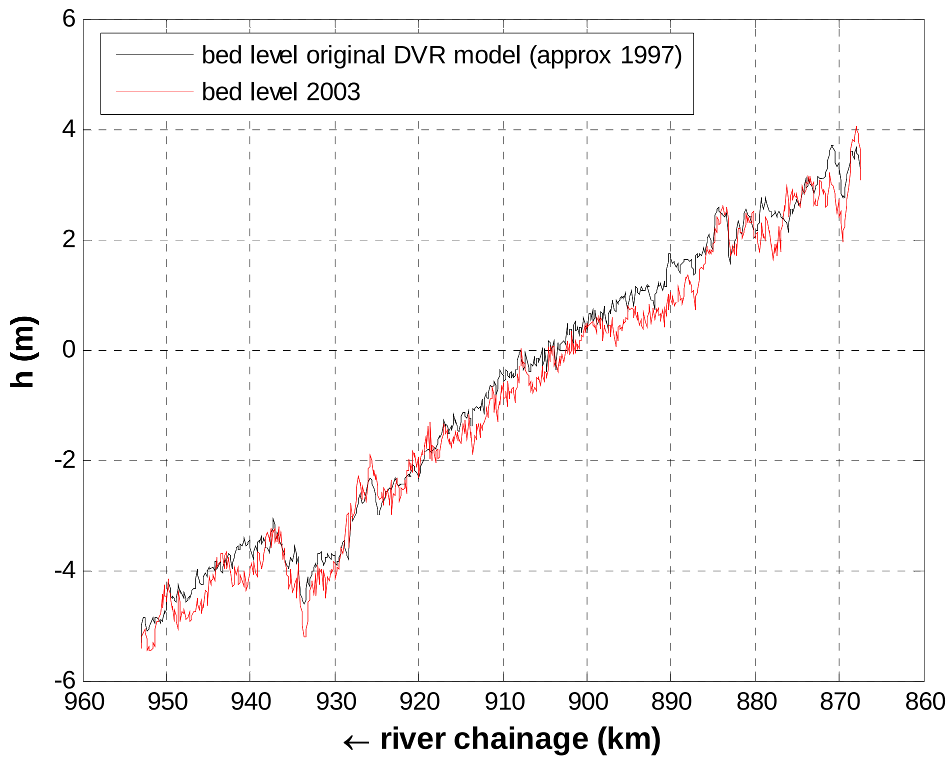

Figure 3.2 Width averaged bed level of the original DVR model (1997, black line) and the bed level of 2003 laser altimetry measurement (red line)

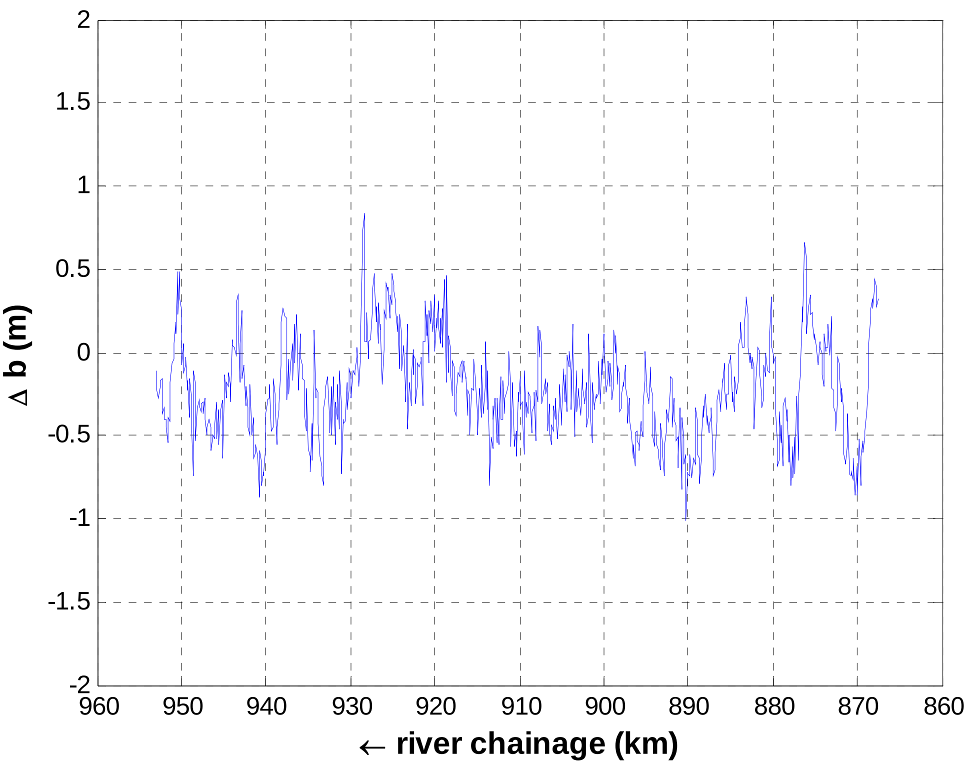

Figure 3.3 Difference between width-averaged bed levels of 2003 and 1997.

3.2.3 Calibration procedure

The calibration was carried out for the Waal branch by adapting the *A* values of the alluvial roughness predictor of van Rijn (1984c), Eq. (3.1), for the defined summer bed reaches.

$$k_S = A \cdot h^{0.7}\left(1 - e^{-B \cdot h^{0.3}}\right) \tag{3.1}$$

Here is a list of the roughness codes for the summer bed reaches that are considered in this calibration:

r_code	***river reach***
413	*pankop - nijmhav*
414	*nijmhav - tielwaal*
415	*tiel - zaltbommel*
416	*zaltbommel - vuren*
417	*vuren - einde Waal*

Each river reach starts and ends at a so-called MSW location.

Based on the deviation between the measured and calculated water levels at the upstream MSW locations, *A* values of each downstream reach were adapted by using the relations given below (Vollebregt & van Velzen, 2004):

$$A_{j+1} = A_j + \frac{\Delta \mathrm{h}_j}{\alpha_j} \tag{3.2}$$

$$\alpha_j = -\frac{\Delta h_j - \Delta h_{j-1}}{A_j - A_{j-1}} \tag{3.3}$$

$$\Delta h_j = h_{measured} - h_{calculated} \tag{3.4}$$

with:

α_j	=	a direction coefficient, slope
h	=	water level
j	=	iteration step
A	=	*A* value in alluvial roughness predictor
Δh	=	difference in water level

Adaptation of the *A* value continued until the difference between measured and calculated water levels Δh was minimized.

3.3 Results

3.3.1 Calibration runs

Delft3D calculations were carried out with an upstream discharge of 772 m^3/s and a water level of 0.72 m + NAP at the downstream boundary, in accordance with the measurements of 3 September 2003.

After several steps of adapting the alluvial roughness of the main channel using the method described in Section 3.2.3, the water level at the MSW-stations agreed well with the measurements. Figure 3.5 shows the differences between the measured and calculated water levels. Apart from some locations, the deviations stay within a range of 5 cm. The largest deviation is found in the downstream reach. As mentioned in section 3.2.1, after km 946 the measured water level increases (Figure 3.4), which is obviously not realistic in case of a unidirectional flow. It could be attributed to the tidal influence. That is the reason why a somewhat lower downstream boundary condition was adopted.

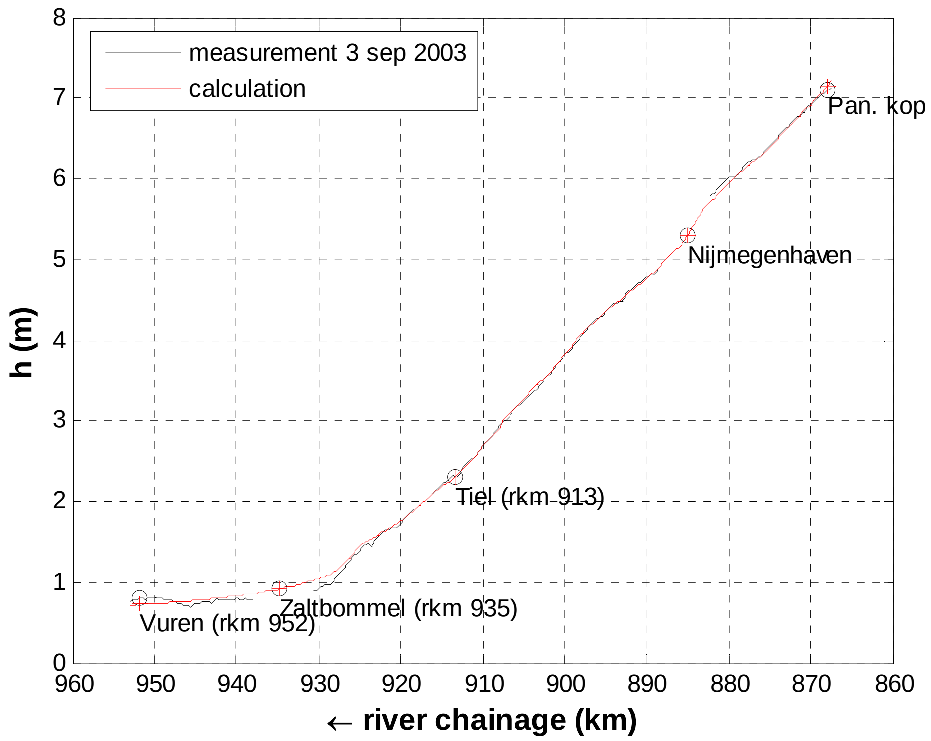

Figure 3.4 Measured (black) and calculated (red) water level (sim6); marker points define the MSW-stations.

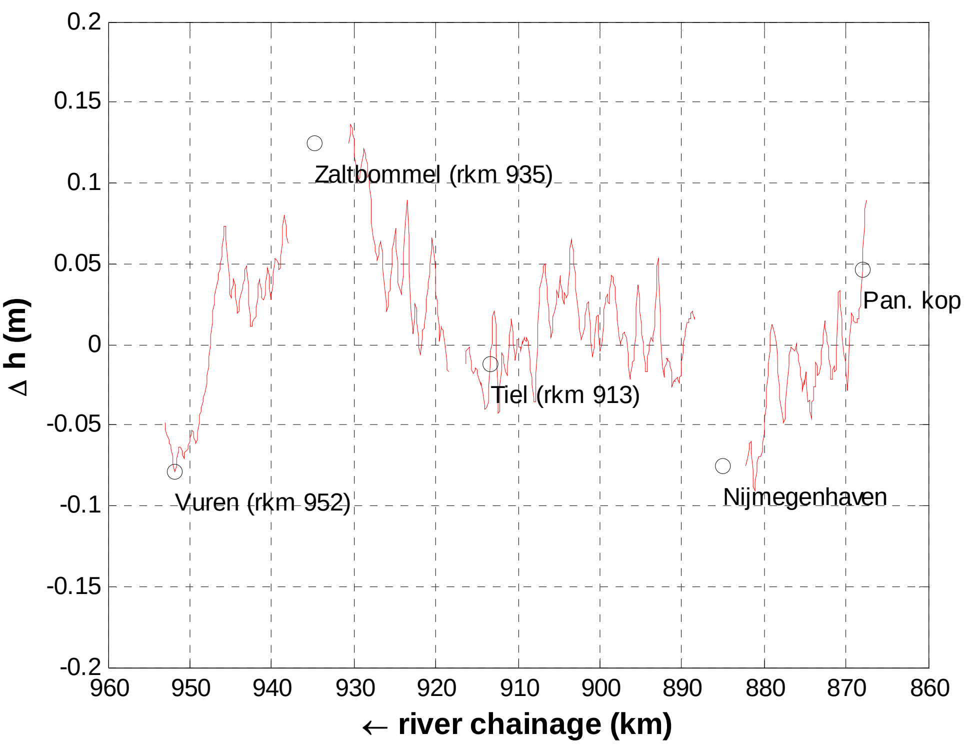

Figure 3.5 Calculated minus measured water level (sim6); marker points define the MSW-stations.

The A values found are presented in Table 3.1. The A values are low to very low in the downstream reach. The following reasons can be suggested:

1. The measured water level in the downstream reach might be wrong. The water level rise after km 946 is an indication.
2. Due to tidal variations the discharge through the downstream section is much lower than the average discharge at Tiel.
3. Under these low discharge conditions, bed forms are smaller and cause lower roughness.

Table 3.1 Calibrated A-values

r_code	***Reach***	**A value**	***Corresponding k_s value for a water depth of 4 m***
431	*pankop - nijmhav*	0.06	0.13
414	*nijmhav - tielwaal*	0.05	0.11
415	*tiel - zaltbommel*	0.025	0.05
416	*zaltbommel - vuren*	0.001	0.002
417	*vuren - einde Waal*	0.001	0.002

Regarding the 3rd point, the lowest roughness that could be expected would be that of the grain roughness. Assuming a hydraulic roughness of the grains solely, with $k_s = 3 \times D_{90}$, Figure 3.6 gives a comparison between the theoretical k_s value along the river reaches and the calibrated k_s value for an assumed water depth of 4 m. As we can see from Figure 3.6, only in the downstream reach of the Waal the k_s value needed to calibrate the model is lower than the theoretical grain roughness. Therefore, for this lower reach a k_s value of 0.01 m will be maintained as a minimum value, which corresponds with an A value of 0.005 rather than 0.001 as indicated in Table 3.1.

In addition to the above mentioned arguments, the fact that the water surface slope in this most downstream reach is rather small leads to a very high sensitivity of the estimated roughness. This can be explained as follows:

$$C = \frac{Q}{\left(z_w - z_b\right)^{\frac{3}{2}} \cdot i^{\frac{1}{2}}} \tag{3.5}$$

$$\frac{dC}{dz_w} = \frac{Q}{i^{\frac{1}{2}}} \frac{1}{\left(z_w - z_b\right)^{\frac{5}{2}}} \tag{3.6}$$

$$\lim_{i \to 0} \frac{dC}{dz_w} = +\infty \tag{3.7}$$

with:

Q	=	discharge
C	=	Chézy coefficient
z_b	=	bed level
z_w	=	water level
i	=	water surface slope

This means that, for very small slope ($i \rightarrow 0$), small errors in water level lead to large errors in roughness.

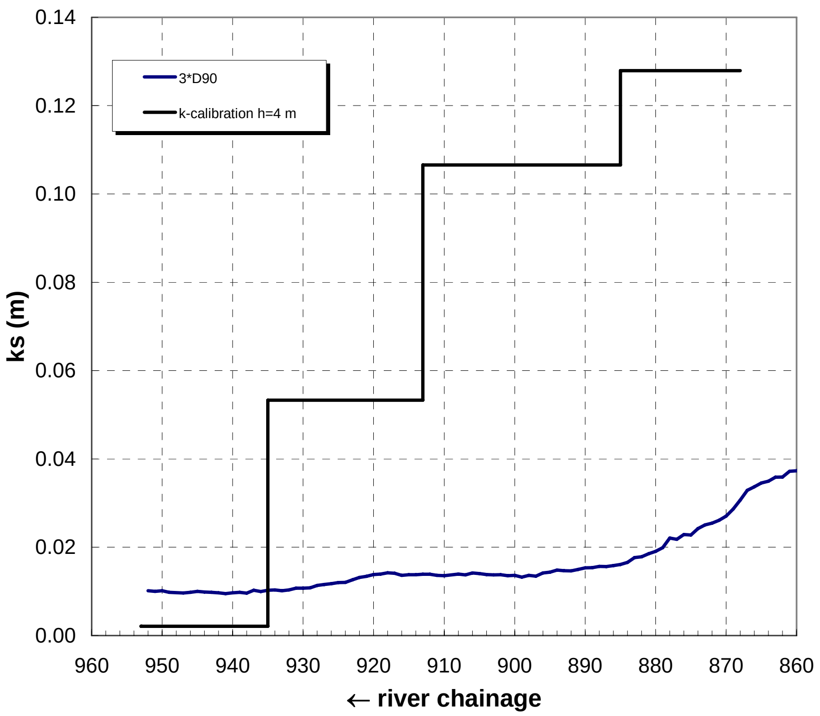

Figure 3.6 Theoretical k_s value based on grain size only (k_s=3·D_{90}) together with the calibrated grain size along the river chainage.

Increasing the downstream *A* value from 0.001 to 0.005 in the most downstream reach, leads to a slight increase of water levels in this reach. This increase amounts to 5 cm (see Table 3.2, Figure 3.7 and Figure 3.8). The effect extends up to Tiel after which it nearly disappears.

Table 3.2 Calibrated alpha-values with threshold of k_s = 3×D_{90}

r_code	***Reach***	***A value***	***Corresponding k_s value for a water depth of 4 m***
431	*pankop - nijmhav*	0.06	0.13
414	*nijmhav - tielwaal*	0.05	0.11
415	*tiel - zaltbommel*	0.025	0.05
416	*zaltbommel - vuren*	0.005	0.01
417	*vuren - einde Waal*	0.005	0.01

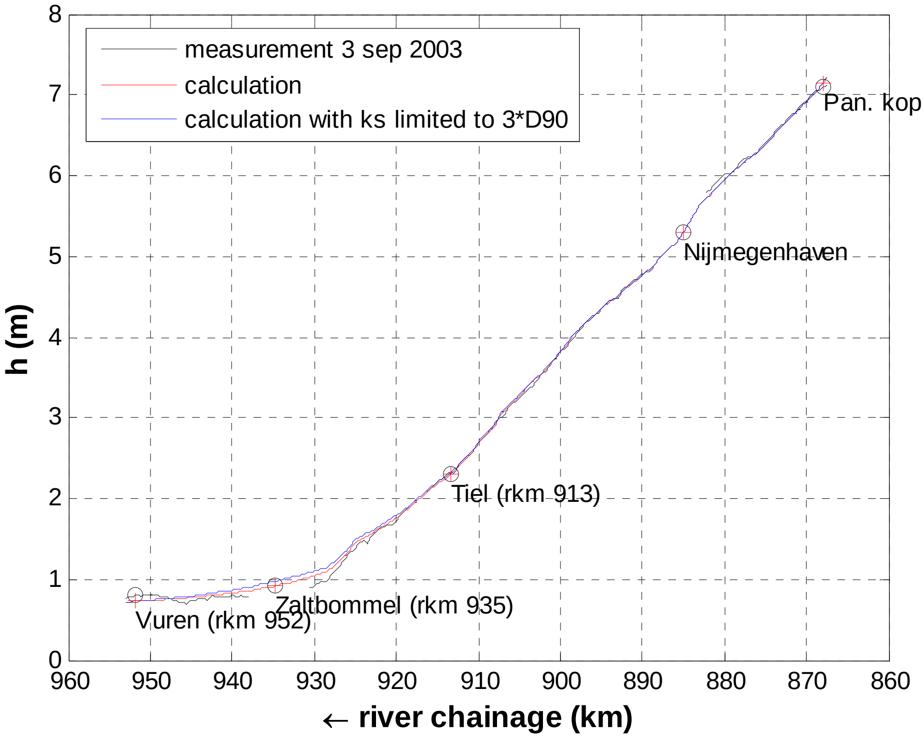

Figure 3.7 Calculated water level (blue) with downstream k_s-value based on grain size, viz. $k_s=3 \cdot D_{90}$ (sim 13). The figure also shows the measured (black) and previously calculated (red) water level of (sim6).

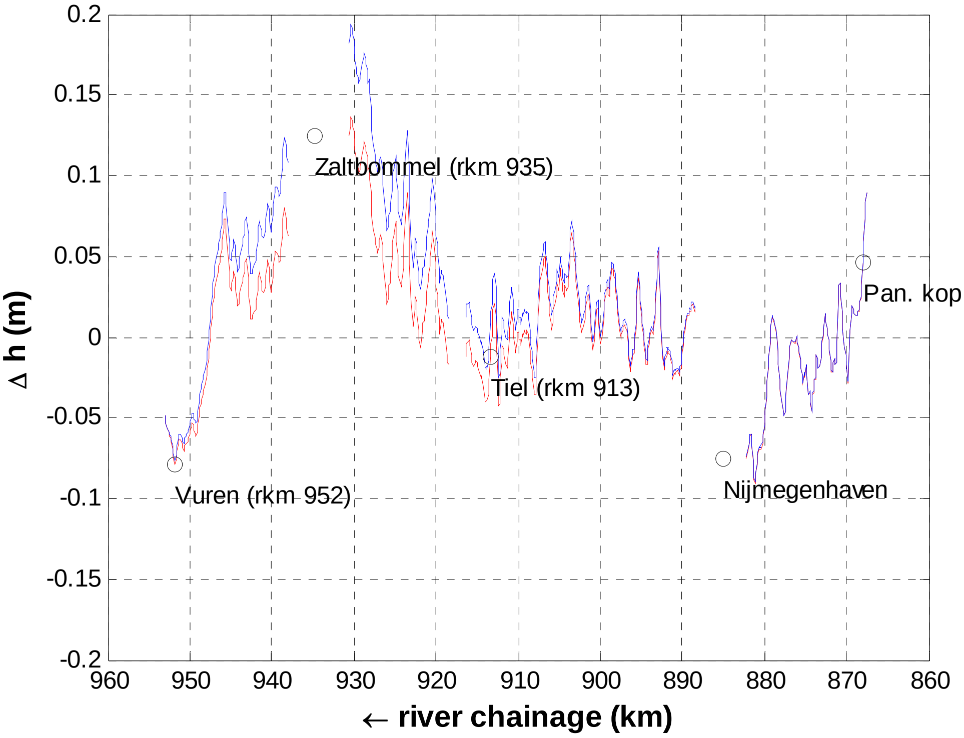

Figure 3.8 Calculated minus measured water level (blue sim6, red sim13)

3.3.2 Verification run

A verification simulation was carried out using the calibrated model with the roughness as described in Table 3.2. The aim is to reproduce the OLR of 2002. A discharge of 818 m^3/s was imposed as an upstream boundary condition and a water level of 0.269 m +NAP was imposed as a downstream boundary condition. The calculated water level is compared with the OLR level of 2002 (see Figure 3.9 and Figure 3.10). The difference in water level given in Figure 3.10 indicates that there is a rather large deviation in the reach between Tiel and Zaltbommel. This will be discussed in Section 3.4.

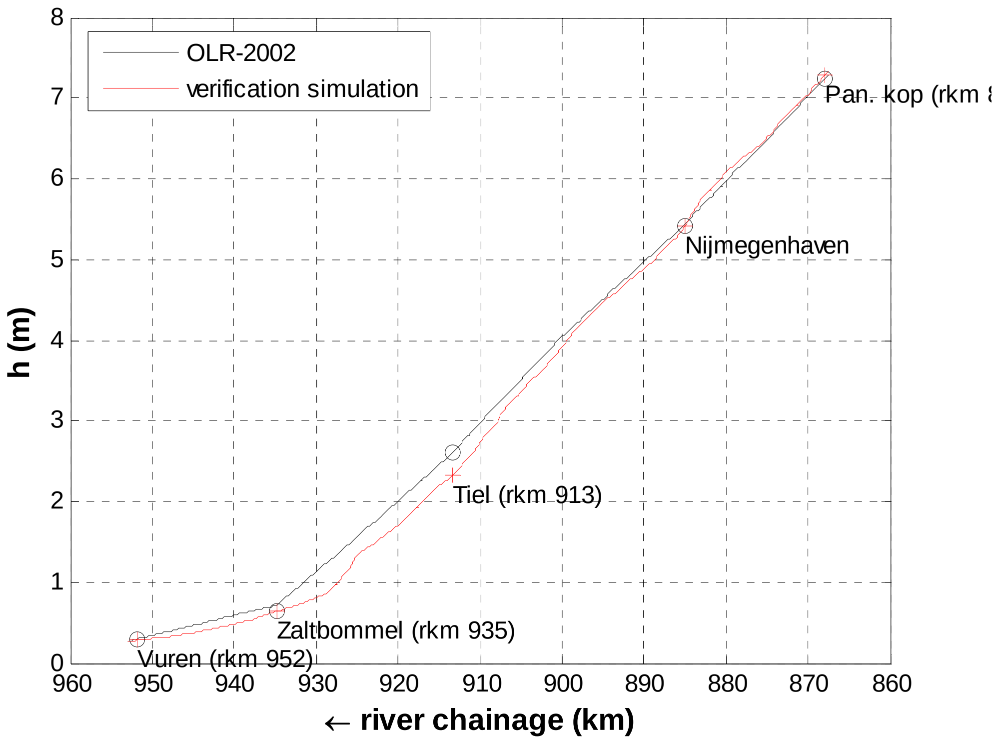

Figure 3.9 OLR-2002 (black line) and calculated (red line) water level (sim14)

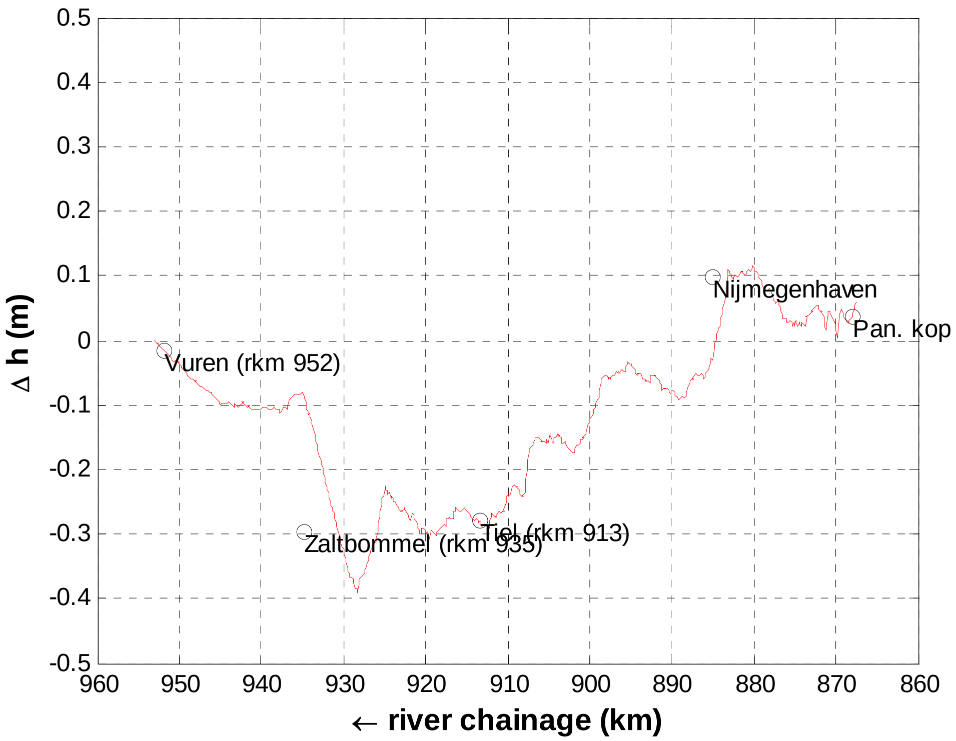

Figure 3.10 Calculated minus measured water level verification run

3.4 Discussion

The Waal branch of the DVR model has been calibrated on the low-water levels of 3 September 2003 for a constant discharge of 772 m^3/s. The calibrated roughness values, viz. the *A* values of the alluvial roughness predictor, are rather low, especially in the downstream reach, indicating low to no additional roughness due to bed forms. However, other causes could be pointed out, like discharge storage in the downstream reach due to tidal movement.

Table 3.3 gives the daily average discharges at Lobith, Tiel and the highest water level at Vuren for September 2 till 4 2003, obtained from Waterbase.nl. Note that Donar discharges are not measured but estimated from stage-discharge curves and for low-flow domain, this empirical relation is uncertain, which adds to the discrepancies between computed and observed water levels. Moreover, the following points are noticed:

1. The average discharge of 3 September slightly deviates from the discharge provided by RIZA.
2. The highest water level at Vuren of 3 September is more than 10 cm lower than the water level from the laser altimetry measurement.
3. It is likely that the laser altimetry measurement was taken at the time of the highest water level for the specific day.

Table 3.3 Discharges and water levels according to Waterbase.nl (Donar)

date	**Q_{Lobith} (m^3/s)**	**Q_{Tiel} (m^3/s)**	**Highest water level at Vuren (m + NAP)**
2 September 2003	989	756	0,73
3 September 2003	992	776	0,63
4 September 2003	994	788	0,55

Although the discharge in the vicinity of Vuren is not provided by www.waterbase.nl, from results of the SOBEK model for 1990 that is available at WL | Delft Hydraulics, it became clear that the downstream discharge during a day may fluctuate with more than 500 m^3/s (storage effect). For 21 September 1990, for instance, of which www.waterbase.nl provides a comparable daily average discharge at Tiel of 773 m^3/s, the highest discharge at Vuren was 945 m^3/s, while the lowest discharge corresponded to 420 m^3/s. The highest water level took place at a discharge of 580 m^3/s. In view of that, we conclude that the hydrodynamic calibration of the downstream reach of the model is somewhat uncertain. According to the calculations the tidal influence reached up to around Tiel, however, this distance is also related to the discharge. Therefore, the calibration is accepted for the upper part of the Waal, for hydrodynamic calculations and for lower discharge only.

With respect to the verification run given in section 3.3.2, the difference in water level given in Figure 3.10 indicates that there is a rather large deviation in the reach between Tiel and Zaltbommel. The calculated water level is up to 0.35 m lower than the OLR of 2002. This should be considered in comparison with the calibration model where in the same reach, the calculated water level reaches up to 0.20 m higher than the measured water level. This underscores the fact that the hydrodynamic calibration for the most downstream part of the river is uncertain. In the absence of additional data, e.g. a tidal boundary condition, we have the impression that this is the best possible at this stage. It is worth mentioning, however, that the OLR level in the lower Waal is based on statistics and not a physical backwater curve. Nevertheless, for the sake of dredging activities in the downstream reach of the Waal, an underestimation of the OLR is more critical than an overestimation, i.e. dredging volume would be larger in the case of underestimated OLR. Considering that the previous dredging case study (Mosselman et al. 2007) indicated that no dredging took place in the most downstream part of the Waal, this seems to be a more appropriate starting point with respect to dredging.

4 Global morphological calibration

4.1 Introduction

Past morphological model applications studying the Rhine branches in the Netherlands, including the previously developed DVR model, had different sediment transport formulations for each branch. Hence, linking the entire river would lead to discontinuities at the boundaries between branches. In this phase of developing the DVR model, we make the model operational in its entirety. This chapter presents the global model calibration. The objective of the global calibration is to ensure that the model operates correctly for all the river branches using the same transport formula and avoiding discontinuities between the different branches.

In this chapter we carry out a morphological calibration for the Bovenrijn, the Waal and the Pannerdensch Kanaal. We calibrate the model for 1D as well as 2D morphological behaviour. The 1D morphological calibration focuses on cross-sectional averaged quantities and the 2D calibration addresses 2D patterns of river bed such as bar-pool formation. The global morphological calibration presented in this chapter is limited to the model containing the domains of the Bovenrijn, the Waal and the Pannerdensch Kanaal with a particular emphasis on the Waal.

Within the scope of this chapter, we also briefly elucidate the approach we followed to incorporate all three Rhine branches into a single model. Moreover, we give a short description about an additional step that has been taken regarding the hydraulic boundary conditions as well as the discharge distribution at the bifurcation.

4.2 Method

4.2.1 Model preparation

Calibration period

For the calibration of previous morphodynamic models of the Rhine branches in the Netherlands, for instance the 1D SOBEK Rijntakkenmodel (Van Vuren & Sloff, 2006), the period 1990-2000 is often used as the calibration period. This is simply because a homogeneous data set of bed level measurements is available for this period. These were single-beam measurements. In 1990 a new policy concerning dredging activities was adopted, stating that net extraction of sediment from the river is not allowed, so as to prevent the large-scale degradation of the river. In conformity to this policy the dredged material is to be dumped elsewhere in the river. However, during the 1990s, Waal programme measures were implemented. Accordingly, the morphological behaviour of the river was influenced by these interventions. Moreover, the results of the 1D SOBEK Rijntakkenmodel indicated that incomplete data of dredging and dumping volumes in the period 1990-1999 made it difficult to reproduce the observed morphological changes properly.

From 1999 onwards, multi-beam bed level measurements are being performed in the main channels of the Rhine branches. These measurements have a larger resolution than the single-beam measurements. Moreover, the measurements took place after the completion of the Waal programme measures.

Accordingly, and in close consultation with RWS-RIZA, we arrived at the conclusion that the best calibration can be achieved by using the bed levels of 1999 multi-beam measurements as initial condition and by using the period between 1999 and 2006 as the calibration period. The trends derived from multi-beam measurements in that period can be used for calibration purposes. By doing so, the calibration period is rather short (around 7 years); in particular when considering the 1D morphological evolution of the Rhine branches. Therefore, the 1D trends (yearly bed level changes, propagation speed of bed disturbances, etc) derived from single-beam measurements will be used complementarily to the trends from multi-beam measurements. With respect to the calibration of the 2D pattern of the river bed the more recent data (multi-beam) are used.

Integration to a single DVR model

The calibration of the DVR model is restricted to the branches Bovenrijn, Waal and Pannerdensch Kanaal. In other words, the branches IJssel and the Nederrijn are not calibrated within the present study. The entire model is composed of 8 domains: the Bovenrijn, 3 domains for the Waal, the Pannerdensch Kanaal, 2 domains for the IJssel, and the Nederrijn. The calibration runs are made without the IJssel and Nederrijn, i.e. using five domains. The Waal is divided into three sub-grids in order to distribute the computation effort equally over multiple processors.

The integration of the three branches into a single model is discussed in the following sections. Since a number of aspects have changed with respect to the previous DVR model (Van Vuren et al. 2006 and Mosselman, et al., 2007), a brief overview of the parameter settings is given herein.

Model specifications

In accordance with the finding from the 1st phase of this project, (Reducing Computation Time of the DVR model: Van Vuren et al., 2007), we use the recommended combination of grid size, hydrodynamic time step, and morphological acceleration factor.

- Δx, Δy: Table 4.1 gives a summary of the grid characteristics.
- Δt: a time step of 0.4 minutes is used. The computational time step of 1.2 minutes as recommended in the previous phase was based on a single-domain computation and proved to cause instabilities near the boundaries in a multi-domain computation.
- Morphological acceleration factor: the morphological acceleration factor ranged from 120 to 600 depending on the discharge see Table 4.2. The maximum morphological acceleration factors recommended in the 1st phase of the project were used.

Table 4.1 Characteristics of the grids used for different branches.

Gridname	Bovenrijn	Waal – part a	Waal – part b	Waal – part c	Pannerdensch Kannal
number of grid cells	55x177	47x296	47x401	47x353	67x137
main channel					
number of grid cells	10	12	12	12	8
grid cell width (m)	~34	~23	~21	26~	~20
grid cell length (m)	~80	~80	~80	~80	~80
aspect ratio	1:2,4	1:3,4	1:3,8	1:3	1:4
floodplains (gradually coarsened in transverse direction up to a factor of 4.0)					
number of cells, left	21	21	21	21	31
number of cells, right	24	14	14	14	28
grid cell width (m)	29-200	16-325	23-151	24-305	16-122
grid cell length (m)	45-135	9-140	50-112	26-156	31-127

Model schematisation

The reference schematisation of the PKB Room for the River studies is used for the projection of hydraulic roughness, bed topography, groynes, summer dikes and steep obstacles in the floodplains. Due to difficulties switching to a newer version of Baseline (V4.02) the older version that has been used earlier was used again; Baseline version 3.3 is used.

As initial settings of the morphological schematisation, e.g. grain size distribution and the definition of the fixed layers (available sediment thickness), the earlier DVR model settings were used (Van Vuren et al., 2006 & Mosselman et al., 2007). During the calibration process they were changed. Note that the grid cells near the heads of the groynes fixed layers were imposed (Mosselman et al., 2007).

The initial topography for the main channel is derived from the multi-beam measurements of 1999 for the Waal and the Bovenrijn, and of 2002 for the Pannerdensch Kanaal. For the floodplain the topography was generated using the Baseline schematisation. In the upstream (German) part of the Bovenrijn multi-beam measurements are not available. Hence, the topography for this part of the model was derived from Baseline and corrected to reflect changes from 1997 to 1999 and to account for the systematic discrepancy between single-beam and multi-beam measurements.

4.2.2 Boundary conditions

At the upstream boundary a discharge hydrograph was imposed as a hydraulic boundary condition. A bed degradation of 3 cm/yr was imposed as a morphological boundary condition in accordance with the large-scale trend (Sieben, 2005).

The representative discharge hydrograph for the calibration period 1999-2006 was derived from the measured discharges of the same period. Figure 4.1 shows the measured discharge duration curves, the averaged duration curve and the schematized duration curve. The resulting representative hydrograph is depicted in Figure 4.2 and Table 4.2.

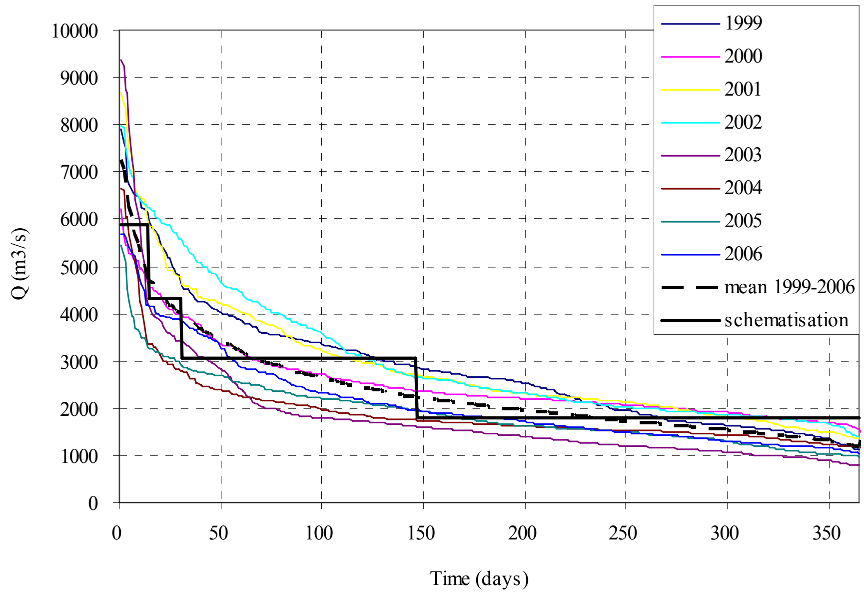

Figure 4.1 Measured duration curves for single years of the calibration period, the averaged duration curve and the schematized duration curve.

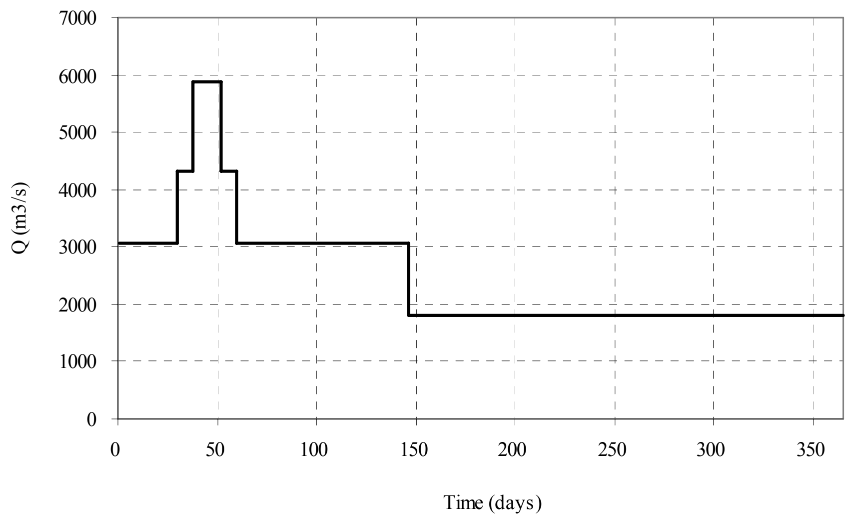

Figure 4.2 Discharge hydrograph used in simulation

Table 4.2 Discharge hydrograph used for simulation

Time [days]	Discharge level in the Bovenrijn [m^3/s]	Morfological acceleration factor [-]
30	3052	480
8	4318	200
14	5866	120
8	4318	200
86	3052	480
219	1794	600

Water level boundary conditions were imposed at the downstream boundaries of the model. For the Waal at km 953, they were derived from the following relation:

$$h_{Waal} = \left(\frac{Q_{Waal}}{1500} \right)^{0.95} - 0.1 \tag{4.1}$$

where Q_{Waal} is the Waal-discharge corresponding to the imposed Bovenrijn discharge derived with SOBEK-simulations[1].

The water levels imposed at the downstream end of the Pannerdensch Kanaal were initially taken from calculations using the complete DVR model including the IJssel and Nederrijn. This resulted in a discharge distribution at the Pannerdensche Kop that does not correspond to the measurements. Too much discharge is going to the Waal at the expense of the discharge in the Pannerdensch Kanaal (Table 4.3). Moreover, the modeled water levels at the Pannerdensche Kop were about 20 cm higher than the measured values (Table 4.4).

Several attempts were made to obtain a better reproduction of the measured discharge distribution; finally the following is applied:

- The water level boundary conditions are deduced from discharge and water level measurements from 2000 (source: Rijkswaterstaat Directie Oost-Nederland, afdeling informatie ANIC).
- The roughness in the Waal is slightly increased by increasing the A parameter of the alluvial roughness predictor of Van Rijn from 0.071 to 0.10:

$$k_S = A \cdot h^{0.7} \left(1 - e^{-B \cdot h^{0.3}} \right) \tag{4.2}$$

where A and B are calibration coefficients and h is the flow depth.

As indicated in Table 4.3 and Table 4.4 these adaptations yield a better reproduction of the the discharge distribution at the Pannerdensche Kop and the water levels in the Pannerdensch Kanaal.

Table 4.3 Measured and modelled percentages of Bovenrijn discharge in the Pannerdensch Kanaal

Q Bovenrijn	% of Bovenrijn-discharge in Pannerdensch Kanaal		
	modeled (old)	measured (2000)	modeled (new)
1794	26.4	31.14	27.9
3052	29.2	32.36	32.3
4318	28.6	32.80	32.5
5866	29.2	32.70	33.4

1. Note that the Waal discharge derived from SOBEK is higher than the Waal discharge deduced from discharge data.

Table 4.4 Measured and modelled water levels at the Pannerdensche Kop.

Q Bovenrijn	Water level at Pannerdensche Kop [m + NAP]		
	modeled (old)	measured (2000)	modeled (new)
1794	8.85	8.76	8.91
3052	10.71	10.51	10.63
4318	12.14	11.87	12.02
5866	13.40	13.17	13.24

Table 4.5 Measured and modelled water levels at the IJsselkop.

Q Bovenrijn	Water level at IJsselkop [m + NAP]	
	model (old)	measured (2000)
1794	8.12	8.30
3052	9.72	9.53
4318	11.16	10.73
5866	12.46	11.81

4.2.3 Calibration of 1D morphological processes

Quantities for calibration

The one-dimensional calibration is focused on the following cross-section-averaged quantities:

- Annual sediment transport volumes/rates,
- celerity of bed disturbances,
- annual bed level changes, and
- period-averaged bed level gradient.

Calibration data set

With respect to the data available for calibration, we use data of the most recent multi-beam measurements 1999-2006 as a primary calibration data set. This period might be considered as somewhat short, however, it is the most accurate data set (all soundings based on multi-beam). The short-term statistics might give a good impression of changes with a length scale in the order of 5 to 10 km. Note that the bed form celerity is in the order of 1.0 km/yr. Accordingly, large-scale changes such as changes of river slope might not be captured in such a short period. We fill this gap by using the trends of the historical data set (1990 – 2000). This becomes more important if large differences appear between the trends based on the multi-beam data and those coming from the historical data set. Therefore, we analysed the difference between trends observed by multi-beam measurements between 1999 and 2006 and single-beam measurements available for the period 1990 - 2000. Note that for the Pannerdensch Kanaal multi-beam measurements were only available between 2002 and

2006, and single beam measurements were only available up to 1994. Thus the calibration data for the Pannerdensch Kanaal covers a shorter period than the data for the other domains.

The measurements in the two periods show some different trends especially in the Bovenrijn. The single-beam measurements show erosion in all but the part close to the Pannerdensche Kop, whereas the multi-beam measurements show erosion at the up- and downstream part but sedimentation in the middle part of the Bovenrijn. For the calibration, we decided to focus on the multi-beam measurement, though single-beam measurement has also been included in the results for the sake of comparison.

Transport formula

The sediment transport formula of Van Rijn (1984a; b) was selected to represent the sediment transport behaviour for all three branches of the Rhine River (see Chapter 3). The formula reads:

$$
\begin{aligned}
S_b &= \alpha_{bed} \cdot 0.1 \sqrt{\Delta\, g\, D_{50}^3}\, D_*^{-0.3} T^{1.5} \\
S_s &= \alpha_{sus} \cdot f_{cs}\, u\, h\, C_a \\
S &= S_b + S_s
\end{aligned}
\tag{4.3}
$$

in which S_b, S_s and S are bed load, suspended load and total transport respectively; T is the dimensionless transport stage parameter; D_* is the dimensionless particle parameter; C_a is the reference concentration, u is depth-averaged velocity, h is the water depth and f_{cs} is a shape factor; see Appendix A for the details.

Calibration parameters

- *Parameters α_{bed} and α_{sus}*: These are the primary parameters that are used to calibrate the overall transport of bed load and suspended load respectively. These are important tuning parameters that affect both the sediment transport rate and the degree of nonlinearity n in the general sediment transport formula $S = m\, u^n$.

- *Critical Shields parameter*, θ_{cr}: previous modelling experience of the Rhine branches in the Netherlands indicates that θ_{cr} is an important calibration parameter and often different branches needed a different θ_{cr} to reproduce the observed morphological behaviour (e.g. Baur & Jagers, 2002; Van Vuren et al., 2006; Mosselman et al., 2007). Observations on the behaviour of the Bovenrijn and the Pannerdensch Kanaal indicate that the conventional value of θ_{cr} yields no transport during low flow conditions in several locations. This leads to predicting the yearly transport volume and the bedform celerity. This may be attributed to the presence of graded sediment in these two branches compared to more uniform sediment in the Waal. In graded sediment, even at low discharge conditions, part of the sediment mixture is still transported. Accordingly, we use the critical Shields parameter as one of the calibration parameters. Note that transport at low discharges is extremely sensitive to the choice if θ_{cr}.

- *Roughness height*[2], k_s: Reference level used in the Van Rijn formula for suspended sediment transport; it affects the reference concentration of suspended sediment. The value of this parameter was given a conventional value of 0.3 for all branches.

- *Standard deviation characterizing the grain size distribution,* σ_g: In Delft3D, if no standard deviation is specified, D_{90} is taken as $1.5 \times D_{50}$. From the analysis of the field data (given in Figure 4.3) we found that D_{90} is around $4 \times D_{50}$. Since $D_{90} = \sigma_g^{\ 1.2816} \times D_{50}$ for a log-normal distribution, σ_g has to be equal to a value of 3. Accordingly, for the present calibration, σ_g was kept constant at a value of 3.0 for all branches.

- *Spatial distribution of bed material* (see Figure 4.3): Offline calculations and test simulations indicated that merely reducing θ_{cr} does not offer a correct estimation of transport and bedform celerity in the Pannerdensch Kanaal and the lower part of the Bovenrijn. Further reduction would lead to overestimation of transport in other locations. Early estimates, in conformity with previous models (Verschelling et al. 2007), showed that the spatial distribution of the grain size has a significant effect on the behaviour of the model. In uniform sediment models, the mixture is characterized by its median grain size D_{50}. The median diameter of the mixture is larger than the fraction diameters of the transported size fractions. Thus, transport starts at higher discharges than in reality. This may explain the need to reduce the D_{50} in the model in branches that are dominated by graded sediment, particularly the Pannerdensch Kanaal.

Calibration procedures

The 1D morphological calibration comprises the following two steps:

- Offline calculations using the hydrodynamic results of the model. These were carried out to roughly tune sediment transport and the celerity of bed disturbances. In this way preliminary parameter settings are found. The rough tuning also necessitates an adjustment of the spatial distribution of the median grain size in each branch within the observed data scatter. The hydraulic and sediment input data for each representative discharge comprise the median grain size along the reaches, velocity and depth (cross-section-averaged) in the main channels, and river width along the reaches. During calibration we focus on the appropriate prediction of celerity of bed disturbance in accordance with the field observation.

- Simulation runs for the evaluation of sediment transport, celerity of bed disturbance, annual bed level changes and time-averaged bed level gradient in comparison with single- and multi-beam measurements for all branches. The calibration is an iterative process. After each simulation some fine-tuning takes place.

2. Not to confuse with roughness height in the alluvial roughness predictor

In order to fine tune the celerity of bed disturbances, simulations with and without trenches are carried out. The celerity of the trenches gives an indication about the speed at which morphodynamic changes occur as well as about the time scale of morphological processes. The bed form celerity along the river reaches is calculated by using the following relationship:

$$u_{bf} = \frac{nS}{h(1-Fr^2)}$$

where S is sediment transport rate, h is flow depth, n is the degree of non-linearity in functional dependence of sediment transport on flow velocity, and Fr Froude number (see Chapter 3 for additional details).

With respect to the large scale morphodynamic response (bed level change and bed level slopes) the amount of sediment entering the branches and the gradients in sediment transport capacity are important. Calibration is focused on both the sediment transport capacity along the branches and the amount of sediment entering a branch. With respect to the first, along with the changes in the hydraulic boundary conditions in the model to provide an improved discharge distribution at the bifurcations for lower discharge in the Pannerdensch Kanaal, slight improvement can be made by adapting the spatial grain size distribution. Regarding the latter one, it is necessary to coarsen the bed material at the right bank of the Bovenrijn near the bifurcation, as observed in the field situation, in order to get the correct trend of sediment entering the branches.

Parameter settings for 1D morphology

Based on offline calculations, the spatial distribution of grain size was decided for all branches (Figure 4.3). Note that in the upstream part of the Bovenrijn there is a large difference between the model and the measurements. This difference could be attributed to graded sediment transport in the Bovenrijn.

After evaluating the performance of several combinations of parameters, two sets of parameters are selected for further analysis:

- the first: $\theta_{cr} = 0.03$, $\alpha_{\text{bed}} = 1.0$, and $\alpha_{\text{sus}} = 0.2$, and
- the second with relatively lower critical Shields parameter: $\theta_{cr} = 0.016$, $\alpha_{\text{bed}} = 0.3$, and $\alpha_{\text{sus}} = 0.2$,

The first set gives an acceptable result for the Waal with some overestimation of celerity in the middle Waal, but, it performs poorly in the other branches, particularly for the lowest discharge. A typical example is depicted in the Figure 4.4 for the case of the Bovenrijn. One can notice the absence of sediment transport in the upper part for the lowest discharge. Also, it seems to underestimate the celerity of bed disturbance. For the Pannerdensch Kanaal we observed the same, but slight improvement was made by decreasing D_{50} that was found to be necessary to get the celerity more or less right. The second set yields reasonable values of celerity and transport rates, particularly during the lowest discharge, and performs quite well in all branches; still the celerity in the Pannerdensch Kanaal is at the low side.

Consequently, we arrived at the conclusion that for this uniform sediment model the second set of parameters is suitable for all branches despite rather low value of critical Shields parameter.

Table 4.6 Final parameter set for the sediment transport formula.

α_{bed}	α_{sus}	θ_{cr}
0.3	0.2	0.016

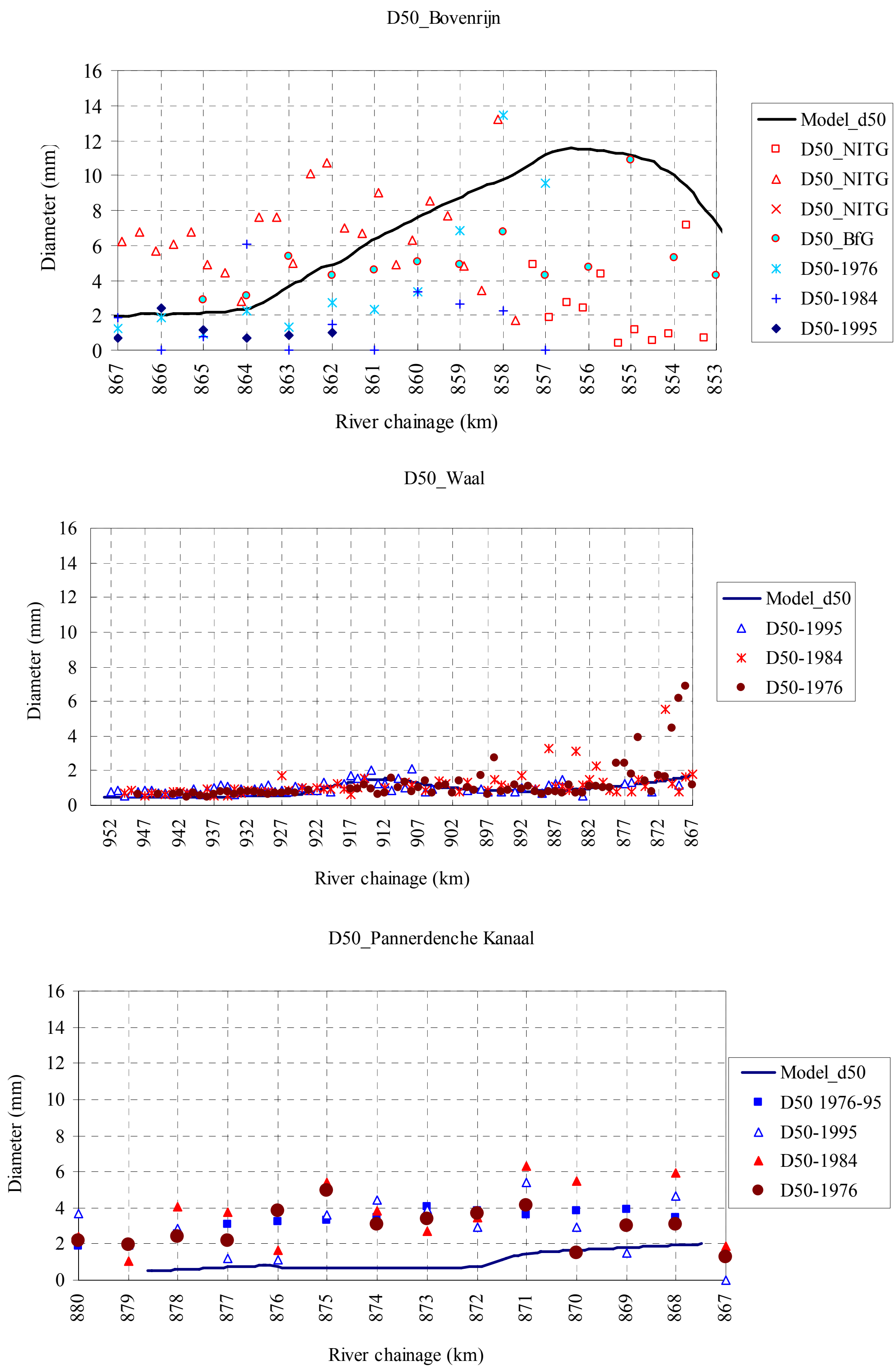

Figure 4.3 Spatial distribution of median diameter along the river reaches

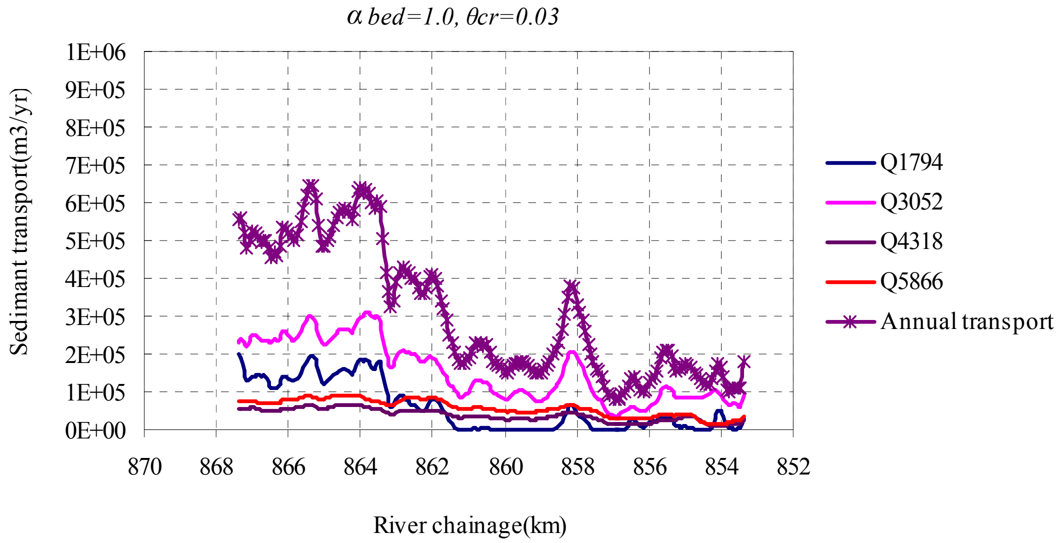

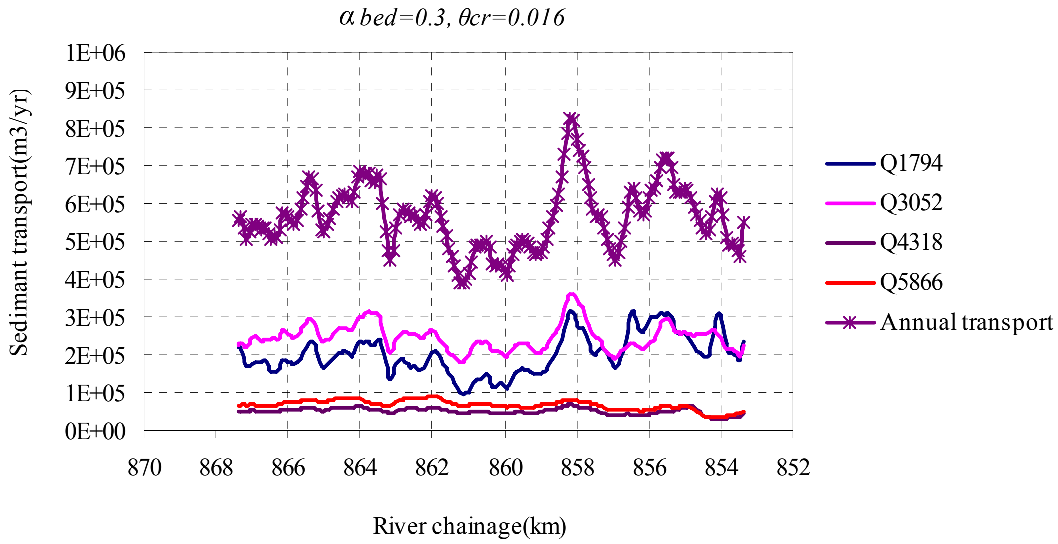

Figure 4.4 Comparison of sediment transport in the Bovenrijn for different discharge levels for respective period with two different parameter settings

Quantitative evaluation of the model settings

For the sake of evaluating the behaviour of the model settings, the behaviour of the final model settings using the formula of van Rijn is compared with the behaviour of the model based on the transport formulae of Mayer-Peter-Muler (MPM) and Engelund-Hansen (EH). Analysis of the annual sediment transport in all Rhine branches was conducted. Van Rijn formula appeared to be effective for all Rhine branches, particularly for the lower discharges. An example comparing the performance of different sediment transport formula is given in Figure 4.5. From the figure we can see that MPM formula behaves comparable to the calibrated Van Rijn formula in the Waal and in the downstream part of the Bovenrijn whereas it yields no transport at all in the upstream part of the Bovenjin. With respect to the formula of Van Rijn, the formula of EH gives a comparable result in the downstream part of the Bovenrijn, upper Waal, and middle Waal, but it underestimates the transport in the upstream part of the Bovenrijn and largely overestimates the transport in the lower Waal. Evidently, each of the formulae MPM and EH, behaves similarly to the calibrated van Rijn formula in part of the model not along the full model where the formula of van Rijn is suitable for the entire model as we will demonstrate later in this chapter.

A comparison of flow and sediment discharge relationship derived based on offline calculation for some selected locations in all branches can be seen in Figure 4.6, Figure 4.7 and Figure 4.8. From Figure 4.6, it can be conferred that, for the upper Waal all formulae give more or less identical result for the lower discharge, while they diverge for the higher discharges. VR formula gives slightly higher transport in lower discharge, whereas EH formula gives excessively high transport in higher discharge. For the middle and lower part of the Waal, bedload transport rate calculated by VR formula gives lower value than EH and MPM, whereas total load transport appears to be an average value of transport rate comparing to EH and MPM. In other words, inclusion of suspended sediment increases the transport rate particularly in the lower part of the Waal. In the same figure (Figure 4.6) the average transport rates as deduced from ten Brinke (2005) are given to have an impression about the measured transport trends. The comparison indicates that the VR formula is closest in behaviour to the measured transport rates. For the upper part of the Pannerdensch Kanaal, all formulae appear to offer identical results for average discharges (Figure 4.7).

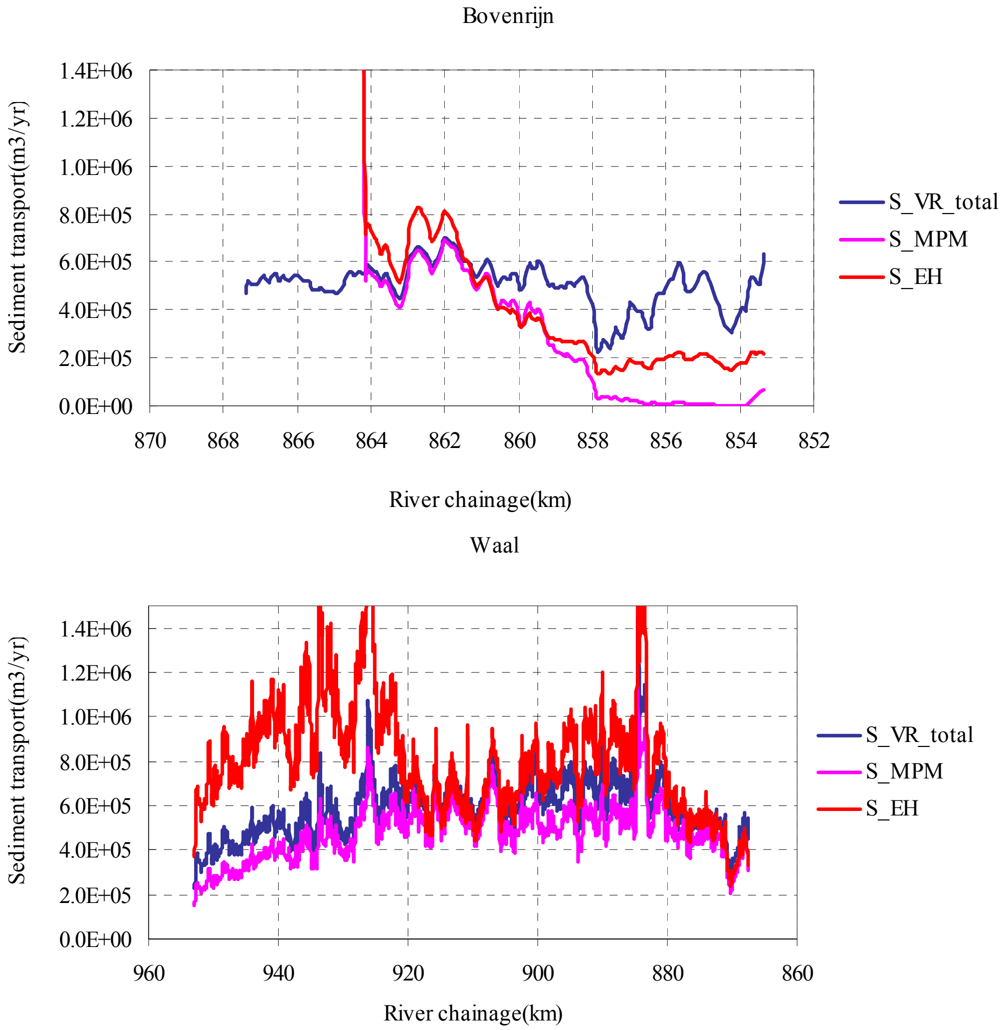

Figure 4.5 Comparison of annual sediment transport calculated by using VR, MPM and EH formulae

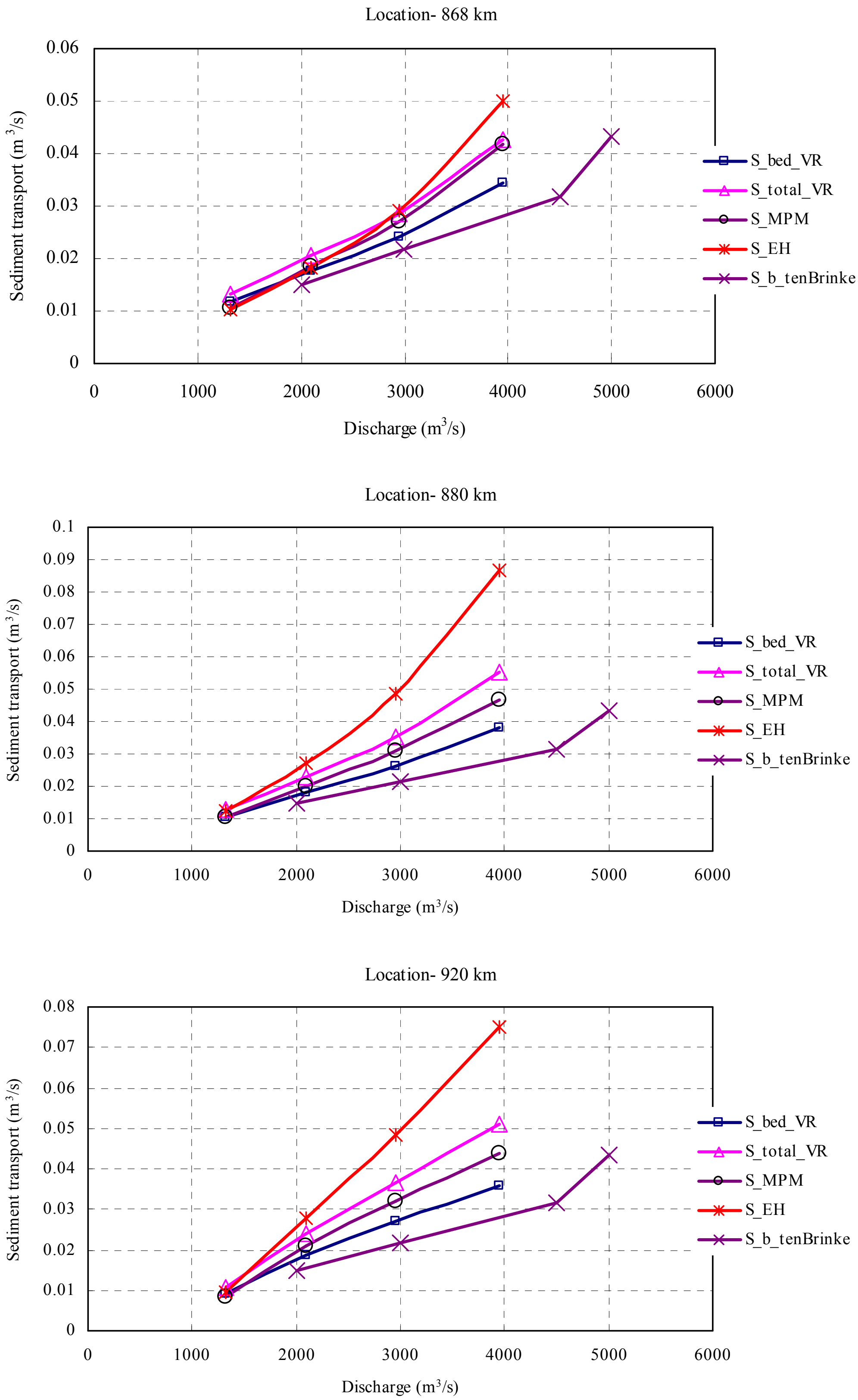

Figure 4.6 Flow discharge and sediment transport relationship in some selected locations in the Waal. *S_b_tenBroinke* is deduced from the bed load transport rates given by ten Brinke (2005) for the Waal.

VR formula seems to give higher transport rate in low discharge, which is important to reproduce transport in low flows. For the lower part of the Pannerdensch Kanaal, all formulae produce similar behaviour with an exception of EH formula that shows quite high transport rate in case of higher discharges. With respect to the Bovenrijn, EH and MPM formulae give quite low transport rate in the upper part, while they produce excessively high transport rate in the lower part (Figure 4.8, top plot). Likewise, the behaviour of these three transport formulae for the Waal can be assessed from Figure 4.8 (lower plot).

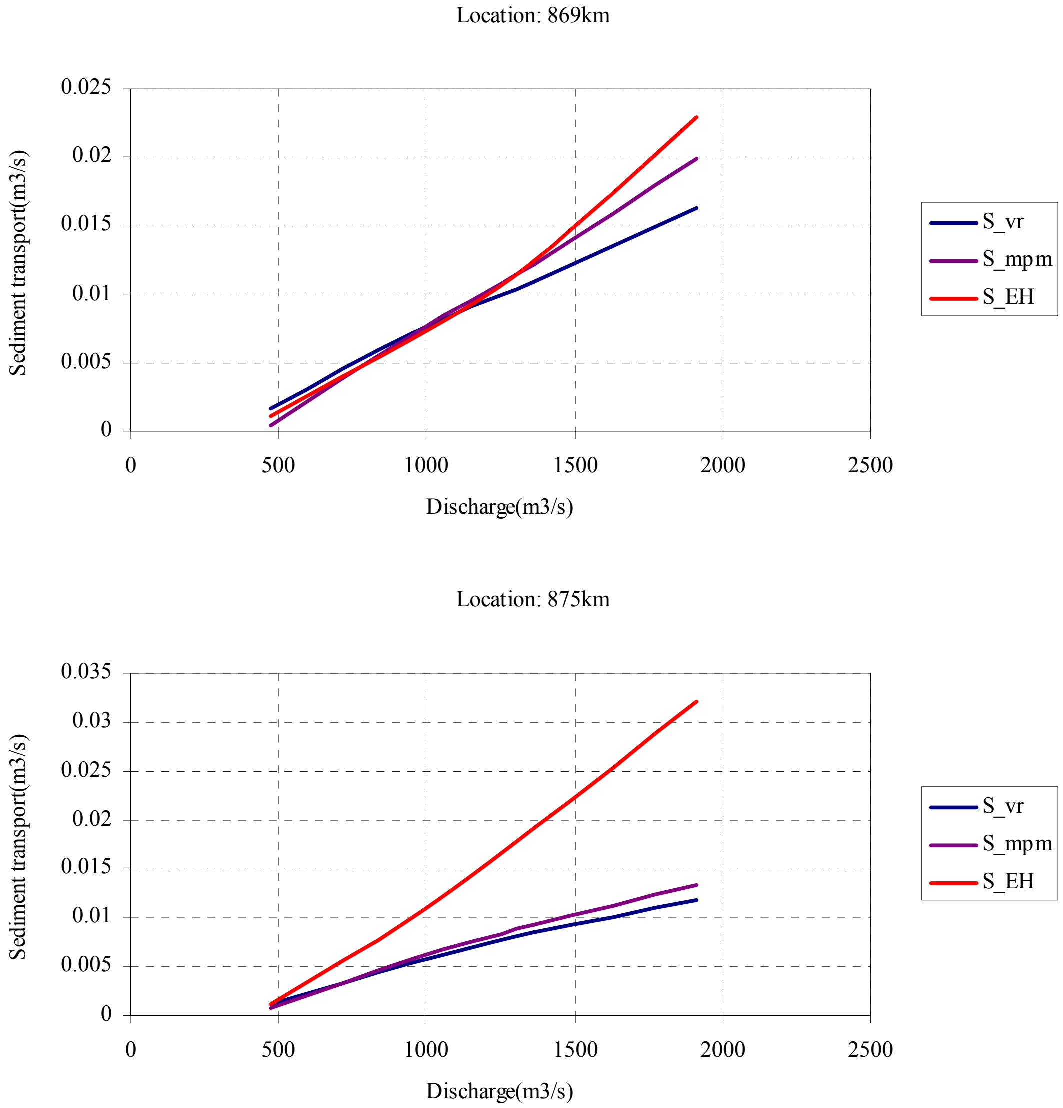

Figure 4.7 Flow discharge and sediment transport relationship in some selected locations in the Pannerdensch Kanaal

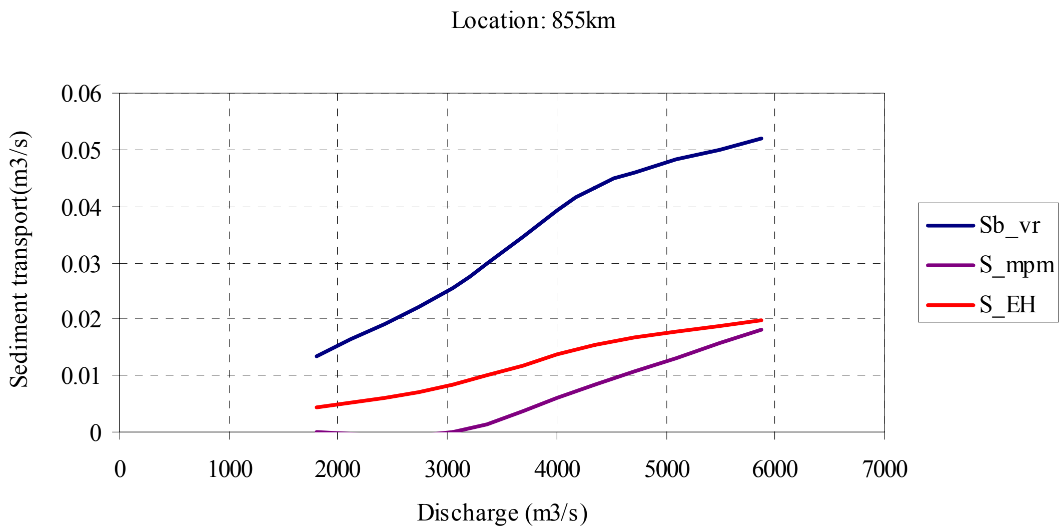

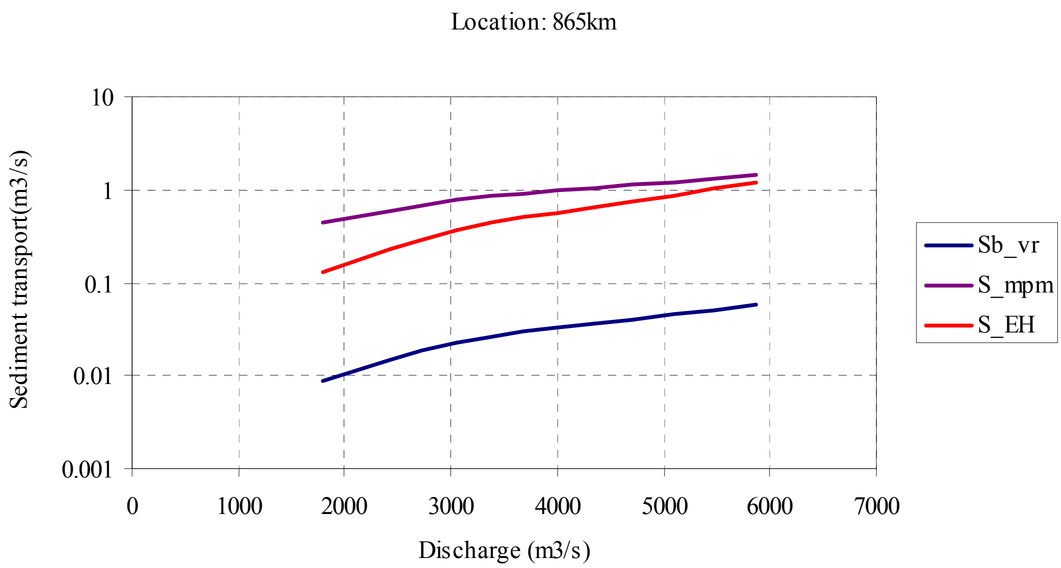

Figure 4.8 Flow discharge and sediment transport relationship in some selected locations in the Bovenrijn

4.2.4 Calibration of 2D morphological processes

Quantities for calibration

The 2D patterns in the river bed are forced by the curvature of the channel and channel width variations. In principle, the 2D patterns do not migrate through the river system. The 2D calibration focuses on a correct reproduction of these patterns. Two important features define the 2D pattern of the river, the amplitude and location, they can be evaluated by:

- the transverse slopes in bends, and
- the position of crossing between two opposite bends

Multi-beam measurements of the period 1999-2006 are used for the calibration. Because of 'breathing' of the river bed due to discharge variations through the year, a time-averaged bed level is derived and used in calibration.

Calibration parameters

For a correct reproduction of the 2D bar-pool patterns, the following two factors are important:

- the spiral motion due to the curvature of the flow, and
- the effect of the transverse bed slope.

In Delft3D these are represented by two calibration parameters:

- E_{spir}: affecting the spiral flow intensity
- A_{shld}: influencing the transverse slope effect.

Calibration procedures and model adaptation

The transverse slope in a river bend depends on the balance between the upslope drag force induced by spiral flow and the down-slope gravitational force, both acting on the grains moving along the bed. The 2D bar pattern in meandering rivers can be considered in general as a combination of the axi-symmetrical solution (theoretical bed slope for infinitely long bend of constant curvature) and a damped solution of the wave equation as a response to variations in radius of curvature and variations in bend direction.

Struiksma et al. (1985) approximate the axi-symmetrical lateral bed slope for infinitely long bend of constant curvature as follows:

$$\frac{\partial Z_b}{\partial y} = A \cdot f\left(\theta\right)\frac{h}{R} \tag{4.4}$$

in which Z_b is the bed level, A is the secondary flow direction coefficient, $f(\theta)$ is a function of the Shields parameter θ, h is the water depth and R is the radius of curvature. The secondary flow direction coefficient is defined as (De Vriend, 1977):

$$A = \frac{2\varepsilon}{\kappa^2}\left(1 - \frac{1}{2}\cdot\frac{\sqrt{g}}{\kappa C}\right) \tag{4.5}$$

in which $E_{spir} = \varepsilon$ a tuning parameter, κ is the von Kármán coefficient (~ 0.4), C is the Chézy coefficient and g is the acceleration due to gravity.

In Delft3D the function $f(\theta)$ is given by:

$$f(\theta) = A_{shld}\theta^{B_{shld}} \tag{4.6}$$

in which A_{shld} and B_{shld} are calibration parameters.
The function $f(\theta)$ can be approximated as (Talmon et al. 1995):

$$f(\theta) = 9\left(\frac{D}{h}\right)^{0.3}\sqrt{\theta} \tag{4.7}$$

in which D_{50} is the median grain size of the bed material.

In practice B_{shld} is taken equal to 0.5 (as in Talmon's formula). The parameter A_{shld} is used as tuning parameter. An initial guess follows often from the formula of Talmon. For the Rhine branches this yields a value between 0.5 and 1.

Eq.(4.5) indicates that via the axi-symmetrical solution, the transverse slope in bends depend on the calibration coefficient E_{spir} that affects the secondary flow direction coefficient A.

The axi-symmetrical situation described in Eq.(4.5) is hardly ever reached in natural rivers, since river bends are limited in length and do not have a constant radius of curvature. Moreover, transverse slopes tend to lag behind variation in flow conditions. Lateral redistribution of flow and sediment motion appears to be important for the bed development. The bed development in a bend is influenced by transitional effects due to a difference between the conditions upstream and those in the bend. The change of curvature induces a change in secondary flow. Transverse bed slope in a bend cannot be predicted solely from local conditions, since non-local effects due to the redistribution of flow and sediment in the first part of the bend can lead to a significant 'overshoot' of the lateral bed slope.

In addition to the above mentioned equilibrium solution, a damped wave is in fact superimposed on top of the equilibrium transverse slope. The dynamic behaviour that is induced with this wave is a function of the ratio between the adaptation length for water motion λ_w and sediment motion λ_s. This ratio is known as the interaction parameter IP ($IP=\lambda_s/\lambda_w$):

$$\begin{aligned}
\lambda_s &= \frac{f(\theta)}{\pi^2}\left(\frac{B}{h}\right)^2 \cdot h \\
\lambda_w &= \left(C^2/2g\right)\cdot h \\
IP &= \frac{\lambda_s}{\lambda_w} = \frac{A_{shld}\theta^{B_{shld}}}{\pi^2}\frac{g}{C^2}\left(\frac{B}{h}\right)^2
\end{aligned} \tag{4.8}$$

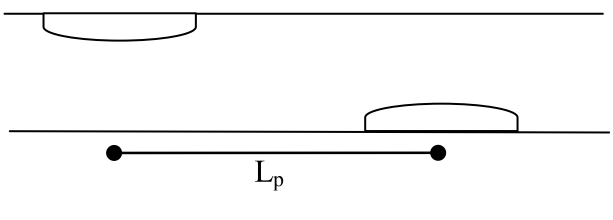

Figure 4.9 Schematic representation of a bar pattern.

So, the interaction parameter is a function of the width-depth ratio and the function for the transverse slope $f(\theta)$ (which includes the calibration parameter A_{shld}). From this, a streamwise wave length L_p (see Figure 4.9) and a damping length L_D can be derived. In Delft3D the wave lengths read:

$$\begin{aligned} \frac{2\pi}{L_p} &= \text{function}\left(IP, n, \lambda_w\right) \\ \frac{1}{L_D} &= \text{function}\left(IP, n, \lambda_w\right) \end{aligned} \tag{4.9}$$

Where L_p and L_D denote the streamwise wave length (length of the point bar) and damping length respectively. The smaller the damping length the closer the bank pattern evolves towards the axi-symmetrical solutions. Eq. (4.9) shows no dependence on the spiral flow direction coefficient A (and so E_{spir}). From this the following can be concluded:

- To tune on the length of the bars (i.e. the position of the crossings between bends) the calibration is restricted to parameter A_{shld} in $f(\theta)$. The position of the crossings between two opposite bend can be shown by plotting the longitudinal profile of the bed levels at the river axis, left and right of the river axis in one figure. This is first step in the calibration process.

After setting the value of parameter A_{shld} (yielding a good representation of the length of the point bar), we continue fine-tuning the amplitude of the bars (without changing the length) by changing calibration parameter E_{spir}. This is second step of the calibration.

Table 4.7 indicates how the parameters A_{shld} and E_{spir} affect the 2D bed deformation.

Table 4.7 Effect of the parameters A_{shld} and E_{spir}

	A_{SHLD}			E_{SPIR}		
	small λ_s/λ_w	λ_s/λ_w ~ the Waal	large λ_s/λ_w	small λ_s/λ_w	λ_s/λ_w ~ the Waal	large λ_s/λ_w
Impact on 2D pattern	-	+	+	-	-	-
Impact of the amplitude	+	+	+	+	+	+

In a strongly damped system with a small interaction parameter IP (e.g. the IJssel), the dynamic effects are suppressed. As a consequence, the free dynamic response does not develop. This means that the position and length of bars are hardly influenced by the dynamic behaviour, but approximates the axi-symmetrical solution. This implies that one can only affect the amplitudes of the bars. The length of the point bar then mainly depends on the local radius of curvature in the flow of the main channel.

In order to have a consistent calibration procedure, we perform the following two steps:

1. calibrate the 2D bar pattern and the location of the crossings with the calibration parameter A_{shld} (with E_{spir} equal to 1),
2. calibrate the bar amplitudes with the calibration parameter E_{spir}.

4.3 Results

4.3.1 One-dimensional morphological behaviour

Sediment budget

Section-averaged values of annual sediment transport derived from the simulation were found to be reasonable for all branches. Nonetheless, there is some deviation when it comes to the sediment distribution at Pannerdensche Kop; the model yields less sediment volume entering from the Waal and more entering to the Pannerdensch Kanaal. Table 4.8 shows a comparison between observed and simulated sediment budget. It is worth mentioning, however, that during calibration we give preference to better reproduction of bedform celerity over sediment budget, see next section.

Table 4.8 Sediment budget for the Rhine branches

River branch	Computed annual transport [m^3/yr]	Observed annual transport (Ten Brinke, 2001) [m^3/yr]
Bovenrijn	250 000 (in) - 480 000 (out) 390 000 (average)	577 000 (out)
Waal	350 000 (in) 410 000 (average)	507 000 (in)
Pannerdensch Kanaal	110 000 (in) – 110 000 (out) 107 000 (average)	70 000 (in) – 97000 (out)

Celerity of bed disturbance

Quantitative comparison between computed and observed bedform celerity, averaged over calibration period, is depicted in Figure 4.10. Cross-section-averaged values derived from simulation were found to be reasonable for all branches, except for the celerity in the Pannerdensch Kanaal which seems to be underestimated (around 0.65 km/year); this could be attributed to a gradual decrease in the flow velocity in the lower part of the Pannerdensch Kanaal (see Figure 4.11).

The comparison of spatial variation of cross-section-averaged bedform celerity is depicted in Figure 4.12, Figure 4.13 and Figure 4.14. It shows that for all river reaches the celerity estimated from measurements has large variations. The calculated celerity for the Bovenrijn (Figure 4.12) and the Waal (Figure 4.13) is very well within the range of variation of the measured celerity. For the Pannerdensch Kanaal, although the sediment budget is close to the observations, it is clear that the calculated celerity is lower than the estimated one; we don’t have a clear reason for this deviation.

The results of the trench migration simulations can be seen in Figure 4.15 to Figure 4.19. These plots give a local estimate of the trench migration speed. Note that the celerity in the lower Waal gradually decreases due to the gradual decrease in flow velocity in that part. It is to be noted that present model does not include any tidal influence in the downstream of lower Waal.

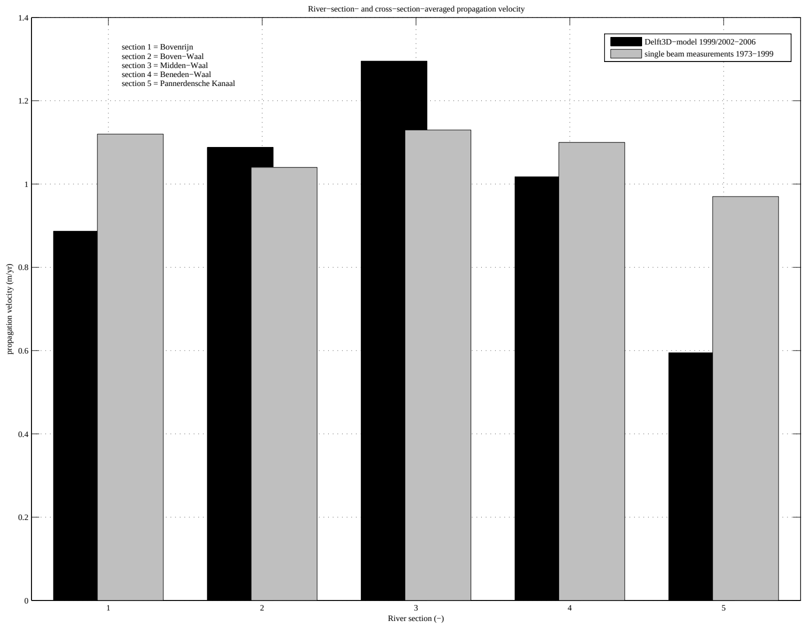

Figure 4.10 Comparison on river-section- and cross-section-averaged bed form celerity in all branches.

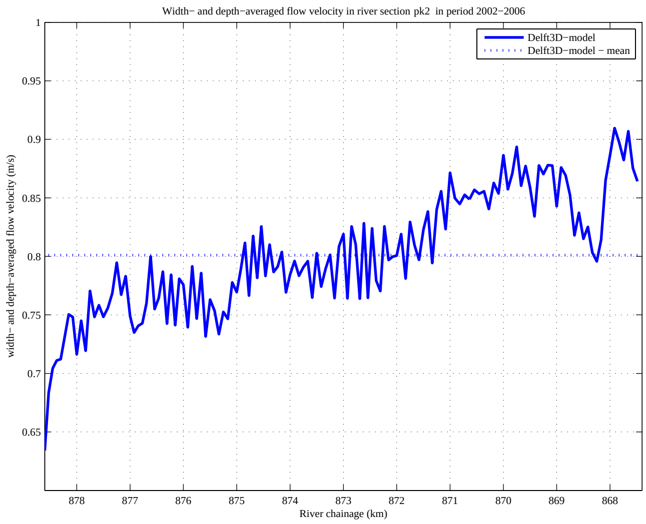

Figure 4.11 Simulated width- and depth-averaged velocity profile along the Pannerdensch Kanaal.

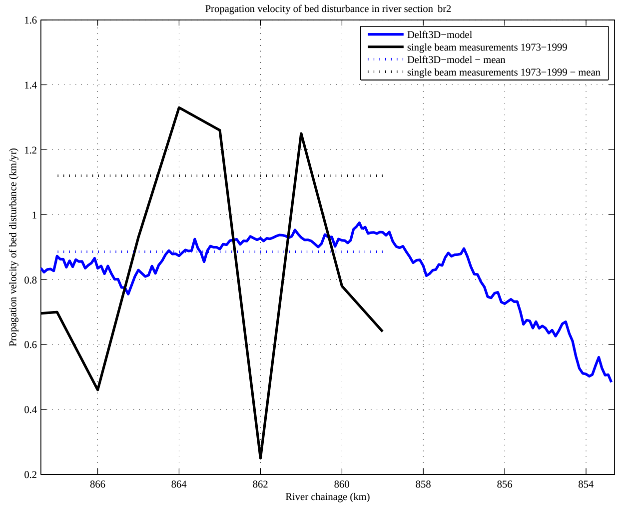

Figure 4.12 Celerity of bed disturbance in the Bovenrijn derived from simulation result and measurement.

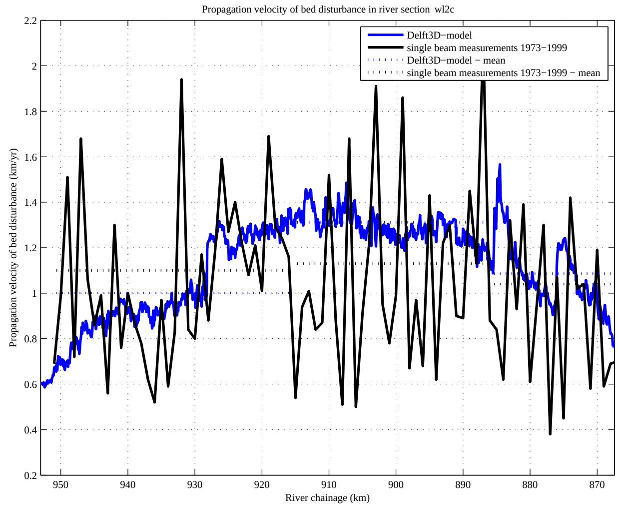

Figure 4.13 Celerity of bed disturbance in the upper Waal derived from simulation result and measurement.

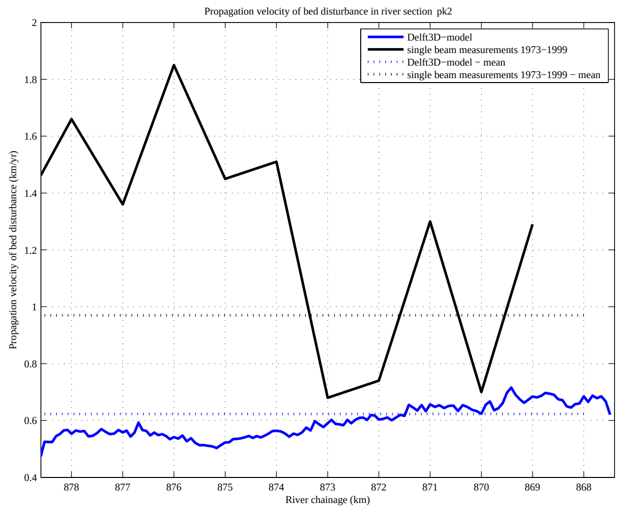

Figure 4.14 Celerity of bed disturbance in the Pannerdensch Kanaal derived from simulation result and measurement.

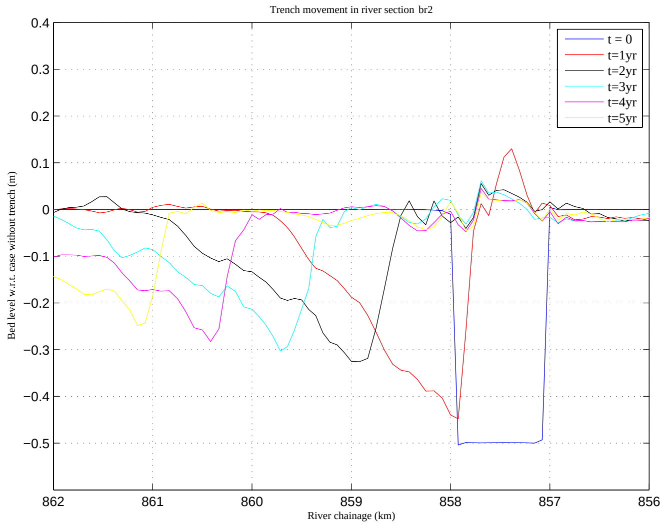

Figure 4.15 Propagation of trench located in a randomly selected reach of the Bovenrijn

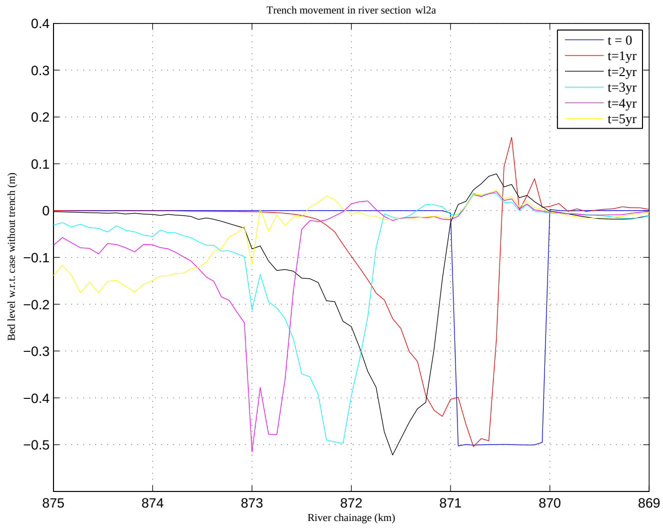

Figure 4.16 Propagation of trench located in a randomly selected reach of the upper Waal

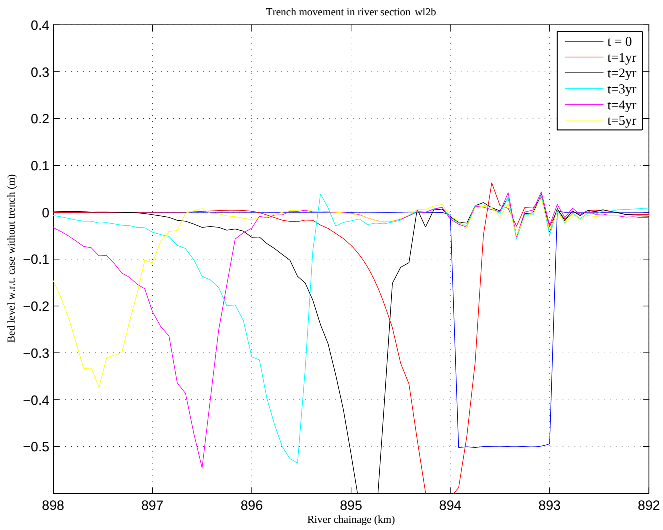

Figure 4.17 Propagation of trench located in a randomly selected reach of the middle Waal

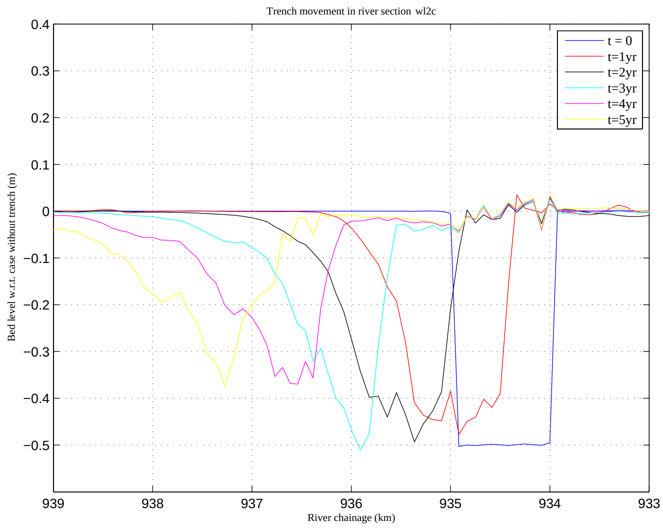

Figure 4.18 Propagation of trench located in a randomly selected reach of the lower Waal

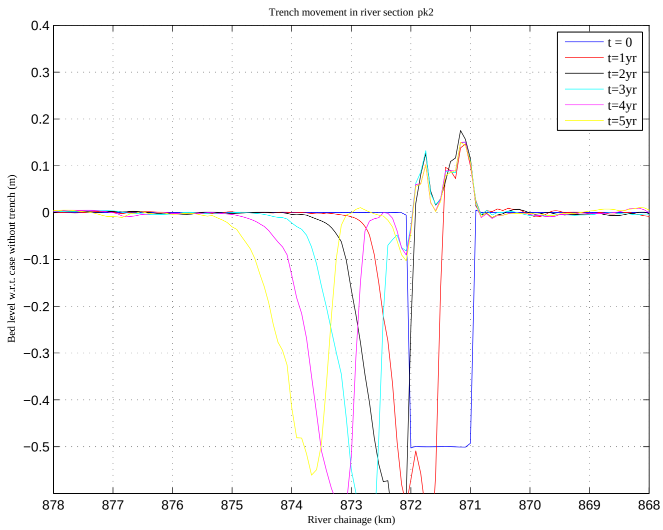

Figure 4.19 Propagation of trench located in a randomly selected reach of the Pannerdensch Kanaal

Annual bed level changes

The model ability to predict cross-section-averaged bed level changes are evaluated in comparison to bed level changes estimated from measurements. Figure 4.20 gives an impression of yearly-averaged bed level changes in some river sections. Spatial variation of cross-section-averaged bed level changes are given in Figure 4.21 to Figure 4.27; for the Waal, figures are depicted by separating five different reaches for clarity (indicated by river section-1 to 5 respectively). For the sake of comparison, bed level changes derived from the single-beam measurement are also included in the plots.

The results show good agreement between the calculations and the multi-beam measurements; with some discrepancy in the most upstream part of the Waal (Figure 4.22). This maybe attributed to the dredging activities conducted in this region during 2000. Similar behaviour can be seen in the most downstream part of the Waal (Figure 4.26). That can be attributed to the tidal influence in this region, which is not considered by the model.

It is worth mentioning that the result in the Pannerdensch Kanaal given in Figure 4.20 indicate no bed level changes. However, from Figure 4.27 we can see that there are some changes that indeed average to zero. The behaviour of the Pannerdensch Kanaal as seen in the later figure indicate that the modelled bed level changes has the same order of magnitude as found in the multi-beam measurements.

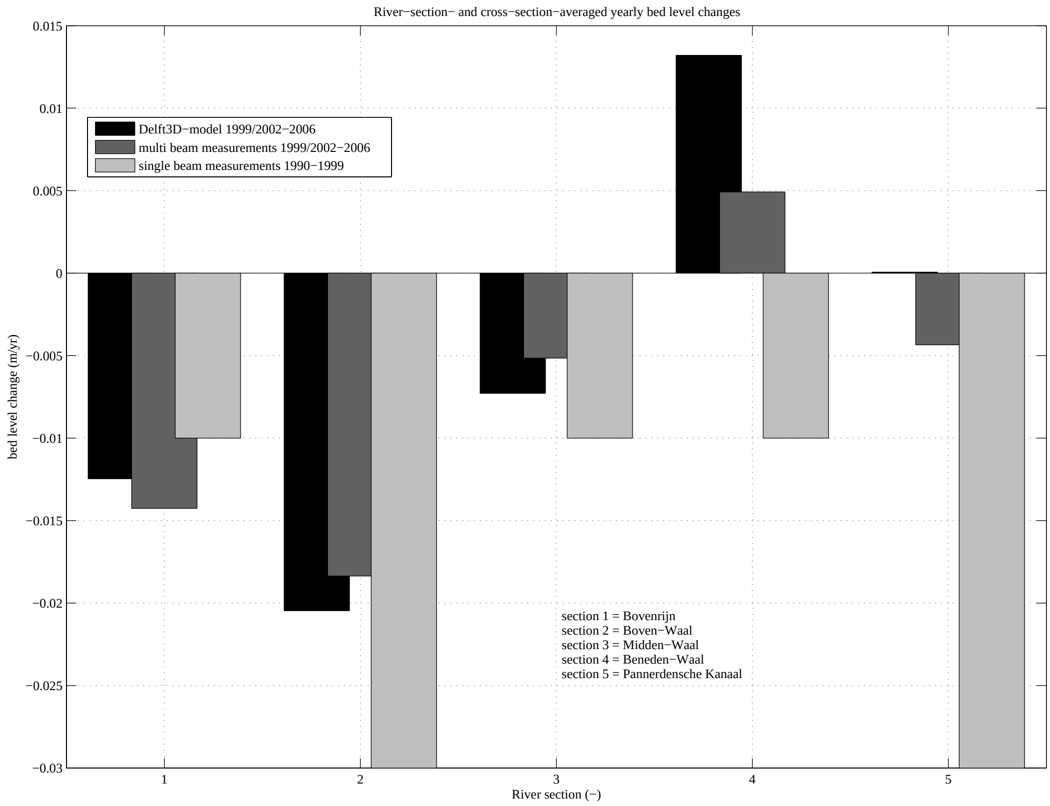

Figure 4.20 Comparison of cross-section-averaged annual bed level changes in river sections

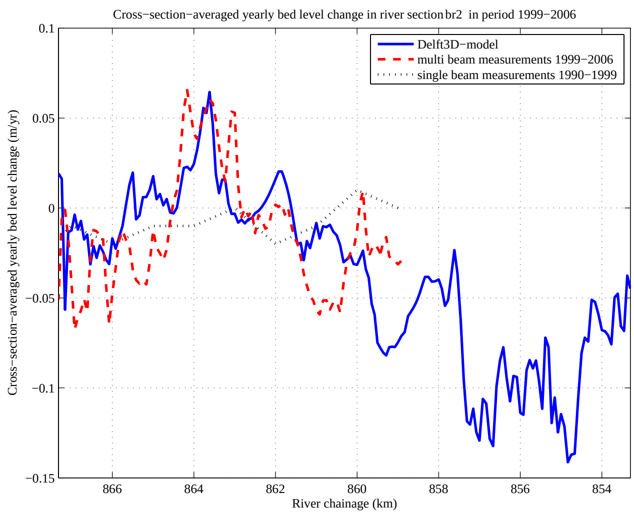

Figure 4.21 Longitudinal profile of cross-section-averaged annual bed level changes in the Bovenrijn: comparison of simulation result with multi-beam and single-beam measurement

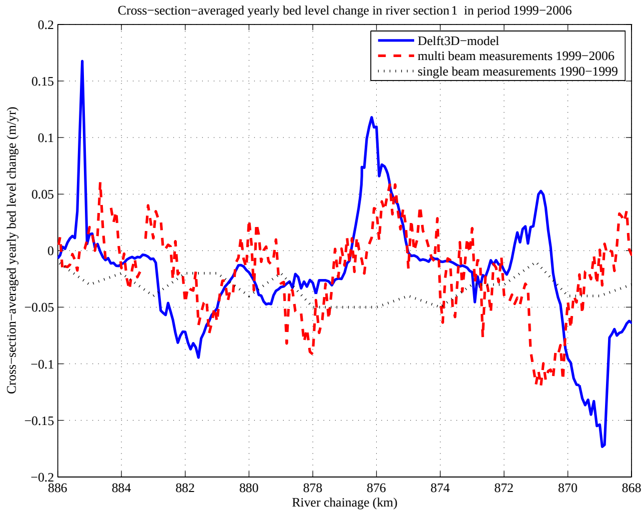

Figure 4.22 Longitudinal profile of cross-section-averaged annual bed level changes in the Waal section 1

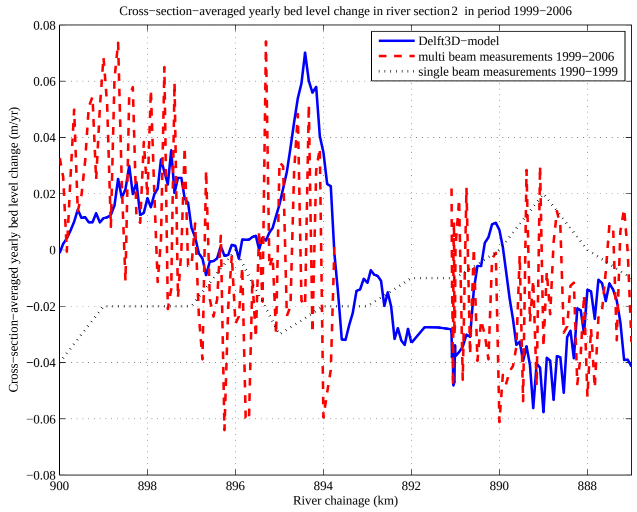

Figure 4.23 Longitudinal profile of cross-section-averaged annual bed level changes in the Waal section 2

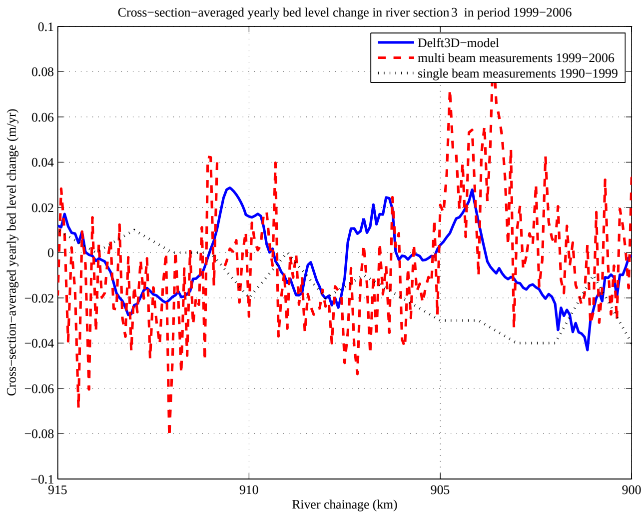

Figure 4.24 Longitudinal profile of cross-section-averaged annual bed level changes in the Waal section 3

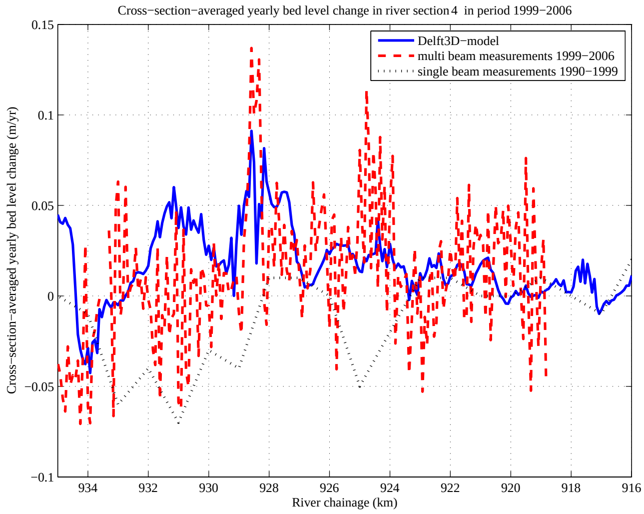

Figure 4.25 Longitudinal profile of cross-section-averaged annual bed level changes in the Waal section 4

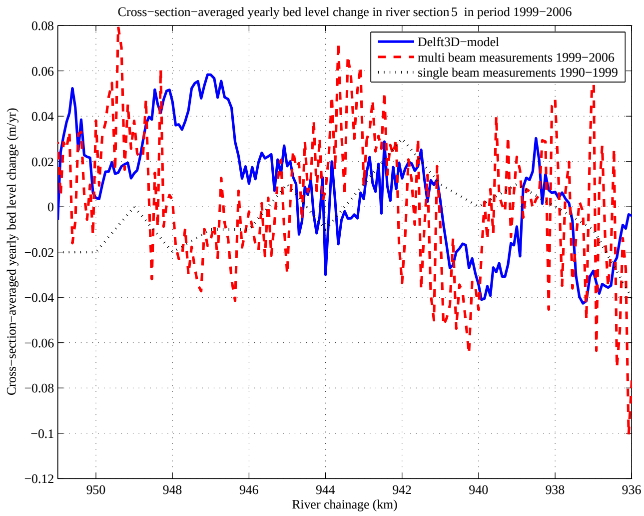

Figure 4.26 Longitudinal profile of cross-section-averaged annual bed level changes in the Waal section 5

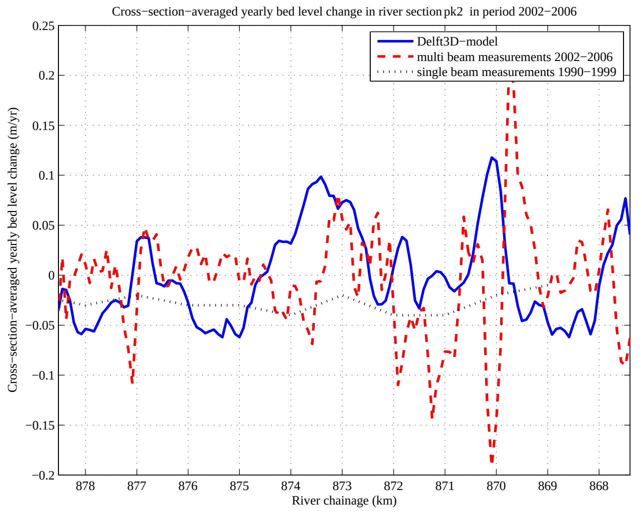

Figure 4.27 Longitudinal profile of cross-section-averaged annual bed level changes in the Pannerdensch Kanaal

Time-averaged bed level gradient

The model ability to predict time-averaged bed level gradients are evaluated in comparison to the measurements. Figure 4.28 gives the comparison between calculated and measured, single- and multi-beam values for cross-section-averaged bed level gradient in all branches. Spatial variation of cross-section-averaged and time-averaged bed level gradient are given in Figure 4.29 to Figure 4.35. The model yields acceptable result for all branches the results has a better agreement with the multi-beam measurements.

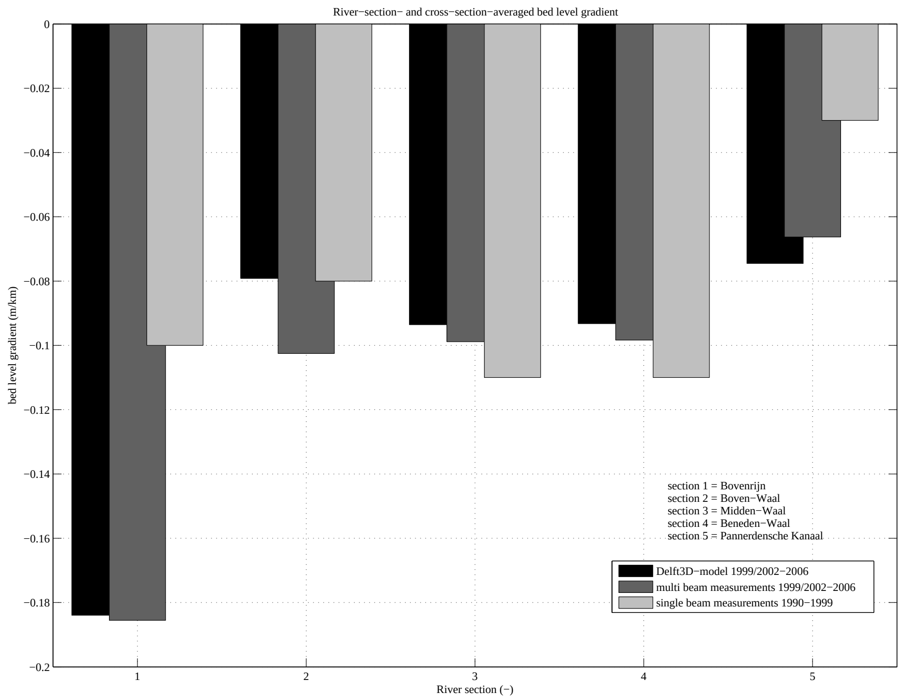

Figure 4.28 River section- and cross-section-averaged bed level gradient at different river sections

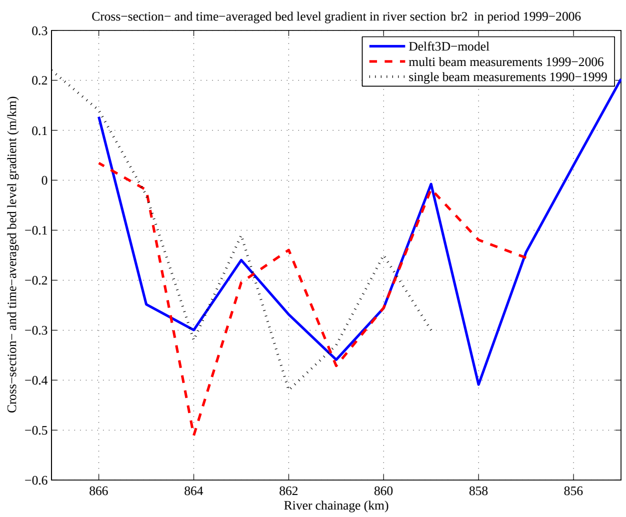

Figure 4.29 Cross-section- and time-averaged bed level gradient in the Bovenrijn

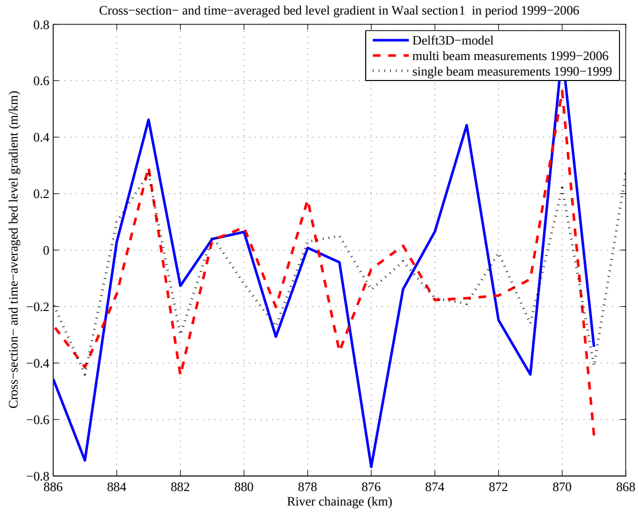

Figure 4.30 Cross-section- and time-averaged bed level gradient in the Waal (section-1)

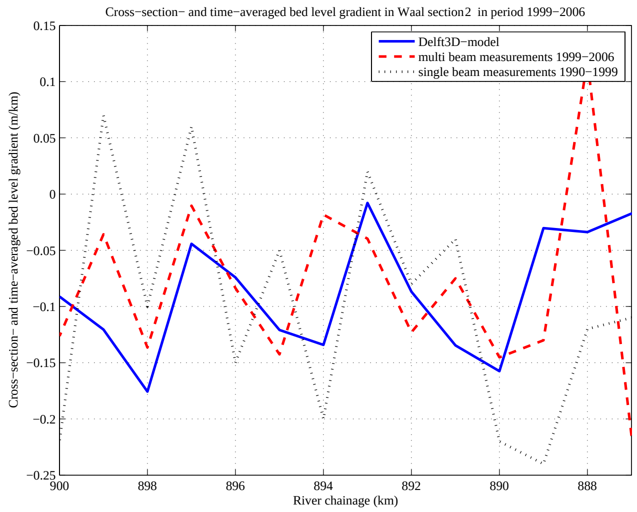

Figure 4.31 Cross-section- and time-averaged bed level gradient in the Waal (section-2)

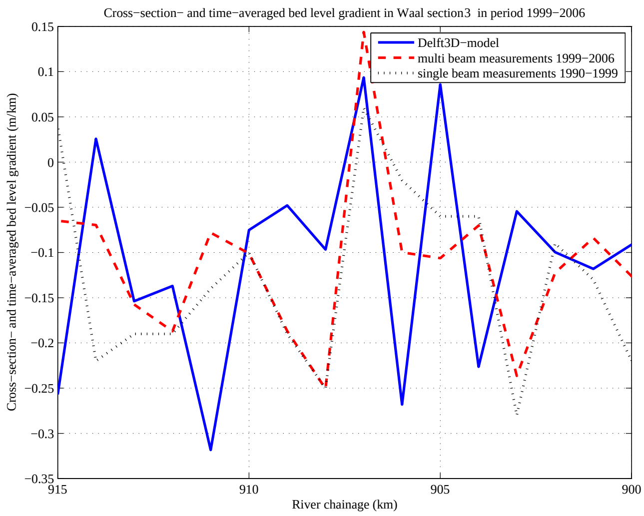

Figure 4.32 Cross-section- and time-averaged bed level gradient in the Waal (section-3)

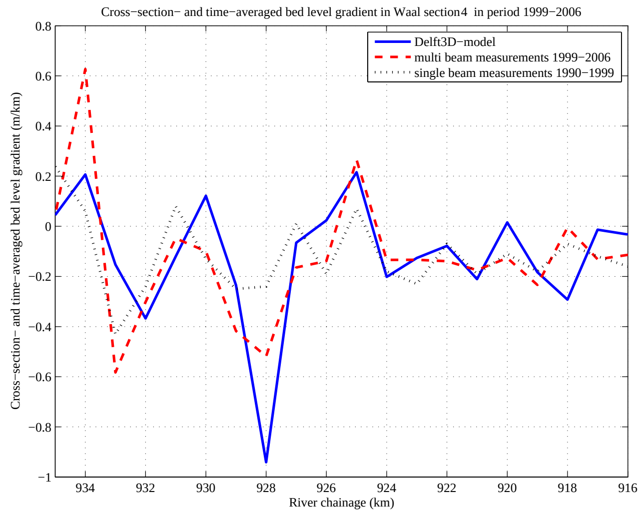

Figure 4.33 Cross-section- and time-averaged bed level gradient in the Waal (section-4)

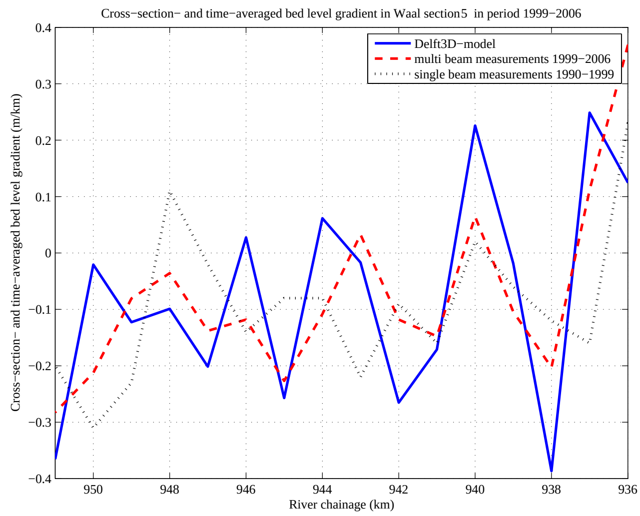

Figure 4.34 Cross-section- and time-averaged bed level gradient in the Waal (section-5)

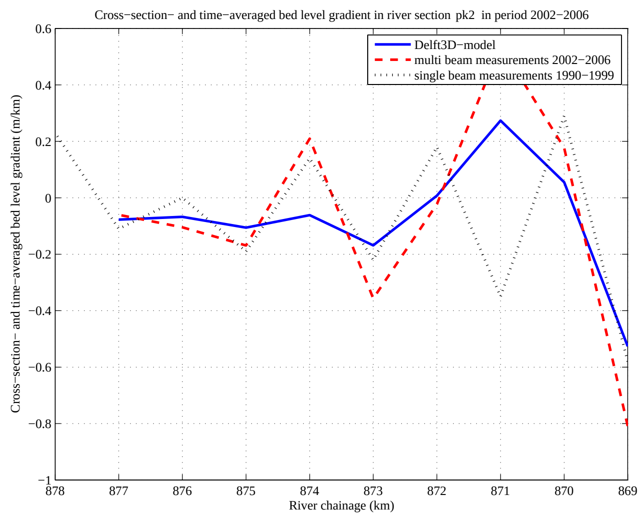

Figure 4.35 Cross-section- and time-averaged bed level gradient in the Pannerdensch Kanaal

4.3.2 Two-dimensional morphological behaviour

Parameter settings

As described in previous Section 4.2.4, the 2D bar pattern and the location of the crossings can be tuned by using the calibration parameter A_{shld}. For the sake of completion, the impact of calibration parameter A_{shld} on the 2D bar pattern and location of crossings for all branches is given in Appendix B.

Based on several simulations, we selected a reasonable value of parameter A_{shld} for each branch (see

Table 4.9). The average value of A_{shld} derived empirically by using Eq. (4.7) was compared with the selected values. A conventional value of parameter B_{shld} was taken, namely 0.5 for all branches.

Table 4.9 Parameter A_{shld} for the Rhine branches

River branch	A_{shld} (Simulation)	A_{shld} (Empirical)
Bovenrijn	1.1	0.9
Waal	0.7	0.7
Pannerdensch Kanaal	0.95	0.7

We tested three different values of this parameter, we finally selected E_{spir}=1.0 for all branches.

Bar pattern

For the final parameter settings the amplitudes and locations of crossings of the bars can be evaluated from Figure 4.36 to Figure 4.38. Moreover, , the bar pattern at different locations can be assessed from Figure 4.39 to Figure 4.41 for all branches. Comparison was made for the period of 7 years for the Bovenrijn and the Waal, and for the period of 4 years for the Pannerdensch Kanaal as the multi-beam measurement data is available only for the period of 2002-2006 for the Pannerdensch Kanaal.

Bar amplitude

Parameter E_{spir} results in an amplification of bar height as it has an effect on the steepness of transverse bed slope. Three different values of this parameter, namely 1, 1.2 and 1.4, and finally selected E_{spir}=1.0 for all branches. Result with the selected E_{spir} can be seen in the same figures as above (Figure 4.36-Figure 4.41). Additional results that show the effect of this parameter are illustrated in Appendix B.

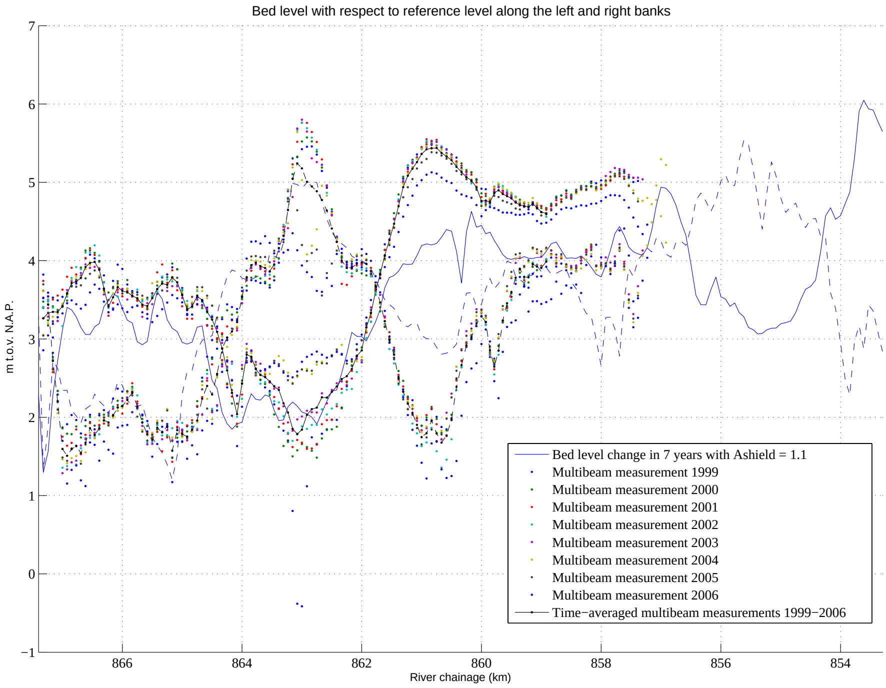

Figure 4.36 Bed changes with respect to the reference level along the left and right bank of the Bovenrijn

Figure 4.37 Bed changes with respect to the reference level along the left and right bank of the Waal section-1

Figure 4.38 Bed levels with respect to the reference level along the left and right bank of the Pannerdensch Kanaal

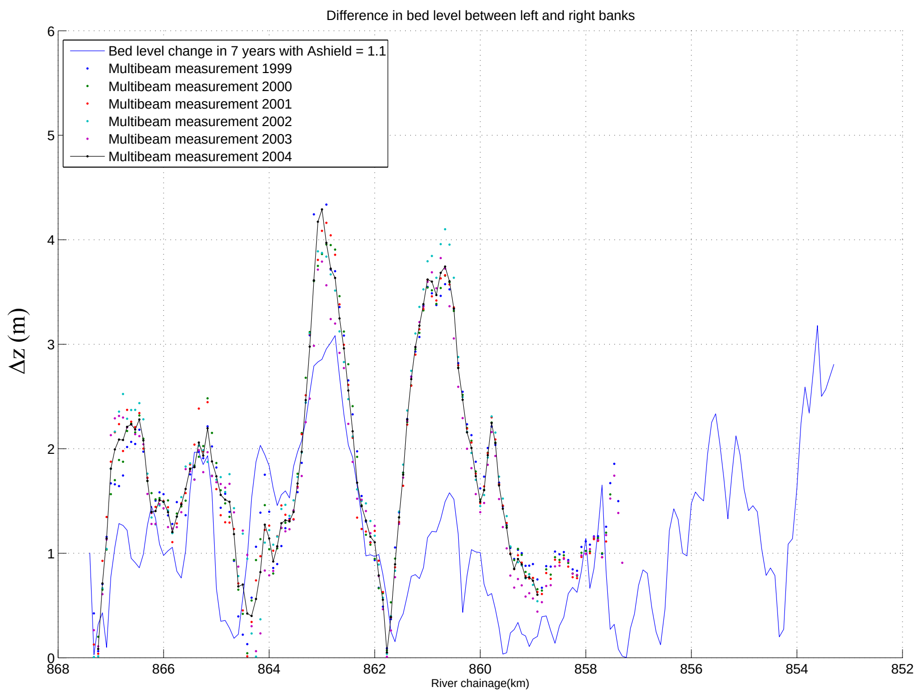

Figure 4.39 Difference in bed level between left and right bank of the Bovenrijn

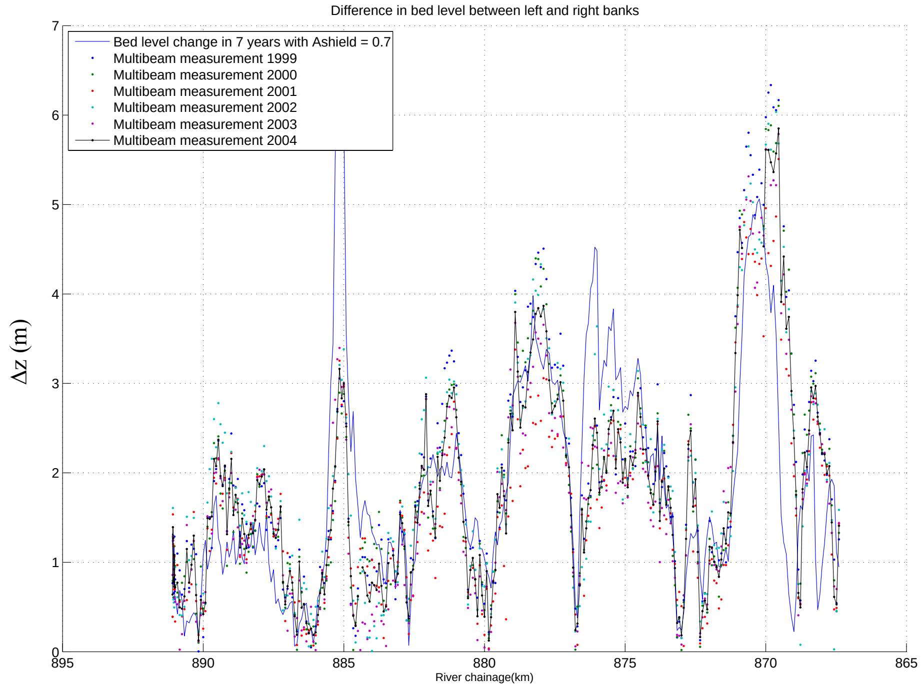

Figure 4.40 Difference in bed level between left and right bank of the Waal section-1; see Appendix B for Waal sections 4 to 5.

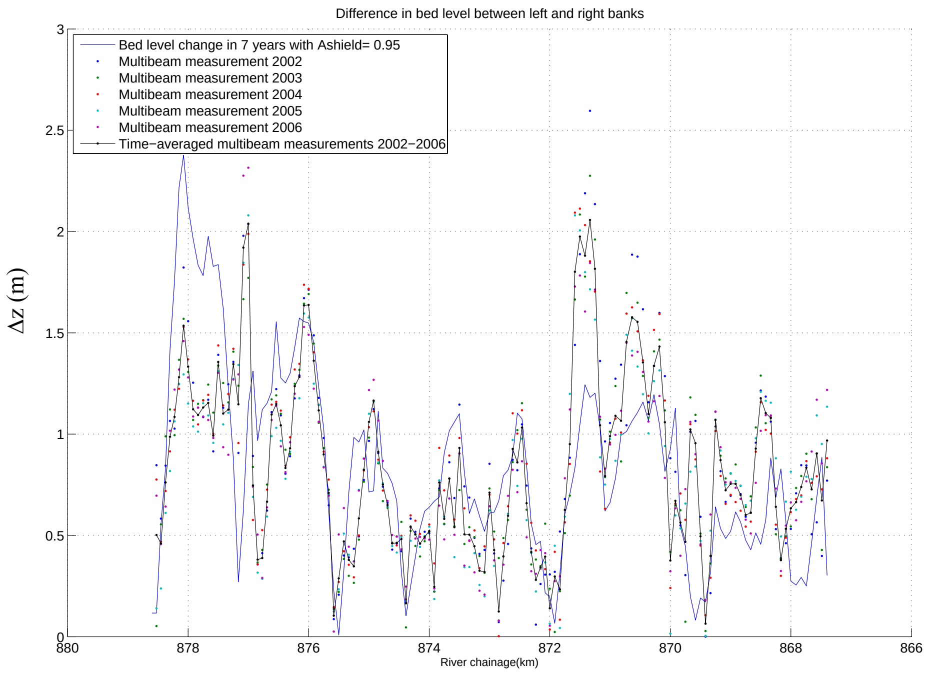

Figure 4.41 Difference in bed level between left and right bank of the Pannerdensch Kanaal

4.4 Discussion and conclusions

4.4.1 Parameter settings of transport formula

- The value of the critical Shields parameter (θ_{cr}) that was selected appears to be rather low as we preferred a lower value of θ_{cr} in combination with a low overall transport parameters α_{bed} and α_{sus}. We tested relatively higher value of θ_{cr} (still lower than conventional value of 0.047) and α_{bed}, which also appeared to be acceptable for the reaches noticeably with the higher flow velocities. However, observations have shown the occurrence of transport during low flows (Frings, 2005). It should be noticed that the low discharge period covers 60% of total duration. Since the model includes the uniform sediment approach, it is obviously unable to treat the problem associated with transport process of graded sediment with the transport of fine materials during lowest discharge. Consequently, we are bound to adapt a decrease of the critical Shields value in order to get close to the observed behaviour particularly in the Pannerdensch Kanaal.

4.4.2 1D morphological behaviour

- With respect to the annual sediment transport at the bifurcation, the model shows some inconsistency with the observation of Ten Brinke (2001) on the sediment transport entering to the Waal and the Pannerdensch Kanaal. The model underestimates the sediment transport entering into the Waal and overestimates the amount entering into the Pannerdensch Kanaal. The reason behind this could be that the consideration of the sediment coarsening in the lower part of the Bovenrijn (near the right bank) towards the Pannerdensch Kanaal seems to be still improper; thereby the model is unable to replicate properly the sediment transport in the bifurcation. However, further coarsening of the sediment diameter in this region (right bank at the end of the Bovenrijn and upstream part of the Pannerdensch Kanaal) yields a lower celerity of bed disturbances in the Pannerdensch Kanaal. Preference is given to the proper reproduction of celerity.

- With respect to the celerity, on the other hand, the calculated celerity in the Pannerdensch Kanaal is still rather low. In the lower part of the Pannerdensch Kanaal, there is a gradual decrease in flow velocity, the reason behind which is still unclear. This decrease in flow velocity resulted in a rather low celerity of bed disturbance. We attempted to force the model to get it right by decreasing further the grain size; however it did not produce much effect in this particular reach. An identical behaviour can be observed in the lower part of the Waal, where the bed form celerity seems to decrease rapidly. That can also be attributed to the low flow velocity in that region.

- The model result for cross-section-averaged annual bed level change shows rather consistent trend in comparison with the multi-beam measurement except for a part of the lower Waal and some regions in the Pannerdensch Kanaal.

- The cross-section and time-averaged annual bed level changes along the reaches also show rather consistent features in comparison with the multi-beam measurement.

4.4.3 2D morphological behaviour

- With respect to the 2D morphological behaviour, the model result for all branches shows good agreement with the multi-beam measurements. Nonetheless, some noticeable inconsistency still exists, for instance, in the middle part of the Bovenrijn the model severely underestimated the bar height in both bends. This can be slightly improved by using a higher value of A_{shld}, though it does not appear to have a significant influence. The same problem seems to occur in the middle part of the Pannerdensch Kanaal. We attempted to influence it by changing calibration parameters. However, it did not offer any significant change. On the whole, the model results show acceptable trend of 2D morphological pattern in terms of the bar-pool and crossings locations as well as the bar amplitude in comparison to the measurements.

4.4.4 Conclusion

- As a whole, model performance appears to be reasonable for the quantitative evaluation of 1D and 2D morphological behaviour considering the implementation of a single sediment transport formula with a single parameter setting for all three branches.

- It appears that a number of problems associated with the morphological calibration originates from the hydrodynamic characteristic of the Rhine branches particularly in some specific regions that cannot be handled properly merely on the basis of the parameter settings or the adjustment in the spatial distribution of median grain size. Some local effects appear to play a dominant role for the morphodynamic behaviour in these regions, particularly in the Pannerdensch Kanaal and the lower part of the Waal. It is of significance to have a careful look at these problems. Consideration of graded sediment process and tidal influence seems to be of significance to improve the model performance.

5 Morphological calibration for dredging activities

5.1 Introduction

The main reason for the development of the advanced 2-D morphodynamic model of the Dutch Rhine branches is to come up with an instrument that enables river managers to:

- investigate the impact of climate change and long-term morphology on the river's navigability, and
- evaluate river intervention measures to keep the Rhine navigable

Intervention measures are divided into two groups
1- Interventions in the sediment budget by means of dredging and dumping (sediment management); and
2- re-normalisation measures, e.g. semi-fixed layers in deep bends, movable groynes or longitudinal dams. Since the large-scale 19^{th} and 20^{th} century normalisations, the river manager uses dredging as a structural means of maintaining and improving the navigation conditions.

This chapter discusses the performance of the calibrated DVR model of the previous chapter with respect to the predictability of dredging activities. The focus is primary on dredging activities in the Waal.

Section 5.2 describes the model preparation and the calibration procedure used to fine-tune on the amount of maintenance dredging carried out in the period between 2000 and 2006. We address the sensitivity of dredging volumes to 1) the presence of bed forms that easily form nautical bottlenecks, 2) the dimensions of the navigation channel, and 3) the dredging & dumping strategy. Results are presented and discussed in Section 5.3. Conclusions and recommendations follow in Section 5.4.

5.2 Method

5.2.1 Model preparation

Calibration period

The calibrated DVR model of the previous chapter is used as a starting point for the calibration of the dredging activities. Since the calibration on dredging focuses on the River Waal, the model of the Waal domain is used in a standalone mode. The calibration period of the morphological calibration processes is 1999 to 2006. Since dredging data are available for that period, the same calibration period is taken for the calibration of dredging activities.

Boundary conditions

For the morphodynamic calibration a schematisation of the discharge time series at the upstream boundary of the Bovenrijn was derived from daily discharge data in the period 1999-2006. The focus of the calibration on dredging is on the predictability of yearly averaged dredging volumes in this period. This justifies the use of a representative discharge hydrograph of this period.

The discharge hydrograph at the upstream boundary of the Waal, viz. the Pannerdesche Kop, is derived from a hydrodynamic simulation using the calibrated DVR model including all model domains. The water levels at the downstream boundary are computed with the following relation:

$$h_{\mathrm{Waal,\ kmr\ 953}} = \left(\frac{Q_{\mathrm{Waal}}}{1500}\right)^{0.95} - 0.1 \qquad (5\text{-}1)$$

in which Q_{Waal} is the discharge level at the upstream boundary.

Table 5.1 presents the upstream and downstream boundary conditions of the Waal model that are used in the calibration.

Table 5.1 Upstream and downstream boundary condition in the Waal model.

Time [days]	Discharge level at the upstream boundary [m^3/s]	Water level at the downstream boundary [m + NAP]
30	2067	1.26
8	2918	1.78
14	3905	2.38
8	2918	1.78
86	2067	1.26
219	1297	0.77

The upstream morphological boundary condition of bed level degradation was set at a rate of 2 cm/year.

Schematisation of dredging activities

The criteria for the dimensions of the navigation channel in the Waal specify that a navigation channel width of 150 m and depth of 2.8 m is guaranteed during 95% of the time. Tell recently, the depth criterion was only 2.5 m but it was increased to 2.8 m. The discharge which is exceeded during 95% of the time is known as ‘the agreed low-water discharge’ (OLA) and is defined to have a value of 1020 m^3/s at Lobith. This value is updated every 5 years. The corresponding water level, known as ‘the agreed low-water level’ (OLR), is used as a reference water level that corresponds to the OLA discharge. In the low flow season, the navigation channel dimensions are tested against the set criteria and dredging takes place when and where necessary. In order to improve the navigability, an increase of the navigation channel dimension from 150 m to 170 m width is planned.

Yossef et al. (2006) and Mosselman et al. (2007) describe the dredging and dumping functionality in Delft3D. The following model settings were used:

1. For computing dredging volumes the navigation channel dimensions were set at 150 m width by 2.5 m depth. The client provided a *shape file* indicating the course of this navigation channel (indicated by the red lines in Figure 5.1). The navigation channel is positioned in the deeper outer bends that alternately turn from the left to the right side and back of in the main channel of the sinuous Waal. Dredging is purely restricted to this navigation channel. For a proper registration of the dredging activities the *shape file* is split into km-blocks. When dredging takes place, a clearance depth of 0.3 m is added on top of the required dredging depth.

2. Deposition of the dredged material occurs 2 to 7 km upstream of the dredge location, between the normal lines indicating the boundaries of the main channel. The client also provided a *shape file* indicating the main channel (indicated by the blue lines in Figure 5.1). In principle it is possible to dump the dredged material in the navigation channel, as long as the dimensions are fulfilled. Obviously, the dredged volume is only deposited at locations that have sufficient depth (including the clearance depth of 0.3 m). In accordance with dredging, the *shape file* indicating dumping locations is also split into km-blocks. The dredge-km blocks are linked with the dump-km blocks, positioned 2 to 7 km upstream. The dredged volume is deposited in the first available location. If it is not possible to dump the entire volume in one go in a km-block, the remainder is dumped in the following km-block available.

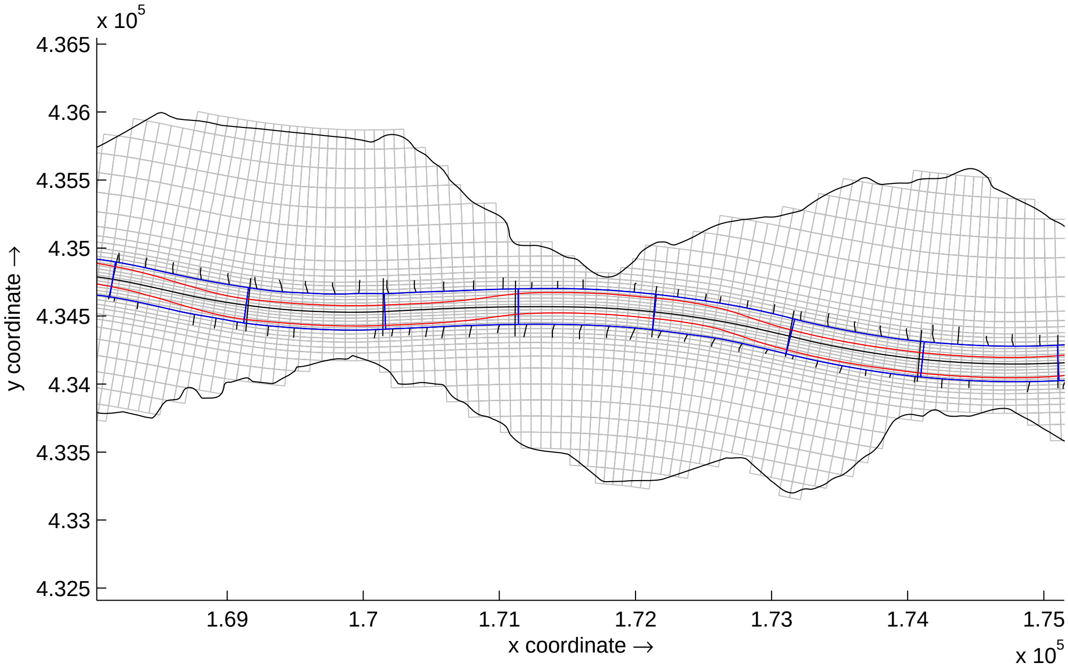

Figure 5.1 Example of shape files indicating the dredging (red lines) and dumping (blue lines) area in a subsection of the Waal.

3. Dredging activities are restricted to the low-water period with a discharge of 1297 m^3/s and take place instantaneously. At every time step during the low-water period, the necessity of dredging is assessed. No use is made of discharge predictions to anticipate future shoals.

4. The OLA discharge of 818 m^3/s (Waal discharge), for a duration of 6 hours, is added to the discharge time series given in Table 5.1. This discharge level corresponds with the OLA of 1020 m^3/s in the Bovenrijn at Lobith. The discharge level is added to enable an update of the OLR that may change due to morphodynamic changes during the simulation period. The OLA of 818 m^3/s in the Waal goes along with an OLR of 0.27 m + NAP at the downstream boundary of the model.

Agreed low-water level (OLR)

The OLA and hence the OLR are officially updated every five years. The present OLR dates back to 2002. Mosselman et al. (2007) indicate that an un-calibrated version of the DVR model overpredicted the OLR with more than 25 cm. As a consequence an under-prediction of the estimated dredging volumes follows.

In Chapter 3 of this report the DVR model was hydraulically calibrated for the measured low-water period of 2003, in order to improve the OLR prediction. To that end, the calibration parameter A in the alluvial roughness predictor of Van Rijn has been changed. This roughness predictor reads as follows:

$$k_s = A \cdot h^{0.7}\left(1 - e^{-B \cdot h^3}\right) \qquad (5\text{-}2)$$

Figure 5.2 shows the difference between the official OLR2002 and the OLR derived from a simulation with the un-calibrated DVR model and the calibrated hydraulic model. The figure indicates that this difference is still large after the hydraulic calibration, up to 0.35 m. This is remarkable, especially when considering the small difference between the water level computations and measurements during the low-water event of 2003, see Figure 5.3.

This can be explained as follows. The official OLR2002 is a statistically derived water level, viz. a water level that is exceeded during 95% of the time. This implies that the OLR does not represent the ‘actual’ back-water curve present during a low-water event such as in 2003. The hydraulic calibration was focussed on the back-water curve observed during the low-water event of 2003. As a consequence the OLR derived with the calibrated hydraulic model strongly deviates from the official OLR2002.

The OLR2002 is officially used for dredging purposes. Therefore, more preference is given to the prediction of the OLR than to the prediction of the low-water levels. In order to obtain a better prediction of the OLR, a new parameter setting was derived, see Table 5.2. As indicated in Figure 5.2, when it comes to OLR prediction, the model with new parameter setting performs much better than the calibrated hydraulic model. The differences between the official OLR and the computed OLR are at most 0.1 m. Obviously, this model with the modified parameter settings performs less well for the low-water event of 2003, see Figure 5.3. The model with the modified settings will be used in this chapter for the OLR calculations.

Table 5.2 Parameter setting of parameter A in the alluvial roughness predictor.

Traject	Parameter A – hydraulic calibration	Parameter A – modified setting for OLR calculation
Pannerdensche Kop - Nijmegen	0.06	0.03
Nijmegen - Tiel	0.05	0.04
Tiel – Zaltbommel	0.025	0.04
Zaltbommel – Vuren	0.005	0.04
Vuren – end of the Waal	0.005	0.04

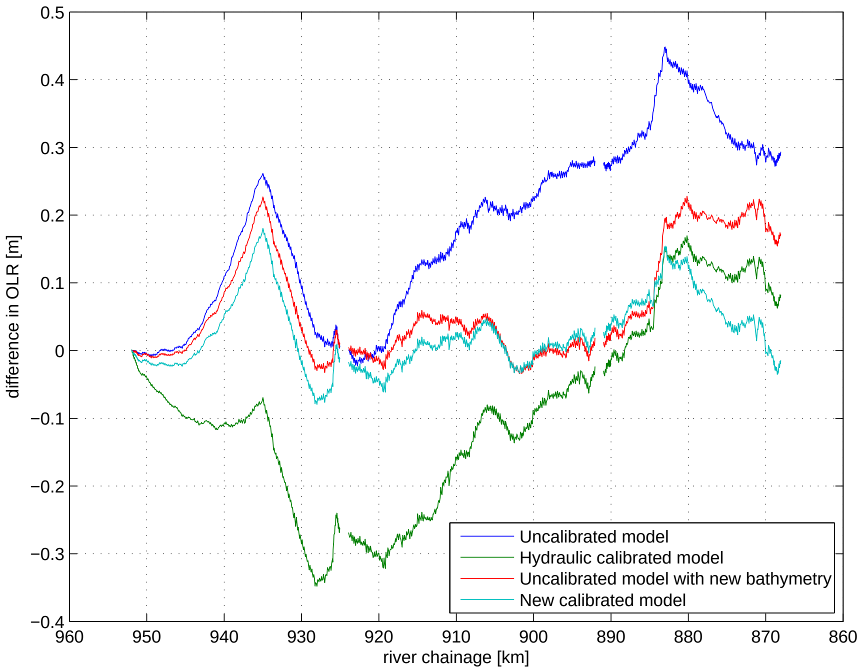

Figure 5.2 Difference between the official OLR2002 and the OLR derived from model simulations.

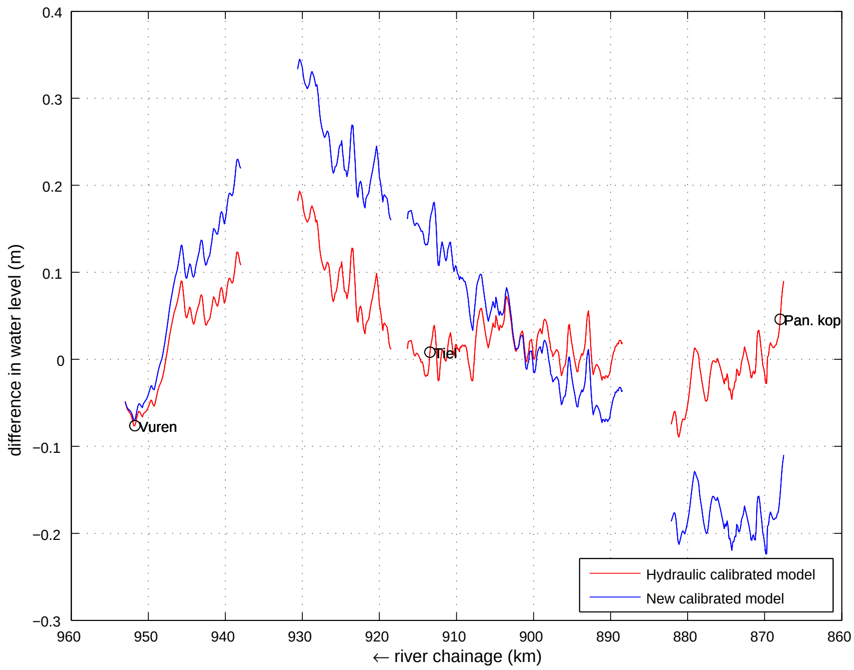

Figure 5.3 Difference between the water levels computations and measurements during the low-water event of 2003.

5.2.2 Calibration procedure

Quantities for calibration

The focus of the calibration is on the following quantities:

- dredging volumes
- dredging & dumping locations

Calibration data set

In the 19th and 20th century large amounts of sand were extracted from the river and probably, only part of that reported. In 1935, a first regulation was introduced which gave license-holders the permission to dredge certain amounts of sediment. Measures to further reduce the dredging activities were implemented in 1974. In 1991 a new dredging policy was adopted, prescribing that net extraction of sediment was no longer allowed. Dredging for navigation channel maintenance was permitted, but in conformity with the new policy, the dredged volume has to be deposited elsewhere in the river.

For calibration purpose, two data sets were used. The first set covered the dredging activities in the period 2000-2002 and the second one covered the period 2005-2006. Figure 5.4 shows the dredging volumes in the Waal during these periods.

The dredging activities in Figure 5.4 can be split in two categories:

- Structural dredging activities that are induced by geometry of the river, for instance at the sharp river bends near Hulhuizen (km 870), Erlecom (km 875), Haalderen (km 880), Nijmegen (km 885) and St. Andries (km 928).
- Incidental dredging activities which is related to the removal of bed forms that are developed during high water conditions forming nautical bottlenecks in the low-water period (mainly in the Midden Waal in the reach between km 887-915).

In both data sets the criteria for navigation channel dimensions were the same (150 m wide and 2.5 m deep). However, Figure 5.4 shows that the dredging volumes differ between the two periods. The dredging volumes in the period 2005-2006 are much lower than in the period 2000-2002. This difference cannot be explained by differences in morphological behaviour in response to different discharge hydrographs (see Figure 5.5). The reason of this difference is perhaps related to the difference in applying the dredging strategy as described by the contracts with dredging companies.

In the period 2000-2002, according to the dredging specifications, every year after the high-water season the navigability was checked when the discharge at Lobith drops below 3000 m^3/s. The agreed low-water reference level was then projected on the actual state of the river, whence the actual dimensions of the navigation channel can be derived. If the requirements were not met, dredging took place. An extra clearance on top of the required depth of approximately 0.3 m was accounted for. If the discharge dropped below 2000 m^3/s at any time during the dry season, another check is carried out.

In the period 2005-2006, dredging took place according to a performance-contract with a dredging company. The exact dredging procedure was not prescribed. The only requisite was to maintain the navigation channel requirements of 150 m by 2.5 m during discharges above a threshold value of 1020 m^3/s. This gave the dredging companies more flexibility to decide when to start dredging and what clearance depth to take into account. In the low-water period, the minimum observed depth (MGD, *Minst Gepeilde Diepte*) is determined every day until the discharges become too high. If a dredging company fails to meet the required criteria, a fine is imposed. Apparently, under this contract, the dredger focused on the structural dredging locations near the river bends Erlecom, Haalderen, Nijmegen and St. Andries.

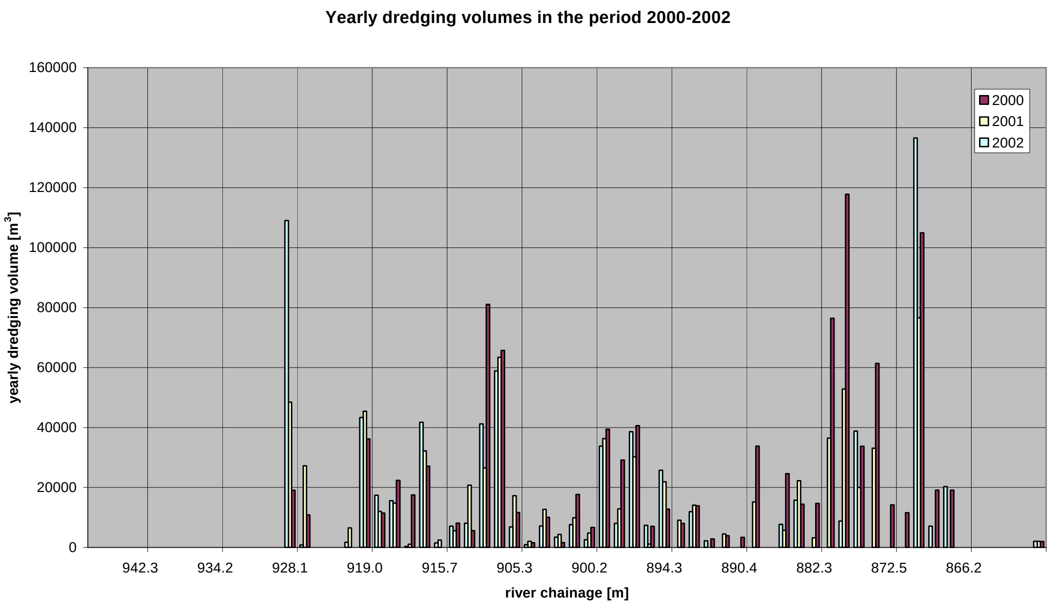

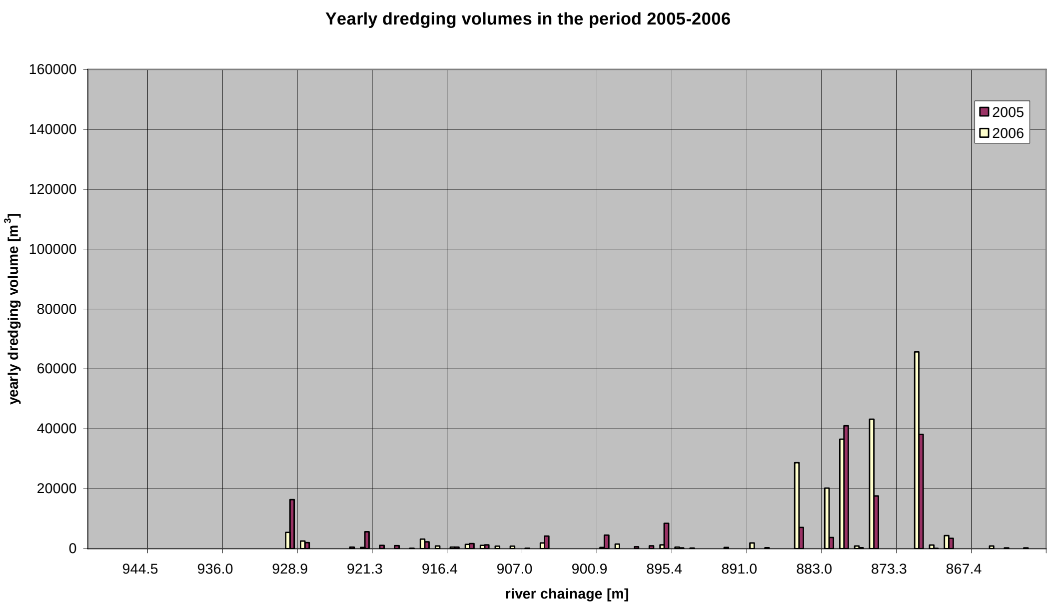

Figure 5.4 Dredging volumes in the Waal in the period 2000-2002 and in the period 2005-2006.

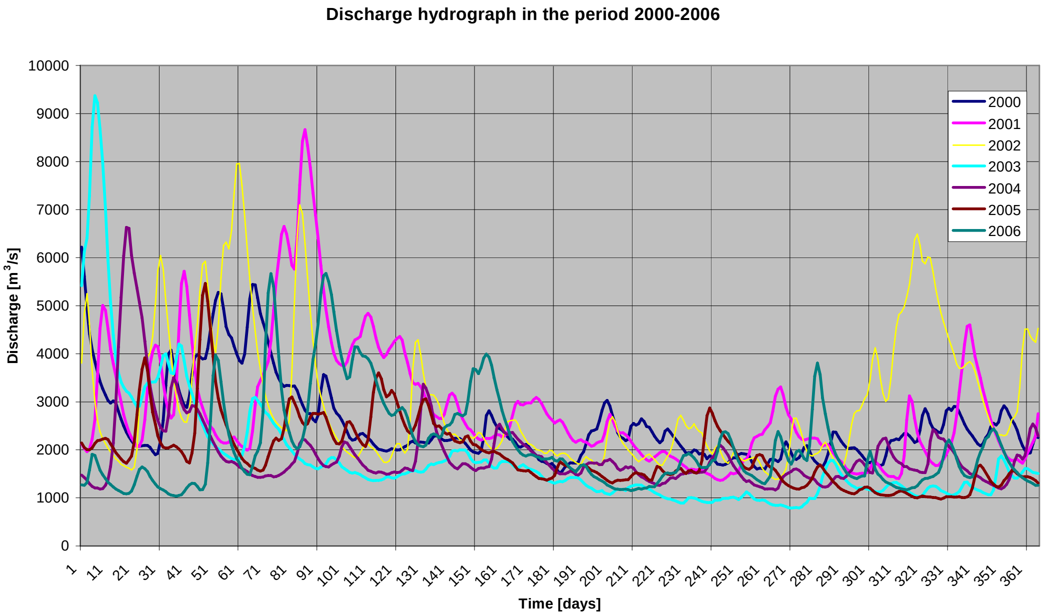

Figure 5.5 Discharge hydrograph in the period 2000-2006.

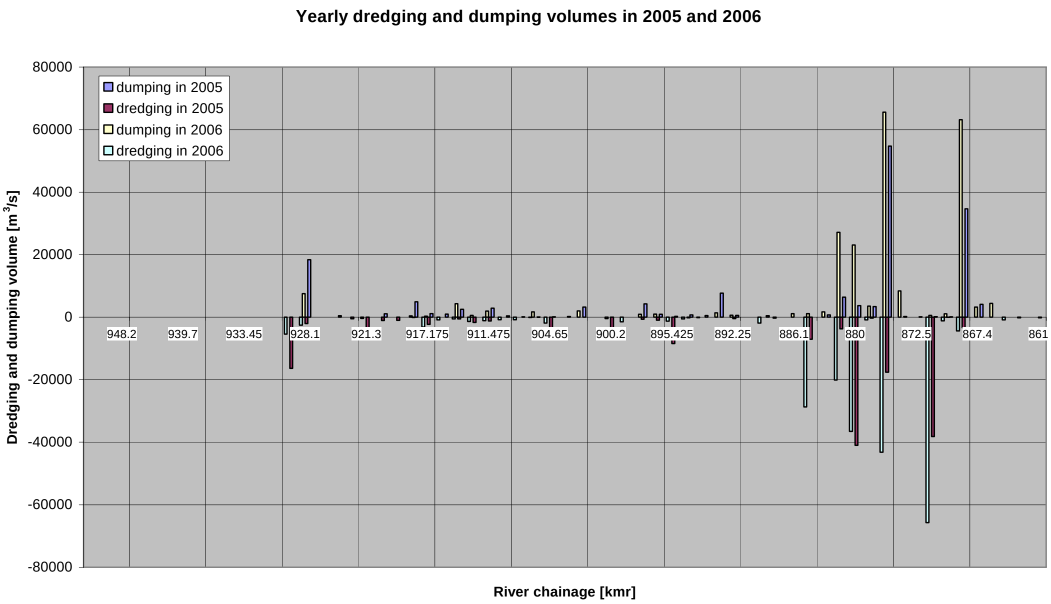

Figure 5.6 Dredging and dumping volumes in the Waal in the period 2005-2006.

The combination of dumping and dredging data is presented for the period 2005-2006 in Figure 5.6. In general most of the dredged material was dumped 2 km upstream. Dumping data were missing in the data set of 2000-2002. For the calibration it is assumed that the dredged material was dumped 2 km upstream from the dredge location.

5.2.3 Calibration parameters

In order to calibrate the DVR model on dredging volumes, the following calibration options are evaluated:

1. **Dune height:** herein we evaluate the impact of the presence of bed forms that easily form nautical bottlenecks on dredging volumes. Currently, the DVR model does not yet include a dune height predictor. This functionality is being developed and calibrated in the next phase of this project.

   Since part of the dredging activities is related to the removal of bed forms, the presence of bed forms in the DVR model is tested. In Van Vuren and Ottevanger (2006), the normative bed level for navigation that accounts for bed forms is defined as follow:

$$Z_{rep}(x,t) = \overline{Z}(x,t) + \alpha\sigma(x,t) \qquad (5\text{-}3)$$

   in which:

   Z_{rep} normative bed level for the navigation depth in [m]+NAP
   $\overline{Z}$ bed form averaged bed level [m]+NAP
   σ spatial variation in the bed level due to the presence of dunes [m]
   α constant parameter (to be chosen between 0 and 1)

   The bed form averaged bed level $\overline{Z}$ is estimated with the DVR model. The spatial variation σ due to the presence of dune with dune height H can be approximated as follows (when assuming triangular-shaped bed forms):

$$\sigma = \frac{H}{\sqrt{12}} \qquad (5\text{-}4)$$

   In this chapter simulations are performed to evaluate the presence of an extra height to account for the presence of dunes of 0 m, 0.2 and 0.5 m (equivalent to dune heights of 0, 0.7 m and 1.7 m respectively). This height is imposed on top of the bedform-averaged bed level in the Delft3D simulations, Figure 5.7 illustrates the concept.

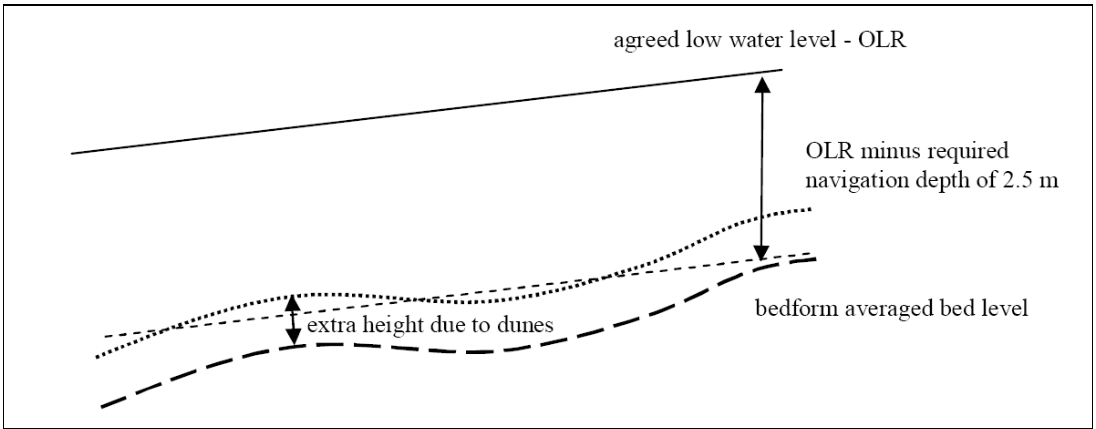

Figure 5.7 Testing the impact of the presence of bed forms on dredging activities, definition sketch.

2. **Navigation channel width:** The shape files given in Figure 5.1 indicate the course of the navigation channel and the dumping areas where the dredged material can be deposited. The dredging & dumping functionality works as follows. When a grid cell lies partly outside the shape file, the cell is not considered within the dredging & dumping functionality. Figure 5.8 clearly shows that the shape file that represents the official course of the navigation channel (red lines), cuts through several grid cells of the computation grid. So in fact, the navigation channel width requirement is checked over a smaller width than intended. The impact of this on the estimated dredging volumes is investigated with an additional simulation using the polygon of the navigation channel width of 170 m (green lines). For the latter channel width the dredging volumes are estimated for a navigation depth of 2.5 and 2.8 m.

3. **Dumping strategy:** In conformity with the new policy, the dredged volume has to be deposited elsewhere in the river. The impact of the distance between the dredging and dumping location is assessed by two simulations: a) dumping 0-5 km upstream, and b) dumping 2-7 km upstream.

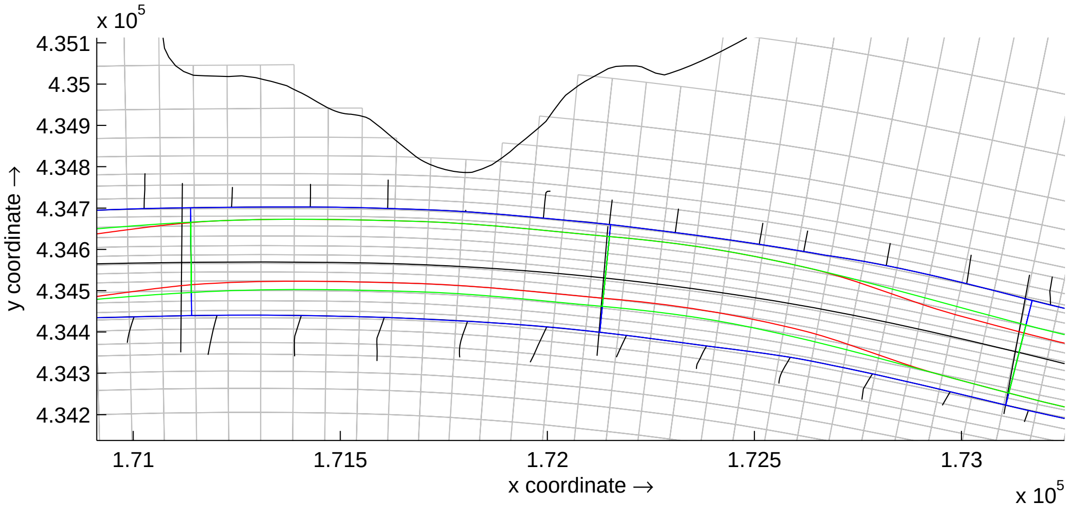

Figure 5.8 The official course of the navigation channel: the red lines indicate the navigation channel of 150 m wide; the green line represents the same for a channel width of 170 m.

5.3 Results

The impact of the presence of bed forms, the course of the navigation channel and the dumping strategy are investigated with the model simulations specified in Table 5.3. The reference simulation contains the following model settings: 1) dunes of 0.5 m are imposed, 2) dumping takes place 2-7 km upstream of the dredge location, and 3) use is made of the shape file indicating the course of the navigation channel with a width of 150 m.

The analysis focuses on the representation of the yearly averaged dredging volumes, and the locations where dredging and dumping takes place. The results are shown in Figure 5.9 (impact of bed forms), Figure 5.10 (impact of the navigation channel dimensions) and Figure 5.11 (impact of dumping strategy).

Table 5.3 An overview of the model simulations to estimate dredging & dumping volumes.

nr.	A. Impact of bed forms	nr.	B. Impact of channel dimensions	nr.	C. Impact of dumping strategy
Ref	dunes of 0.5 m	Ref	150 m x 2.5 m	Ref	dumping 2-7 km upstream
A.1	dunes of 0.2 m	B.1	170 m x 2.5 m	C.1	dumping 0-5 km upstream
A.2	no dunes	B.2	170 m x 2.8 m		

In general the figures indicate that the DVR model is a useful tool to locate the structural dredge locations in sharp river bends at Hulhuizen (km 870), Erlecom (km 875), Haalderen (km 880), Nijmegen (km 885) and St. Andries (km 928). It appears more difficult to predict the incidental dredge locations in the Midden Waal between km 887-915. The latter are more related to the removal of bed forms that are developed during high water conditions and form nautical bottlenecks in the low-water period.

Imposing an extra height to account for the presence of dunes on the bed-form averaged bed levels yields an increase in dredging activities. When imposing an extra height of 0.5 m, dredging volumes at the Midden Waal are better predicted. However, it yields an overestimation of the dredging activities at the structural dredging locations.

The same can be noticed, when widening the width of the navigation channel. As mentioned before, the dredging requirement has not been estimated for the grid cells that lie partly outside the shape file of the navigation channel. This implies that a simulation with the shape file of a navigation channel width of 150 m in fact yields the dredging requirement for a narrower channel. The grid cell width in the main channel is on average 23 m. This means that either 5 or 6 grid cells lie within the shape file. This corresponds with a channel width of 115 m or 140 m.

When using the shape file of a channel width of 170 m, the channel width for which dredging is estimated increases to 140 m to 160 m (6 or 7 grid cells). This better corresponds with the required channel width. Note that the 170 m wide channel is increased from one side (at a location) rather than extending the 150 m wide channel from both sides, which would be needed actually to compensate for cut-cells of the grid on both sides. The total dredging volume increases with a factor of 1.5. Figure 5.10 indicates that dredging volumes increase along the entire river. In particular in the Midden Waal this yields better predictions. The estimated dredging volumes are still very low. Increasing the channel width results in a large overestimation of the dredging volumes at the structural dredge locations. In some locations dredging volumes become up to 5 times larger than observed.

The lower panel in Figure 5.10 gives an indication of the extra dredging requirement for an increase of the channel depth from 2.5 to 2.8 m. The total dredging effort increases with a factor 2. A factor of 1.5 is due to the channel width increase and a factor of 1.4 is due to the navigation depth increase.

The impact of the distance between the dredge and the dump location is illustrated in Figure 5.11. It appears that deposition of the dredged material 2-7 km in upstream direction yields a larger dredging effort than dumping 0-5 km in upstream direction. This is mainly the case for the structural dredge locations. Apparently, the deposition of dredged material occurs more often just upstream of the worst nautical bottlenecks. The figures in Appendix C showing the dumping volumes along the river confirm this assumption. As a consequence, nautical bottlenecks are formed faster, so that extra maintenance dredging is required.

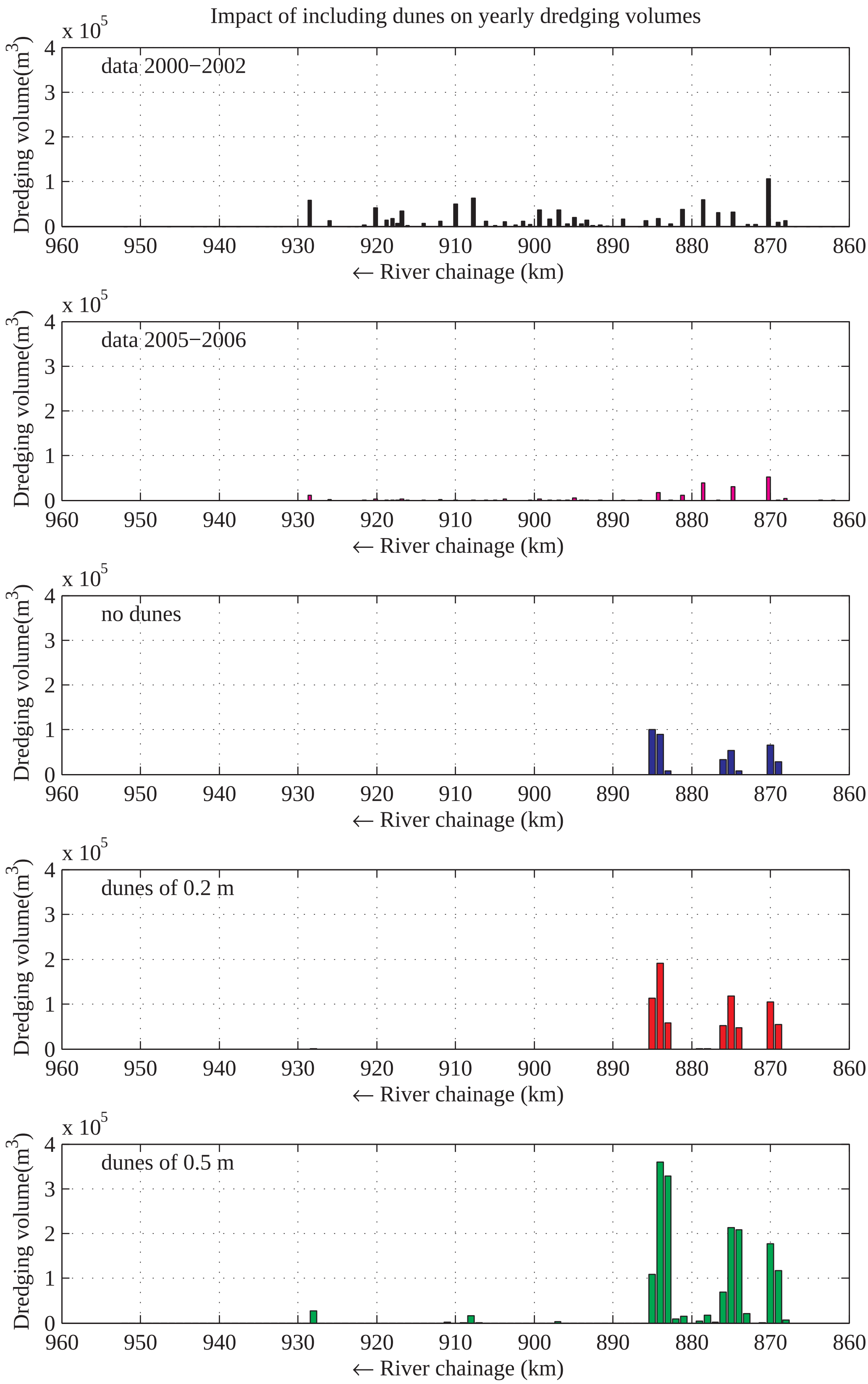

Figure 5.9 The impact of bed forms on yearly averaged dredging volumes (for the model simulation the dredging volumes are averaged over the period 2000-2006).

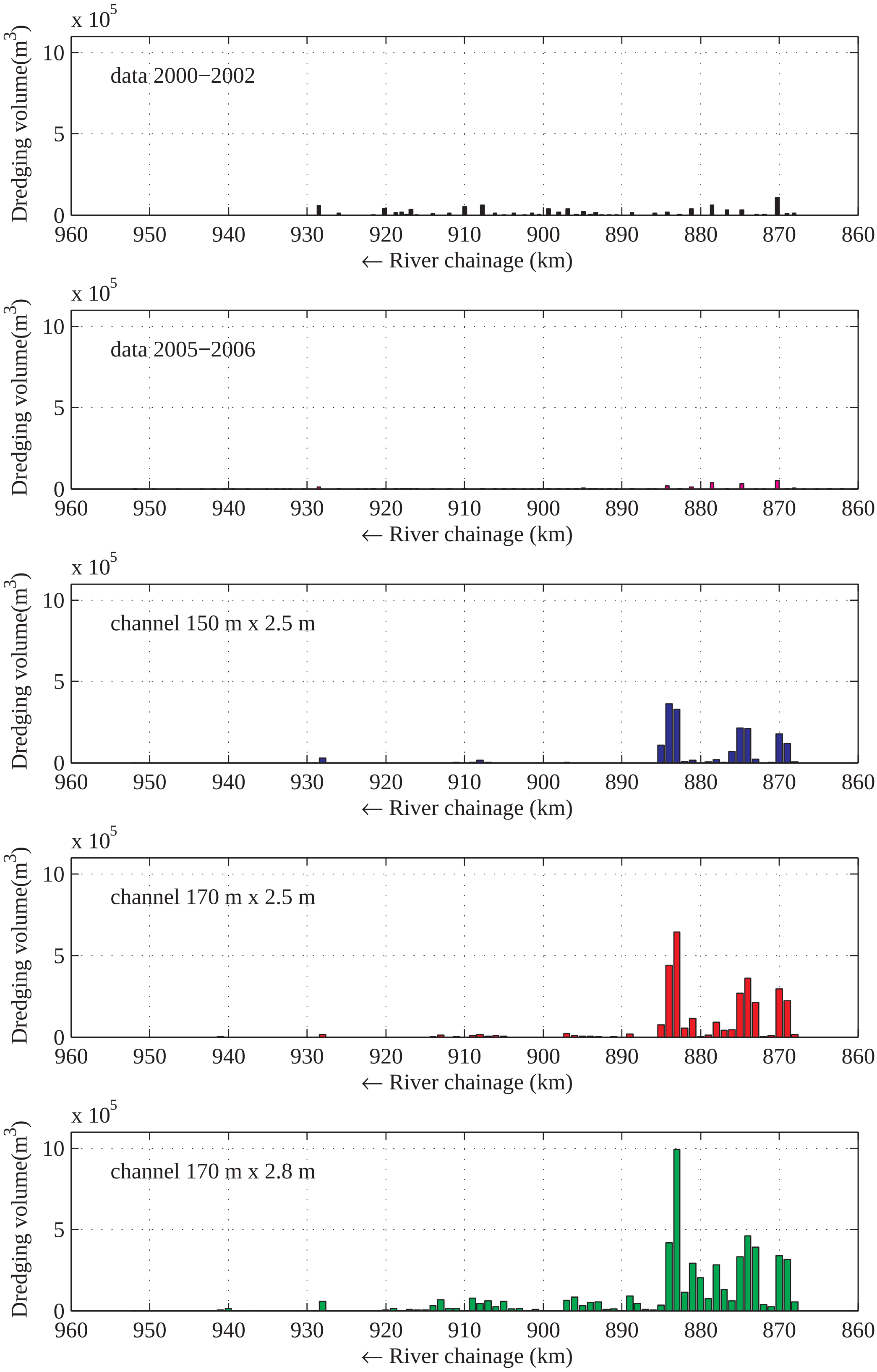

Figure 5.10 The impact of the course of the navigation channel and the navigation depth on yearly averaged dredging volumes (for the model simulation the dredging volumes are averaged over the period 2000-2006).

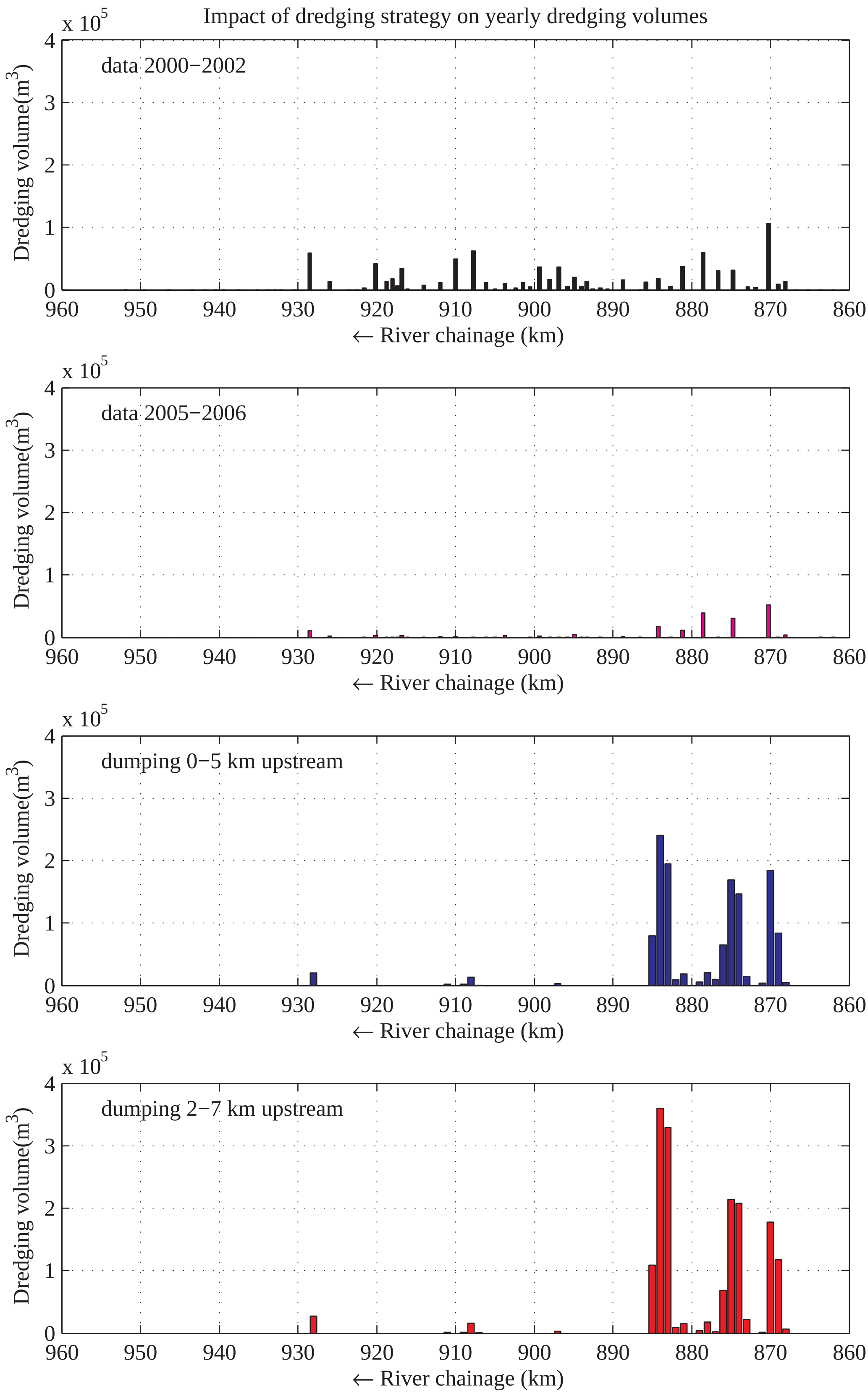

Figure 5.11 The impact of dumping strategy on yearly averaged dredging volumes (for the model simulation the dredging volumes are averaged over the period 2000-2006).

Although the dredging effort is overestimated at the structural dredge locations, it is recommended to use the settings of model B1 (see Figure 5.12 lower panel) in future projects. In this model an extra height of 0.5 m is imposed on top of the bed form averaged bed level, the shape file of a channel width of 170 m is used, and the dredge material is deposited 2-7 km upstream of the dredge location. More detailed morphological calibration of the Boven-Waal would improve the predictability of dredging in this area. Despite the fact that not all dredge locations are detected, simulation B1 does perform quite well for the Midden Waal. Figure 5.12 shows that simulation B1 yields for the Midden Waal dredging volumes of the same order of magnitude as the dredging data.

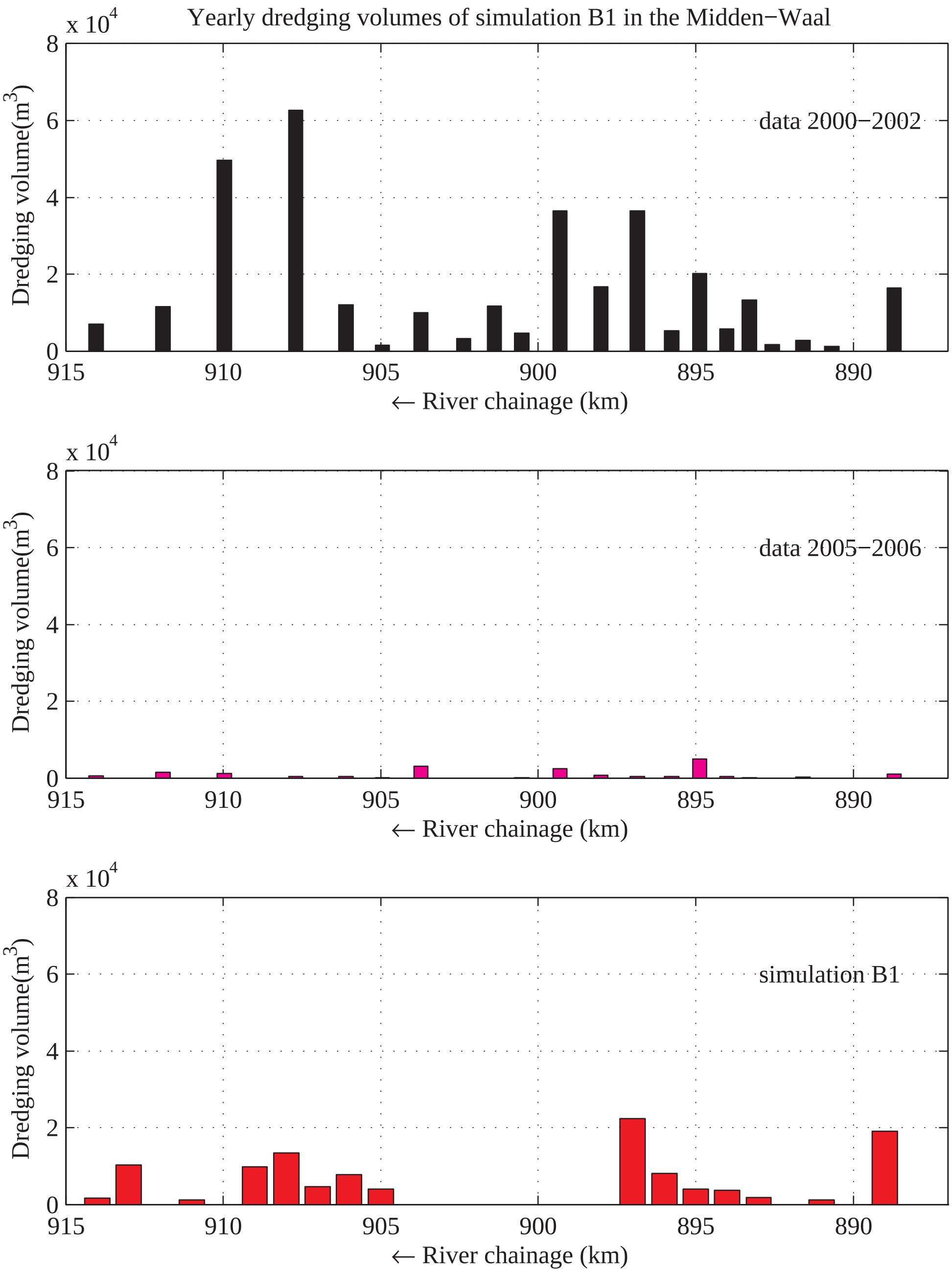

Figure 5.12 Yearly averaged dredging effort for simulation B1 in the Midden-Waal (for the model simulation the dredging volumes are averaged over the period 2000-2006).

Figure 5.13 represents the yearly dredging volumes derived from simulation B1 in the first 7 years of the computations. It seems that the dredging effort increases as a function of time. A simulation of 40 years is used to investigate this behaviour on the long term. Figure 5.14 gives the dredging volumes per year over a period of 40 years for four locations Hulhuizen (km 870), Haalderen (km 880), Nijmegen (km 883) and St. Andries (km 928). After a period of 15 to 20 years the yearly dredging effort becomes more or less constant. Apparently, it takes some years before the morphodynamics are stabilised.

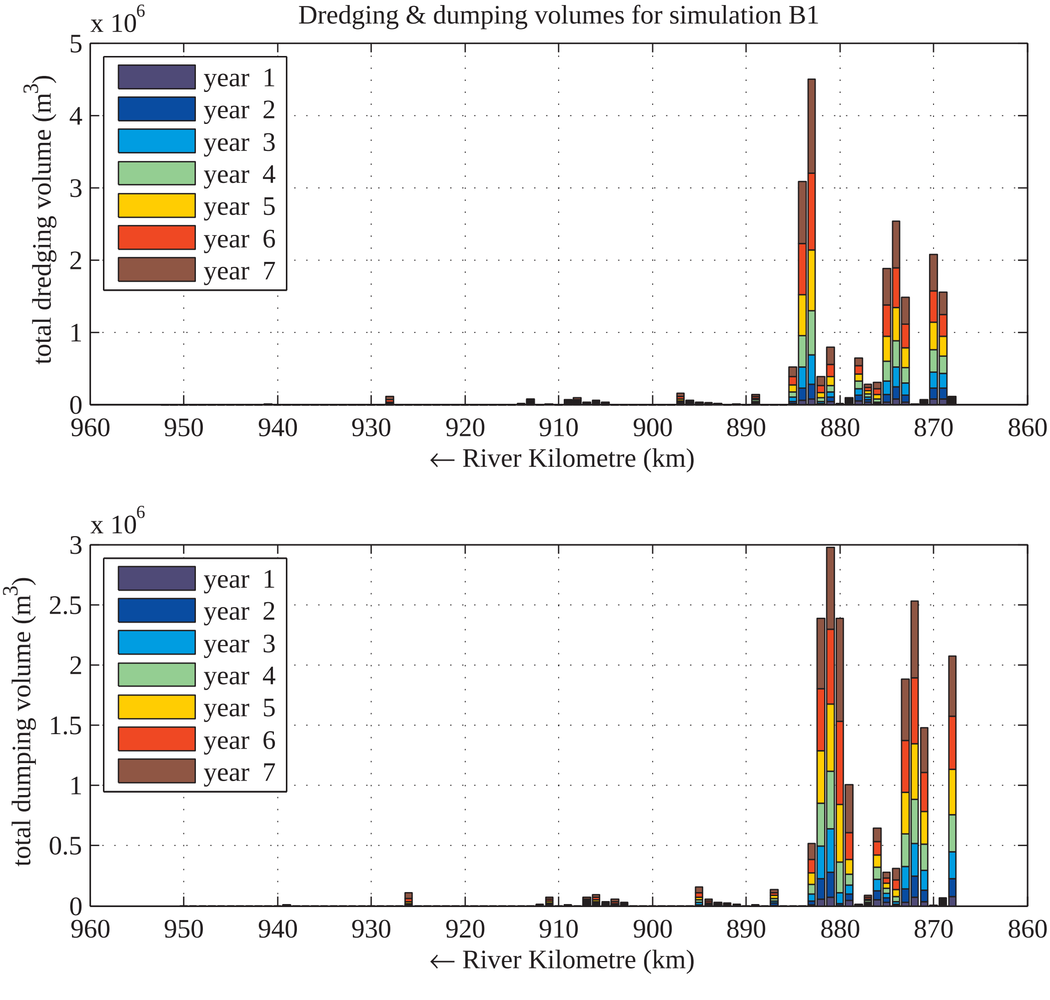

Figure 5.13 Dredging volumes in the period 2000-2006 for simulation B1 (dunes of 0.5 m, shape file of channel width of 170 m, and dumping 2-7 km upstream of the dredge location).

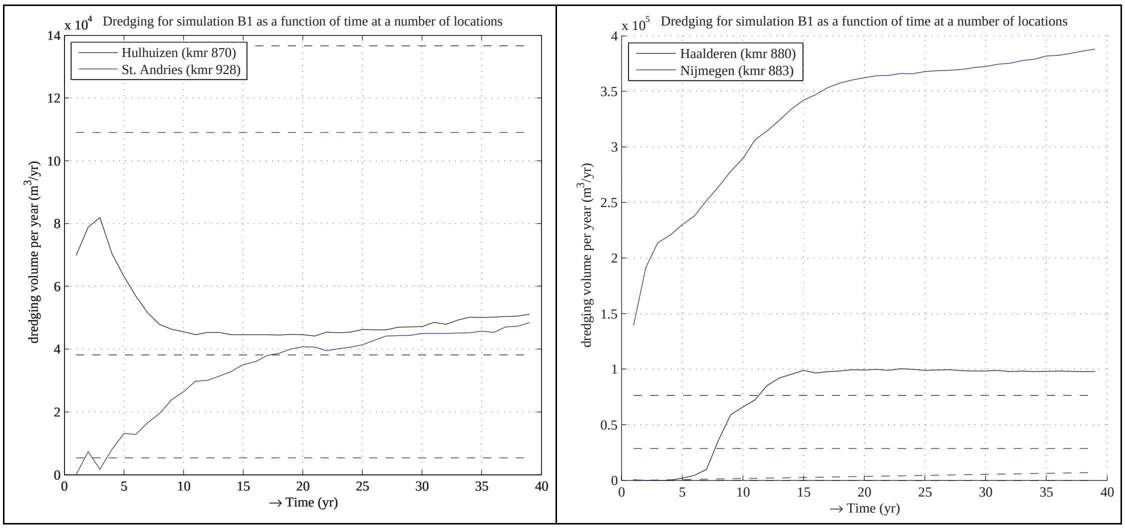

Figure 5.14 Dredging volumes per year over a period of 40 years for simulation B1 at four locations Hulhuizen (km 870), Haalderen (km 880), Nijmegen (km 883) and St. Andries (km 928).

Figure 5.15 and Figure 5.16 show the bed level difference in the Boven-Waal and the Midden-Waal between a simulation with (simulation B1) and without dredging.
Figure 5.15 indicates that for the Boven Waal where dredging activities are relatively high, there are some differences in the morphological pattern because dredging (erosion) mainly occurs in the shallow inner bends and dumping (deposition) in the deep outer bend. Especially in river bends with bottom protection structures at Erlecom (km 873-876) and Nijmegen (km 882-885) lots of dredging takes place in the inner bend (see Figure 5.15). As mentioned before the dredging effort is overestimated in this area and could be improved with a more detailed calibration. In the Midden Waal, dredging activities are much less and morphological changes are minor.

Figure 5.17 gives the cross-sectional and river-section-averaged 1) bed form celerity, 2) annual bed level changes, and 3) bed level gradient in the Boven-Waal, Midden-Waal en Beneden-Waal, for a simulation with (simulation B1) and without dredging. From Figure 5.17 we can deduce that dredging activities had little effect on the large-scale morphological behaviour of the river.

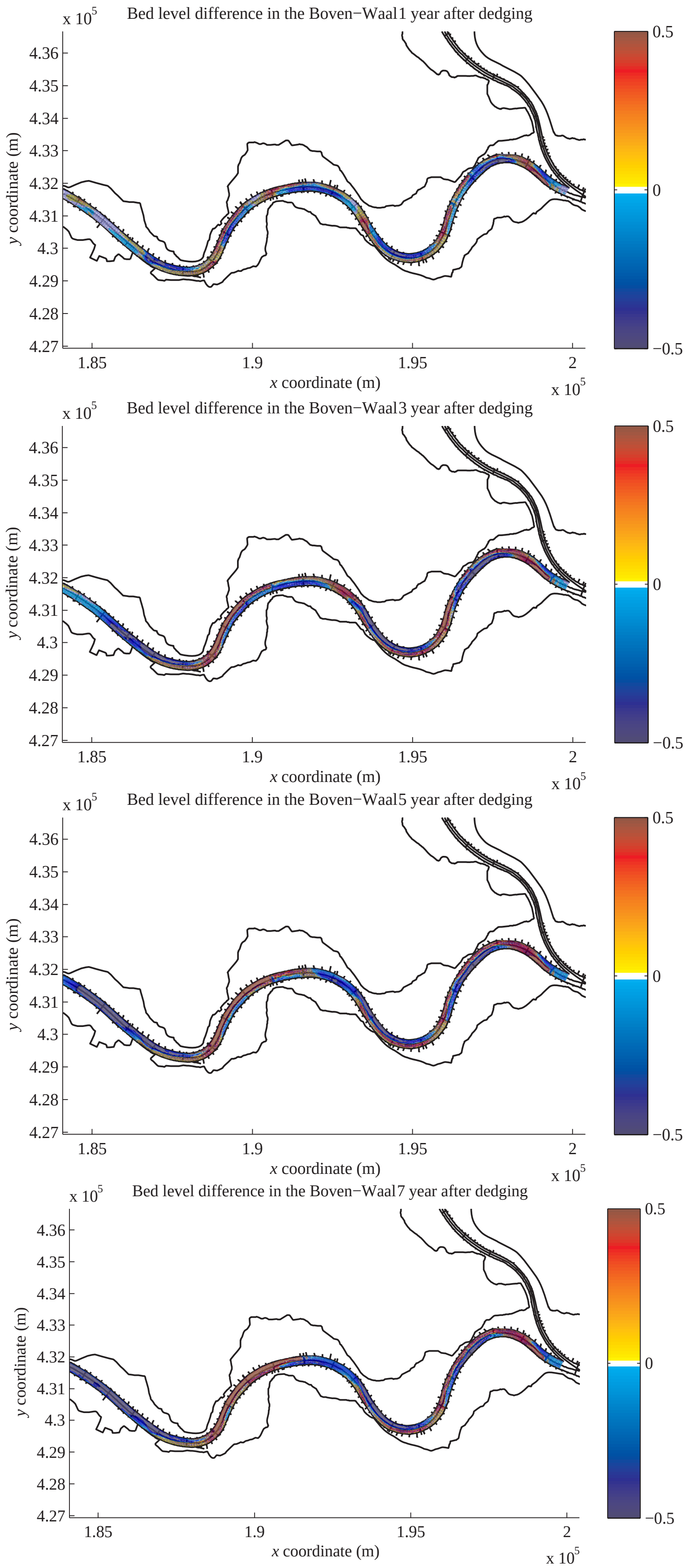

Figure 5.15 Difference in bed level in the Boven-Waal between a simulation with (simulation B1) and without dredging after periods of 1 year, 3 years, 5 years and 7 years.

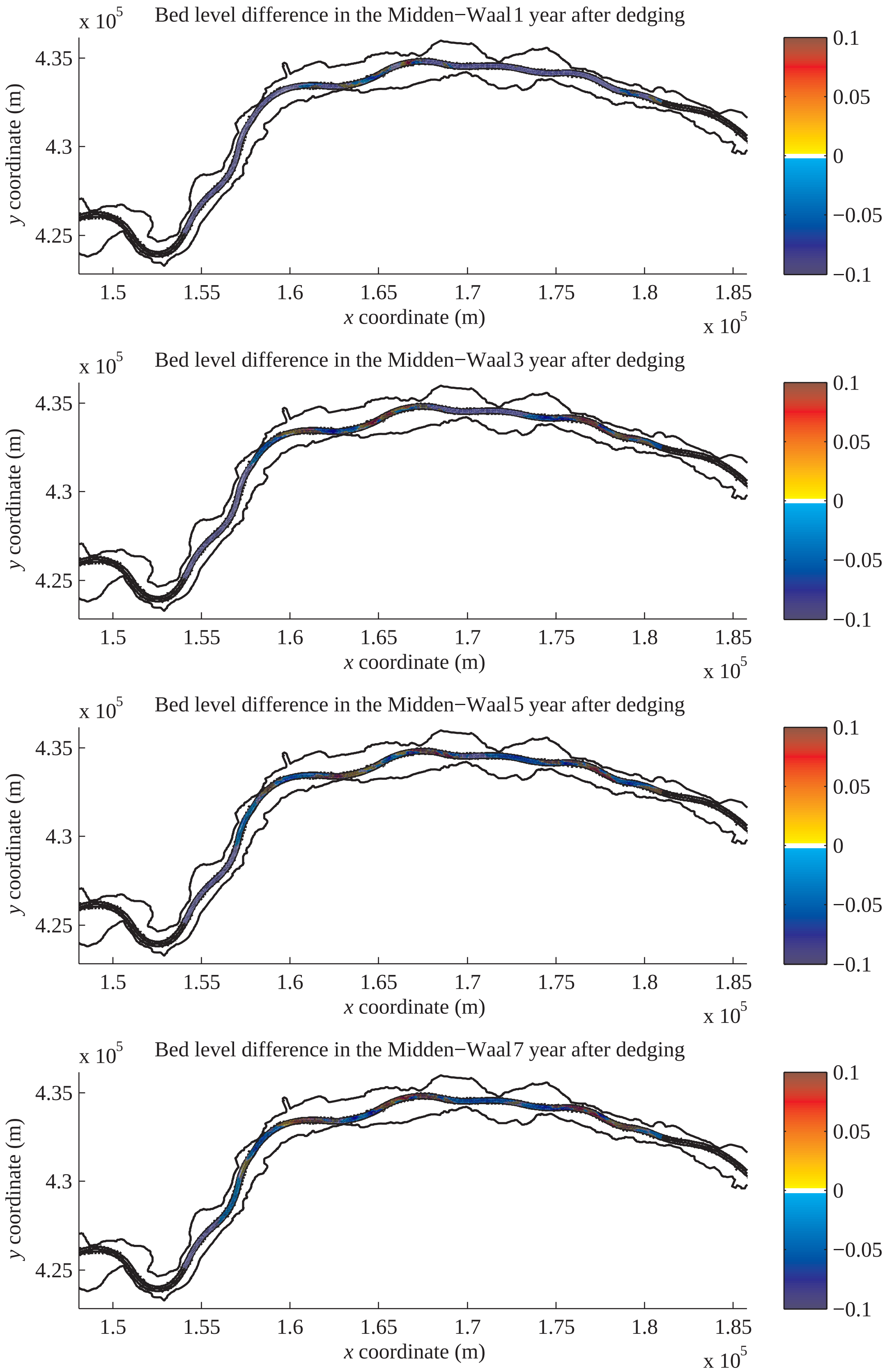

Figure 5.16 Difference in bed level in the Midden-Waal between a simulation with (simulation B1) and without dredging after periods of 1 year, 3 years, 5 years and 7 years.

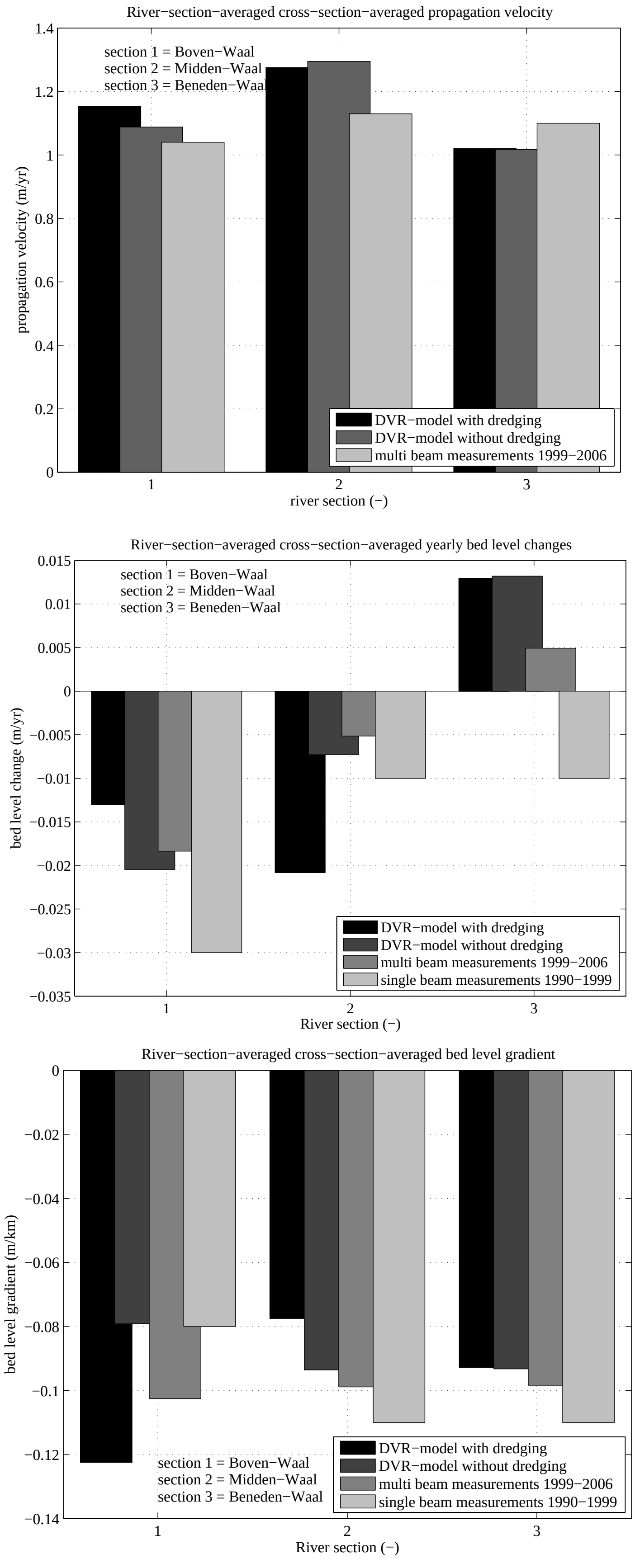

Figure 5.17 Comparison on river-reach- and cross-section-averaged 1) bed form celerity, 2) annual bed level changes, and 3) bed level gradient in the Boven-Waal, Midden-Waal en Beneden-Waal.

5.4 Conclusions and recommendations

- In general, the DVR model is a useful tool to locate the structural dredging activities located in the sharp river bends at Hulhuizen (km 870), Erlecom (km 875), Haalderen (km 880), Nijmegen (km 885) and St. Andries (km 928). It appears more difficult to predict the incidental dredging locations in the Midden Waal between km 887-915 which is mainly related to the removal of dunes that develop during high water and form nautical bottlenecks in the low-water period.
- The study shows the importance of a dune height predictor and a good representation of the navigation channel. We can conclude that including an additional height to account for the presence of dunes and a wider channel to account for the cut-cells of the grid, result in much better predictions of the dredging activities in the Midden Waal. This does not improve the predictions of the structural dredge activities located in sharp river bends.
- In this project a constant dune height was imposed for better reproduction of dredging activities. For a good operational model, it is recommended to use a dune height predictor that predicts the evolution of the bed forms both in time and space for the entire discharge regime (the bed forms that will develop during high water conditions and that partially damp, but form nautical bottlenecks during low-water conditions). In this study, the impact of dunes on the representative bed level for navigation is assessed by assuming triangular shaped dunes. It is recommended to investigate the sensitivity of the results to this assumption.
- In the current implementation of Delft3D, the dimensions of the dredging locations are affected by the grid size. All grid-cells with centre points that lay outside a dredge block are not dredged, i.e. cut-cells are mostly ignored. It is recommended to improve Delft3D dredging functionality by accounting for cut-cells by the dredging blocks.
- At the structural dredging locations, though the dredging locations are well predicted, the volumes are over predicted with a factor of up to 5. This is especially the case in river bends with bottom protection structures at Erlecom (km 873-876) and Nijmegen (km 882-885). It is recommended to have a closer look at the 2D behaviour of these specific locations. Moreover, it is recommended to investigate the interaction between shallow bars and dune development and migration.
- If improvements are made, the model has a large potential for navigation channel assessments. However, implementing a larger number of functionalities in the model leads to a significant increase in computational time. A model simulation with the Waal domain for a period of 40 years, takes approximately 4.4 days, whereas running the entire DVR model with the branches Bovenrijn, Pannerdensche Kanaal and Waal takes about the same. Especially when an online dune height predictor will be implemented, it is recommended to further investigate the possibilities of computation time reduction. The negative drawback of additional computation time could most probably be removed by further development and implementing the lateral inflow and outflow approach of Van Vuren et al. (2007). It is also recommended to consider an approach where foreknowledge (on dredging activities for instance) could be used to reduce the computation time. There are locations with hardly any dredging activities, which do not need to be checked every time step in the low-water season.
- The improved model could be used to evaluate various dredging strategies. The present study focussed on the dumping strategy. It appears that deposition of the dredged

material 2-7 km upstream leads to more maintenance dredging than deposition 0-5 km upstream. For the Boven Waal, it seems that the deposition, just upstream nautical bottlenecks, induces extra maintenance dredging. One of the principal main objectives of upstream deposition is to prevent further large-scale tilting of the bed. It is recommended to evaluate a strategy where deposition of the dredged material is only allowed outside the course of the main channel. A strategy of downstream deposition of dredged material might be interesting from an economical point of view. Further research on this subject is recommended.

- This chapter started with a discussion on the prediction of the OLR. The OLR is a statistically derived reference level. As indicated, the OLR does not necessarily correspond to water levels that are present during a low discharge of the same order of magnitude as the OLA.

6 Conclusions and recommendations

6.1 General

The improvements introduced to the DVR model in this report cover the following aspects:

- Analysis, choice, implementation and testing of an overall sediment transport formula that is suitable for all branches in the model,
- hydrodynamic calibration of the OLR conditions in the Waal,
- global morphological calibration of the entire model using the overall transport formula reached, and finally
- a morphological calibration for the dredging activities in the Waal.

6.2 Overall sediment transport formula

- An alternative sediment transport formula has been analytically evaluated, implemented and tested for the use in the improved DVR model. Criteria were set for the choice of the formula in Section 2.2.
- We reached the conclusion that the sediment transport formula of van Rijn (1984a; b) is the most suitable. Some additional options were introduced to the formula and accordingly implemented in Delft3D.
- The formula was tested successfully to behave as intended. The parameter settings of the formula were optimised as part of the morphological calibration of the model.

6.3 Hydrodynamic calibration

A calibration of the DVR Waal model for low discharge conditions was carried out. The calibration was done by tuning the roughness values of the main channel. This yielded rather low roughness values, lower than what is coming from the Baseline schematisation, especially in the downstream reach of the Waal.

It appeared from the analysis that, in the most downstream reach of the model, there is uncertainty in the water level data at very low discharge conditions. In view of that, we reached the conclusion that the hydrodynamic calibration of the most downstream reach of the model is uncertain. According to the calculations the backwater effect reaches up to around Tiel. The distance is related to the discharge. Therefore, the calibration is accepted for the upper part of the Waal, for hydrodynamic calculations and for lower discharges only.

A verification run with the OLA conditions was conducted. The difference between calculated and deduced OLR water levels indicates that there is a rather large deviation in the reach between Tiel and Zaltbommel. The calculated water level is up to 0.35 m lower than the OLR of 2002. This should be considered in comparison with the calibration model where in the same reach, the calculated water level reaches up to 0.20 m higher than the measured water level.

In the absence of additional data, we have the impression that this is the best possible at this stage. Nevertheless, for the sake of dredging activities in the downstream reach of the Waal, an underestimation of the OLR is more critical than an overestimation, i.e. dredging volume would be larger in the case of an underestimated OLR. Considering that the previous dredging case study (Mosselman et al. 2007) indicated that no dredging took place in the most downstream part of the Waal, this seems to be a more appropriate starting point with respect to dredging. However, for the reason of correctly estimating OLR, additional adjustment to the model parameters has been carried out in Chapter 5.

6.4 Global morphological calibration

The DVR model has been successfully calibrated including the Bovenrijn, Waal and the Pannerdensch Kanaal. The model is successfully operational including all five branches, though the Nederrijn and the IJssel are not calibrated at this stage. A summary of the final model settings is given in Table 6.1.

In general the model calibration has been successful with a correct reproduction of the observed one-dimensional and two-dimensional morphological patterns.

With respect to the 1D morphological behaviour:

- the criteria for calibration were a correct reproduction of:
  - annual sediment transport volumes,
  - celerity of bed disturbances,
  - annual bed level changes,
  - time-averaged bed level slopes,
  - sediment distribution at the bifurcation,

- For the Bovenrijn and the Waal these criteria were successfully met, for the Pannerdensch Kanaal the celerity is slightly underestimated compared to the values inferred from the historical data set.
- The sediment distribution at the bifurcation point Pannerdensche Kop shows some inconsistency with the observations. The model underestimates the sediment transport entering into the Waal and overestimates the amount entering into the Pannerdensch Kanaal. This could be attributed to the sediment coarsening near the right bank of the lower part of the Bovenrijn towards the Pannerdensch Kanaal. This phenomenon is related to graded sediment transport that is not included in this model.

With respect to the 2D morphological behaviour:

- A correct reproduction of the bar amplitude and pattern were the criteria for calibration.
- In general the results for all branches show good agreement with the multi-beam measurements.

Table 6.1 Parameter settings for the DVR model

Parameter	Final settings
Baseline schematisation	Baseline version 3.3 with reference schematisation of the PKB Room for the River study.
Grid used	Grid properties are summarised in Table 4.1
Time step	0.4 minutes
Morphological acceleration factor given per discharge	Q = 1794 m^3/s → 600 Q = 3052 m^3/s → 480 Q = 4318 m^3/s → 200 Q = 5866 m^3/s → 120
Initial bed levels	BR multi-beam data year 1999 → Dutch side (single-beam data 1997) – 0.40 m → German side Waal multi-beam data year 1999 PK multi-beam data 2002
Boundary conditions	Upstream: discretised discharge time series derived from daily discharge measurements at Lobtih for the period 1999-2007, given in Figure 4.2. The discharge was given as a total discharge and distributed in proportion to $h^{1.5}$ per grid cell. Downstream: PK → measured water levels (year 2000) Waal → $h_{Waal} = \left(\frac{Q_{Waal}}{1500}\right)^{0.95} - 0.1$ Upstream morphological boundary condition → bed level degradation of 3 cm/yr
1D parameters	θ_{cr} = 0.016 α_{SUS} = 0.3 α_{BED} = 0.2 D_{50} = Figure 4.3, data from measurement campaigns in 1976, 1984, 1995 and 2000 are used
2D parameters	A_{shld}(BR) = 1.10 A_{shld}(Waal) = 0.70 A_{shld}(PK) = 0.95 B_{shld} = 0.50 E_{spir} = 1.0

PK = Pannerdensch Kanaal
BR = Bovenrijn

Finally,

- It appears that a number of problems associated with the morphological calibration originate from the hydraulic results, e.g. the discharge distribution at the Pannerdensche Kop underestimates the discharge into the Pannerdensch Kanaal. These problems cannot be simply handled using a different set of morphological settings.
- It is recommended to pay attention to the hydraulic calibration of the model through the full discharge range with special attention to the discharge distribution between the main branches.
- It is recommended to conduct an uncertainty analysis for the morphological behaviour of the model.

6.5 Calibration of dredging activities

In Chapter 5 we have carried out initial attempts towards calibrating the DVR model for dredging activities; we focused on dredging volumes and dredging & dumping locations. We were able to distinguish two categories of dredging:

1- Structural dredging activities that are induced by the geometry of the river, for instance at the sharp river bends near Hulhuizen (km 870), Erlecom (km 875), Haalderen (km 880), Nijmegen (km 885) and St. Andries (km 928).
2- Incidental dredging activities which are related to the removal of dunes that are developed during high water conditions forming nautical bottlenecks in the low-water period (mainly in the Midden Waal in the reach between km 887-915).

The results of the calibration indicated that:

- In general, the DVR model is a useful tool to locate the structural dredge activities located in sharp river bends.
- It appears that it is more difficult to predict the incidental dredge locations in the Midden Waal between km 887-915 which is mainly related to the removal of dune development and migration
- The study highlighted the importance of two primary parameters:
  - dune heights, and
  - the dimensions of the navigation channel (dredging blocks), or in other words, the way that the dimensions of the navigation channel is transformed into dredging locations in Delft3D.
- We could conclude that including an additional height to account for the presence of dunes and a wider channel to account for the cut-cells of the grid, results in much better predictions of the dredging activities in the Midden Waal. This does not improve the predictions of the structural dredging activities located in sharp river bends.
- It is recommended to use a dune height predictor that predicts the evolution of the bed forms both in time and space for the entire discharge regime. Moreover, additional investigations on the effects of dune-shape on dredging volume are needed.
- It is recommended to improve Delft3D dredging functionality by accounting for cut-cells of the model grid by the dredging blocks. In the current implementation of Delft3D, the dimensions of the dredging locations are affected by the grid size. All grid-cells with centre points that lay outside a dredge block are not dredged, i.e. cut-cells are

mostly ignored. This yields an effective dredging area smaller than reality. Partial accounting for the area of the grid-cell included in the dredging block would improve the model results with respect to dredging activities.

- At the structural dredging locations, though the dredge locations are well predicted, the volumes are overpredicted with a factor of up to 5. This happens because of the need to include relatively large dune height for a correct reproduction of dredging locations in the Midden Waal. It is recommended to have a closer look at the 2D behaviour of these specific locations. Moreover, it is recommended to investigate the interaction between shallow bars and dune development and migration. Perhaps the implementation of a spatially varying dune height predictor would solve this problem.
- It is recommended to consider an approach where foreknowledge of dredging activities could be used to reduce the number of dredging blocks to reduce computation time. There are locations with hardly any dredging activities, which do not need to be checked every time step in the low-water season.

7 References

Baur, T. & Jagers, H.R.A. (2002), Grensproject Bovenrijn/Grenzprojekt Niederhein – Model construction, calibration and verification. Report Q2496.00, WL | Delft Hydraulics.

De Vriend, H.J. (1977), A mathematical model of steady flow in curved shallow channels. Journal of Hydraulic Research, 15(1), pp. 37-54.

Engelund, F. & E. Hansen (1967), A monograph on sediment transport in alluvial streams. Teknisk Forlag, Copenhagen.

Frings, R.M. (2005), Sedimenttransport op de IJsselkop tijdens hoog- en laagwaterperioden in 2002 en 2004. ICG 05/2. Utrecht: Centre for Geo-ecological Research, Universiteit Utrecht.

Griashanin, K.V. (1990), Dynamics of alluvial flows. Moskva “Transport” ISBN 5-277-01000-9 (in Russian; n = 4 for Dnipr River on p. 302)

Meyer-Peter, E. & R. Muller (1948), Formulas for bed-load transport. Proceedings 2nd Congress IAHR, Stockholm, Paper No.2, pp.39-64.

Mosselman, E. (2005), Basic equations for sediment transport in CFD for fluvial morphodynamics. Chapter 4 in: Computational Fluid Dynamics; Applications in environmental hydraulics, Eds. P.D. Bates, S.N. Lane & R.I. Ferguson, Wiley, pp.71-89.

Mosselman, E., S. van Vuren, M. Yossef, W. Ottevanger & K. Sloff (2007). Case studies Duurzame Vaardiepte Rijndelta. Rapport Q4245.00, WL | Delft Hydraulics.

Mosselman, E., S. van Vuren, M. Yossef, W. Ottevanger & K. Sloff (2007). Case studies Duurzame Vaardiepte Rijndelta. Rapport Q4245, WL | Delft Hydraulics.

Sieben, A. (1998), Combineren van transportformules. Concept interne notitie, Rijkswaterstaat RIZA, WSR, 7 juli 1998 (beperkte verspreiding).

Sieben, A. (2005), Morfologische effecten van herinrichting; PKB ruimte voor de Rivier. Werkdocument 2005.044x, Rijkswaterstaat RIZA.

Sloff, C.J. & Mosselman, E. (1998). Voorbereiding ijking Rijntakkenmodel. Rapport Q2460, WL | Delft Hydraulics.

Struiksma, N., K.W. Olesen, C. Flokstra & H.J. de Vriend (1985), Bed deformation in curved alluvial channels. Journal of Hydraulic Research, 23(1), pp. 57-79.

Talmon, A.M., M.C.K.M. Van Mierlo & N. Struiksma (1995), Laboratory measurements of the direction of sediment transport on transverse alluvial-bed slopes. JHR, 33(4), pp. 495-517.

Ten Brinke, W.B.M (2005), The Dutch Rhine – a restrained river. Veen Magazines B.V., the Netherlands; 2005; ISBN 90 76988 91 9, NUR 933; 228 pp.

Ten Brinke, W.B.M., Bolwidt, L.J., Snippen, E. & Van Hal, L.W.J. (2001), Sedimentbalans Rijntakken 2000. Een actualisatie van de sedimentbalans voor slib, zand, grind van de Rijntakken in het beheersgebied van de Directie Oost Nederland. RIZA rapport 2001.043 .Ministerie van Verkeer en Waterstaat, Directoraal Generaal Rijkswaterstaat, RIZA.

Van Rijn, L. C. (1984a). "Sediment Transport, Part I: Bed Load Transport" Journal of Hydraulic Engineering, ASCE, 110(10), 1431-1456.

Van Rijn, L. C. (1984b). "Sediment Transport, Part II: Suspended Load Transport" Journal of Hydraulic Engineering, ASCE, 110(11), 1613-1641.

Van Rijn, L. C. (1984c). "Sediment Transport, Part III: Bed Forms and Alluvial Roughness" Journal of Hydraulic Engineering, ASCE, 110(12), 1733-1754.

Van Vuren, S. & C.J. Sloff (2006), Verbetering 1-D Rijntakkenmodel vanaf Andernach. Rapport Q4130.00, WL | Delft Hydraulics.

Van Vuren, S. & Ottevanger, W. (2006). Inbouw Duinhoogte- en ruwheidsvoorspellers in Delft3DMOR. Rapport Q4190, WL | Delft Hydraulics.

Van Vuren, S., A. Hauschild, W. Ottevanger, J. Crebas & M. Yossef (2007), DVR: Reducing computation time. Rapport Q4357.10, WL | Delft Hydraulics.

Van Vuren, S., E. Mosselman, C.J. Sloff & B. Vermeulen (2006), Voorspelinstrument duurzame vaarweg; Initiële modelbouw en demonstratieberekeningen. Rapport Q4082.00, WL | Delft Hydraulics.

Verschelling, E., Sloff, K. & Mosselman, E. (2007), Modellering morfologie van Pannerdensche Kop tot Hoek van Holland. Rapport Q4249, WL | Delft Hydraulics.

Vollebregt, E.A.H. en C. van Velzen (2004). Automatisering van de calibratie van WAQUA riviermodellen, Vortech Computing.

Yossef, M., E. Mosselman, B. Jagers, K. Sloff, S. van Vuren & B. Vermeulen (2006), Voorspelinstrument duurzame vaarweg; Innovatieve aspecten. Rapport Q4082.00, WL | Delft Hydraulics.

A Van Rijn (1984)

The formula of Van Rijn (1984) takes the form:

$$S = S_s + S_b \tag{A.1}$$

where:

$$S_b = \begin{cases} 0.053\sqrt{\Delta\, g\, D_{50}^3}\, D_*^{-0.3} T^{2.1} & \text{for } T < 3.0 \\ 0.1 \quad \sqrt{\Delta\, g\, D_{50}^3}\, D_*^{-0.3} T^{1.5} & \text{for } T \geq 3.0 \end{cases} \tag{A.2}$$

First the bed-load transport expression will be explained. In Eq. A.2 T is a dimensionless bed shear parameter, written as:

$$T = \frac{\mu_c\, \tau_{bc} - \tau_{bcr}}{\tau_{bcr}} \tag{A.3}$$

It is normalised with the critical bed shear stress according to Shields (τ_{bcr}), the term $\mu_c \tau_{bc}$ is the effective shear stress. The formulas of the shear stresses are:

$$\tau_{bc} = \tfrac{1}{8}\, \rho_w\, f_{cb}\, u^2 \tag{A.4}$$

$$f_{cb} = \frac{0.24}{\left[\log_{10}\left(12h/\xi_c\right)\right]^2} \tag{A.5}$$

$$\mu_c = \left(\frac{18\log_{10}\left(12h/\xi_c\right)}{C'}\right)^2 \tag{A.6}$$

where $C_{g,90}$ is the grain related Chézy coefficient:

$$C' = 18\log_{10}\left(\frac{12h}{3D_{90}}\right) \tag{A.7}$$

The critical shear stress is written according to Shields:

$$\tau_{bcr} = \rho_w\, \Delta\, g\, D_{50}\theta_{cr} \tag{A.8}$$

in which θ_{cr} is the critical Shields parameter for initiation of motion, which is a function of the dimensionless particle parameter D_*:

$$D_* = D_{50}\left(\frac{\Delta g}{\nu^2}\right)^{\frac{1}{3}} \tag{A.9}$$

The suspended transport formulation reads:

$$S_s = f_{cs}\, u\, h\, C_a \tag{A.10}$$

In which C_a is the reference concentration, u depth averaged velocity, h the water depth and f_{cs} is a shape factor of which only an approximate solution exists:

$$f_{cs} = \begin{cases} f_0(z_c) & \text{if } z_c \neq 1.2 \\ f_1(z_c) & \text{if } z_c = 1.2 \end{cases} \tag{A.11}$$

$$f_0(z_c) = \frac{(\xi_c/h)^{z_c} - (\xi_c/h)^{1.2}}{(1-\xi_c/h)^{z_c}(1.2 - z_c)} \tag{A.12}$$

$$f_1(z_c) = \left(\frac{\xi_c/h}{1-\xi_c/h}\right)^{1.2} \log_e(\xi_c/h) \tag{A.13}$$

where ξ_c is the reference level or roughness height (can be interpreted as the bed-load layer thickness) and z_c the suspension number:

$$z_c = \min\left(20, \frac{w_s}{\beta\kappa u_*} + \phi\right) \tag{A.14}$$

$$u_* = u\sqrt{\frac{f_{cb}}{8}} \tag{A.15}$$

$$\beta = \min\left(1.5, 1 + 2\left(\frac{w_s}{u_*}\right)^2\right) \tag{A.16}$$

$$\phi = 2.5\left(\frac{w_s}{u_*}\right)^{0.8}\left(\frac{C_a}{0.65}\right)^{0.4} \tag{A.17}$$

The reference concentration is written as:

$$C_a = 0.015\alpha_1 \frac{d_{50}}{\xi_c}\frac{T^{1.5}}{D_*^{0.3}} \tag{A.18}$$

The following formula specific parameters have to be specified as input to the model.

w_s	the settling velocity of the sediment [m/s]
α_1	coefficient (should be *O(1)*)
ξ_c	reference level (bed load layer thickness) or roughness height [m]
d_{90}	D_{90}-particle diameter [m]

It is recommended to introduce the following changes:

1. Reduce Eq. A.2 to

$$S_b = \alpha_{BED} \cdot 0.1\sqrt{\Delta\, g\, D_{50}^3}\, D_*^{-0.3} T^{1.5} \tag{A.19}$$

with α_{BED} calibration parameter for bed load transport component, and for consistency we use α_{SUS} instead of α_1 as a calibration parameter for suspended load transport component. Both calibration parameters are user specified inputs.

2. Use a variable fall velocity (w_s) that is internally calculated based on the sediment size rather than using a user specified input value.

3. Introduce the possibility to specify a user defined critical Shields parameter θ_{cr}. This option is introduced inline with the experience from modelling the Bovenrijn, where a rather low critical Shields parameter is needed to reproduce its morphological behaviour correctly.

B Global morphological calibration – supplementary results

B.1 Effect of the parameter A_{shld} on bed changes with respect to the reference level along the left and right bank

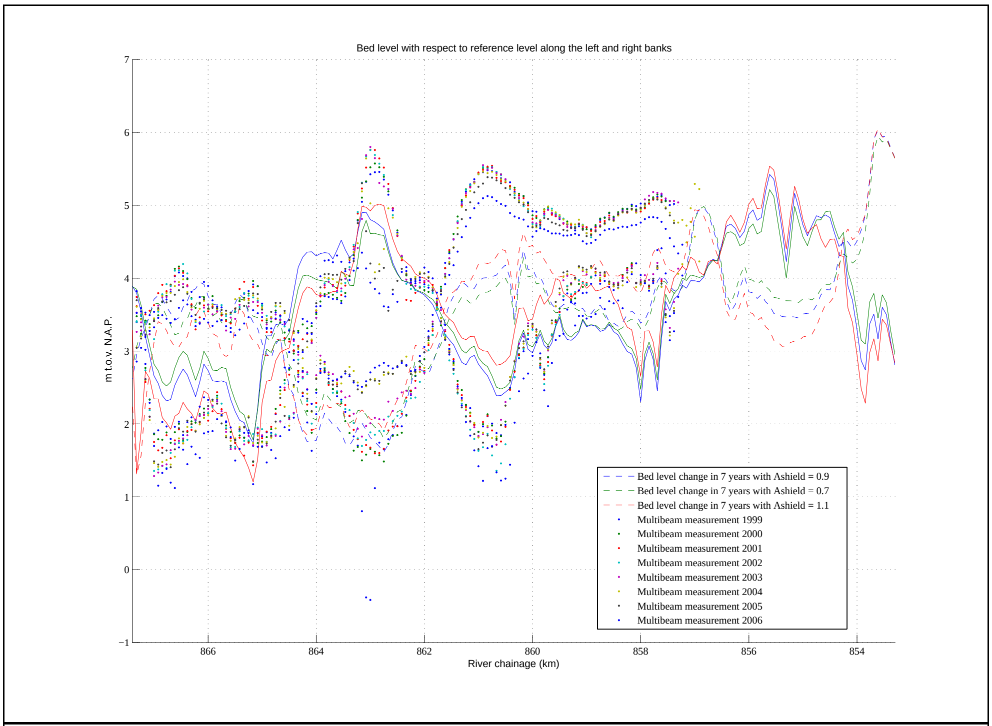

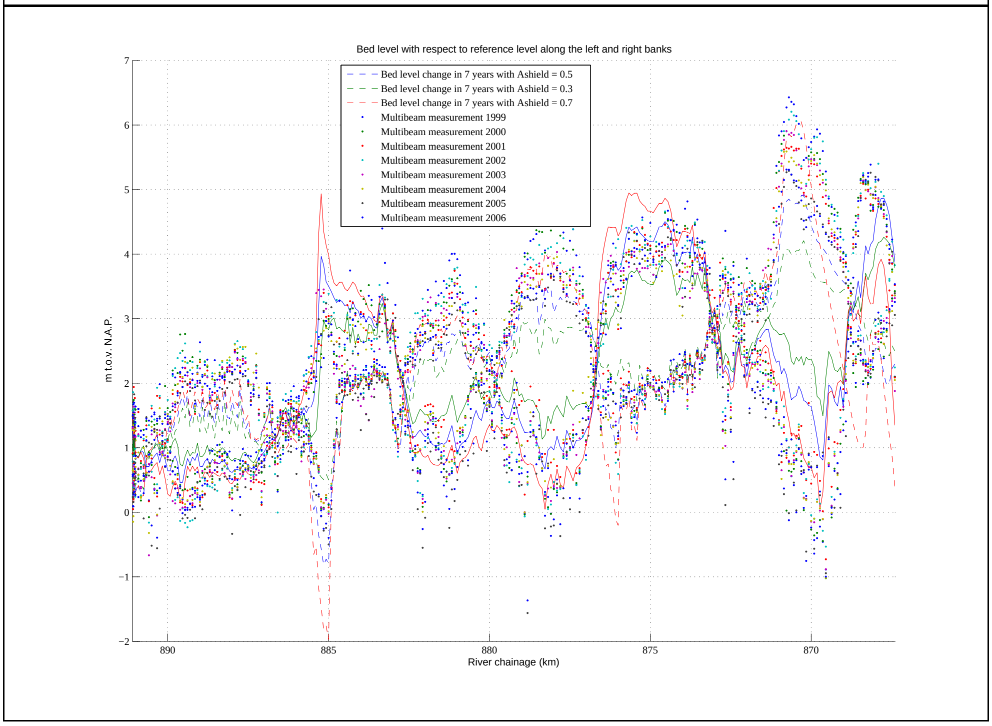

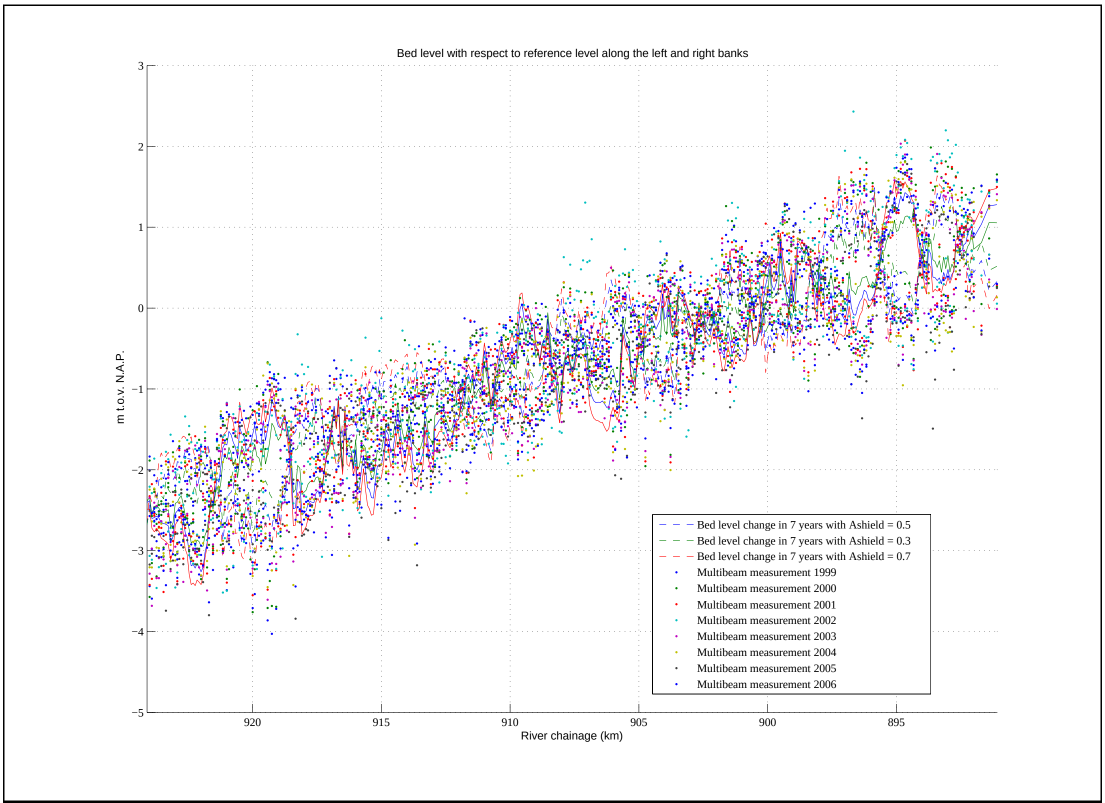
Bed level with respect to reference level along the left and right banks
m t.o.v. N.A.P.
River chainage (km)
Bed level change in 7 years with Ashield = 0.5
Bed level change in 7 years with Ashield = 0.3
Bed level change in 7 years with Ashield = 0.7
Multibeam measurement 1999
Multibeam measurement 2000
Multibeam measurement 2001
Multibeam measurement 2002
Multibeam measurement 2003
Multibeam measurement 2004
Multibeam measurement 2005
Multibeam measurement 2006

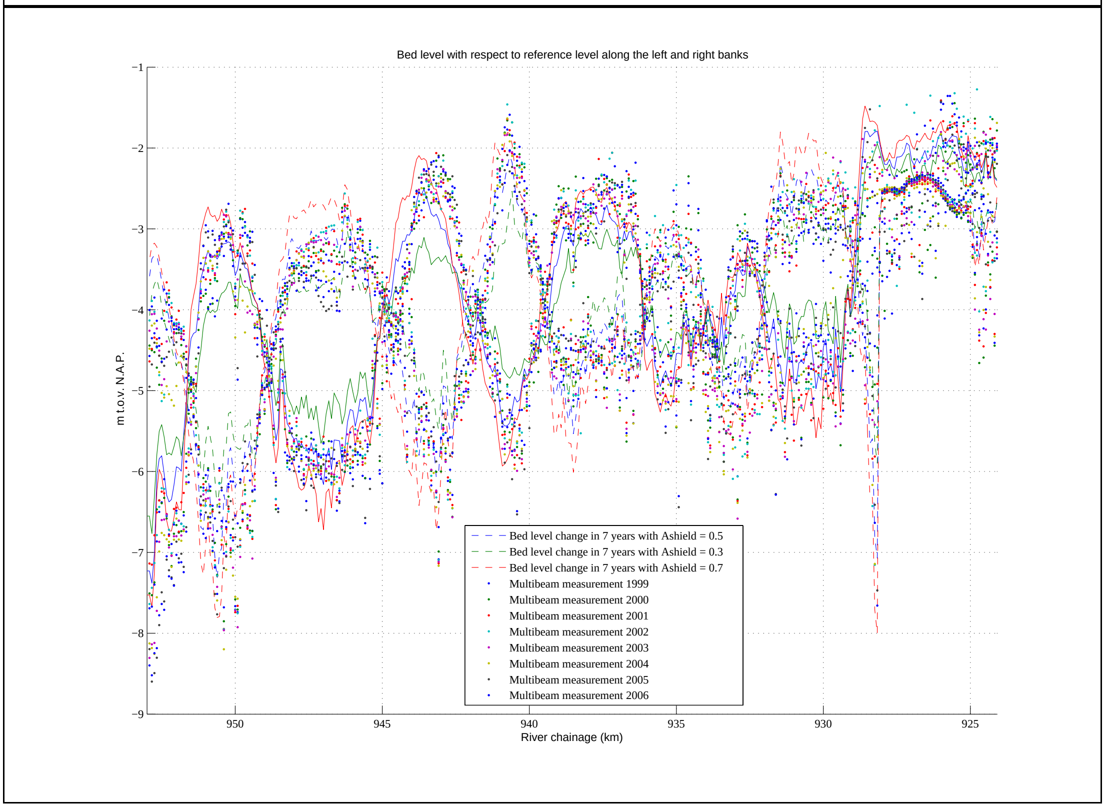
Bed level with respect to reference level along the left and right banks
m t.o.v. N.A.P.
River chainage (km)
Bed level change in 7 years with Ashield = 0.5
Bed level change in 7 years with Ashield = 0.3
Bed level change in 7 years with Ashield = 0.7
Multibeam measurement 1999
Multibeam measurement 2000
Multibeam measurement 2001
Multibeam measurement 2002
Multibeam measurement 2003
Multibeam measurement 2004
Multibeam measurement 2005
Multibeam measurement 2006


Bed level with respect to reference level along the left and right banks
m t.o.v. N.A.P.
River chainage (km)
Bed level change in 4 years with Ashield = 0.75
Bed level change in 4 years with Ashield = 0.55
Bed level change in 4 years with Ashield = 0.95
Multibeam measurement 2002
Multibeam measurement 2003
Multibeam measurement 2004
Multibeam measurement 2005
Multibeam measurement 2006

B.2 Effect of the parameter Ashld on bar pattern

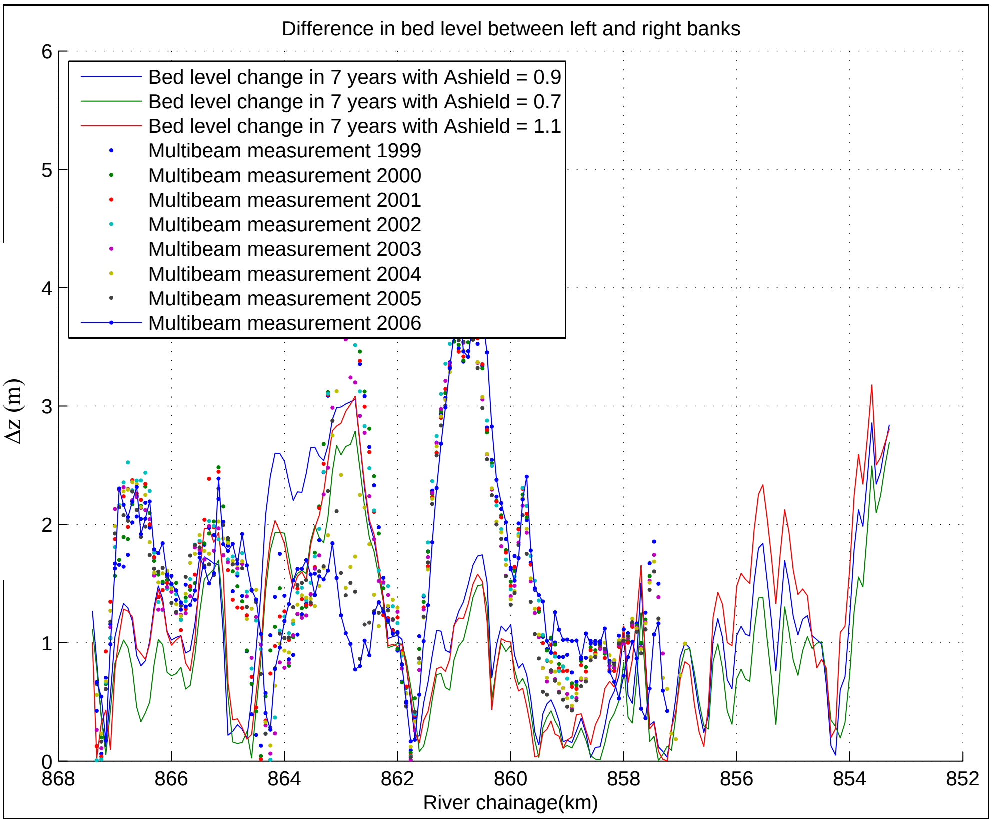

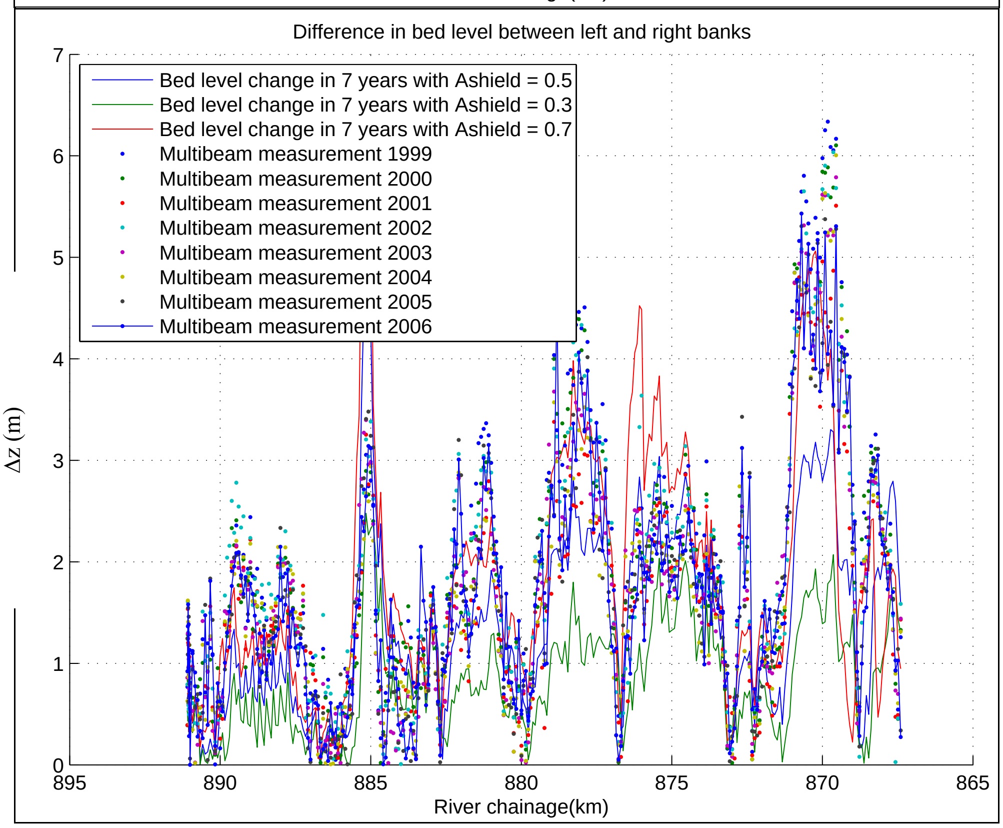

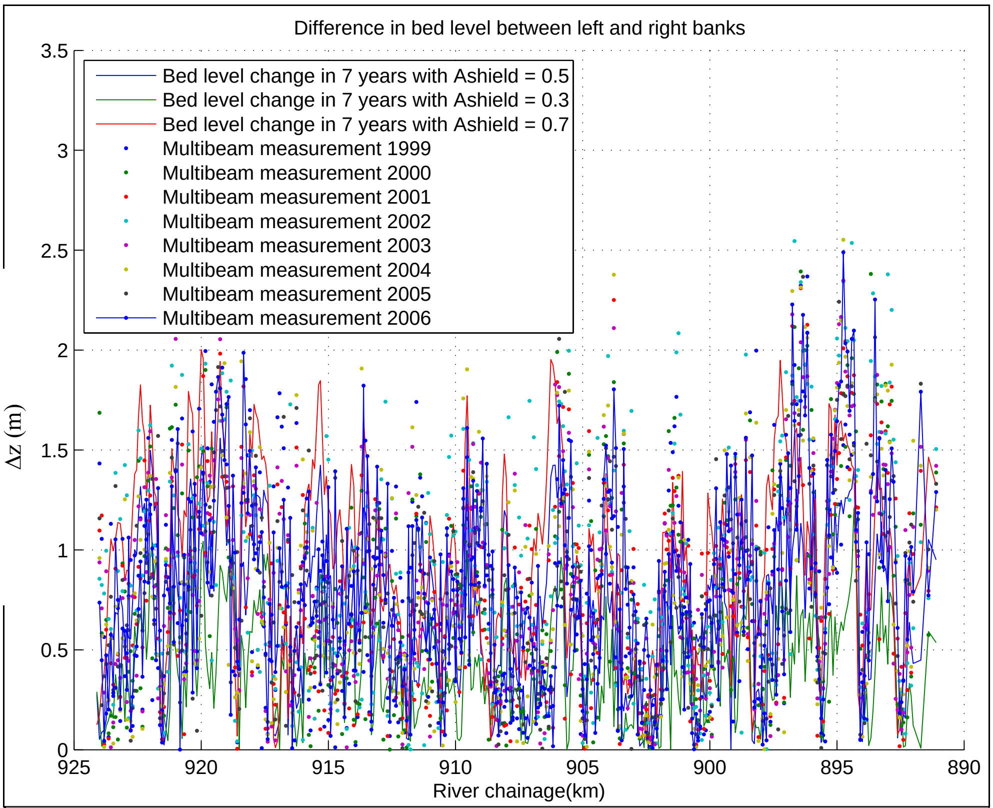
Difference in bed level between left and right banks
Bed level change in 7 years with Ashield = 0.5
Bed level change in 7 years with Ashield = 0.3
Bed level change in 7 years with Ashield = 0.7
Multibeam measurement 1999
Multibeam measurement 2000
Multibeam measurement 2001
Multibeam measurement 2002
Multibeam measurement 2003
Multibeam measurement 2004
Multibeam measurement 2005
Multibeam measurement 2006
Δz (m)
River chainage(km)

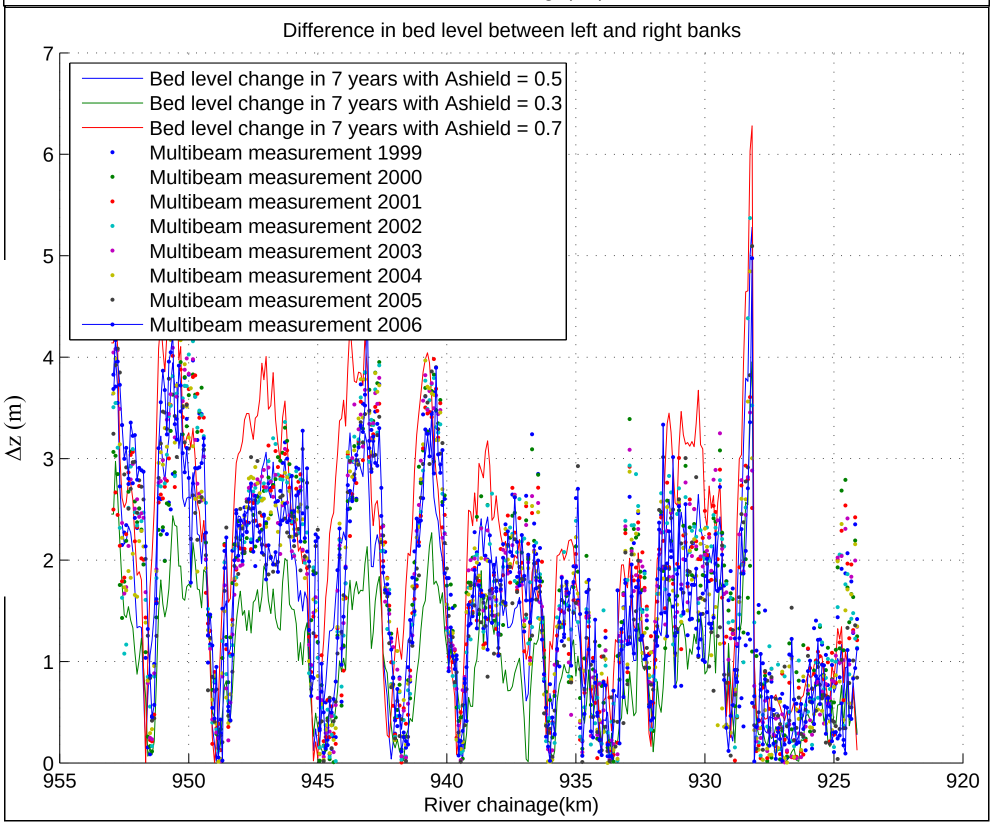
Difference in bed level between left and right banks
Bed level change in 7 years with Ashield = 0.5
Bed level change in 7 years with Ashield = 0.3
Bed level change in 7 years with Ashield = 0.7
Multibeam measurement 1999
Multibeam measurement 2000
Multibeam measurement 2001
Multibeam measurement 2002
Multibeam measurement 2003
Multibeam measurement 2004
Multibeam measurement 2005
Multibeam measurement 2006
Δz (m)
River chainage(km)

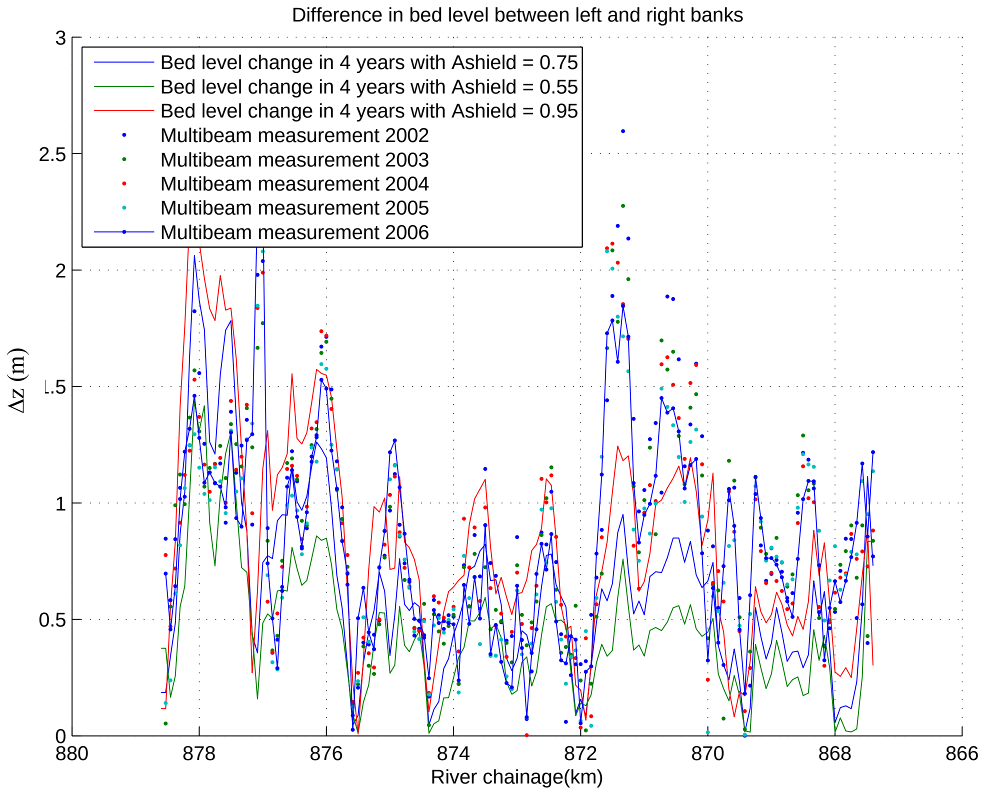
Difference in bed level between left and right banks
Bed level change in 4 years with Ashield = 0.75
Bed level change in 4 years with Ashield = 0.55
Bed level change in 4 years with Ashield = 0.95
Multibeam measurement 2002
Multibeam measurement 2003
Multibeam measurement 2004
Multibeam measurement 2005
Multibeam measurement 2006
Δz (m)
River chainage(km)
3
2.5
2
1.5
1
0.5
0
880
878
876
874
872
870
868
866

B.3 Effect of the parameter E_{spir} on bed changes with respect to the reference level along the left and right bank

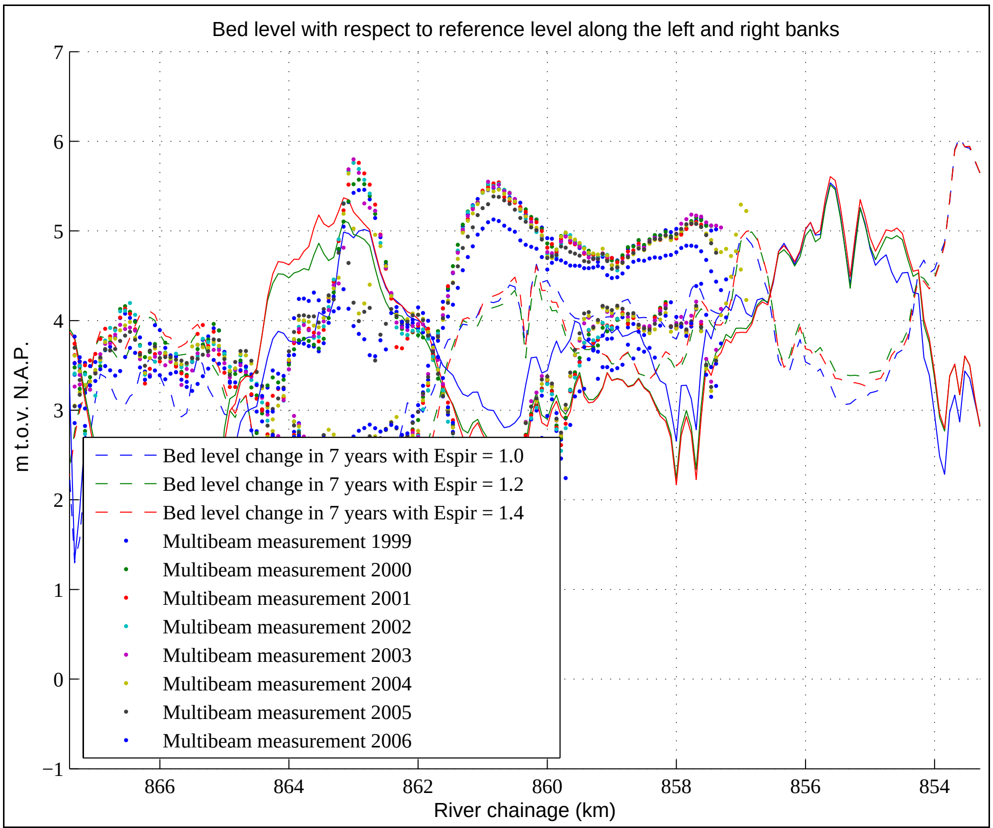

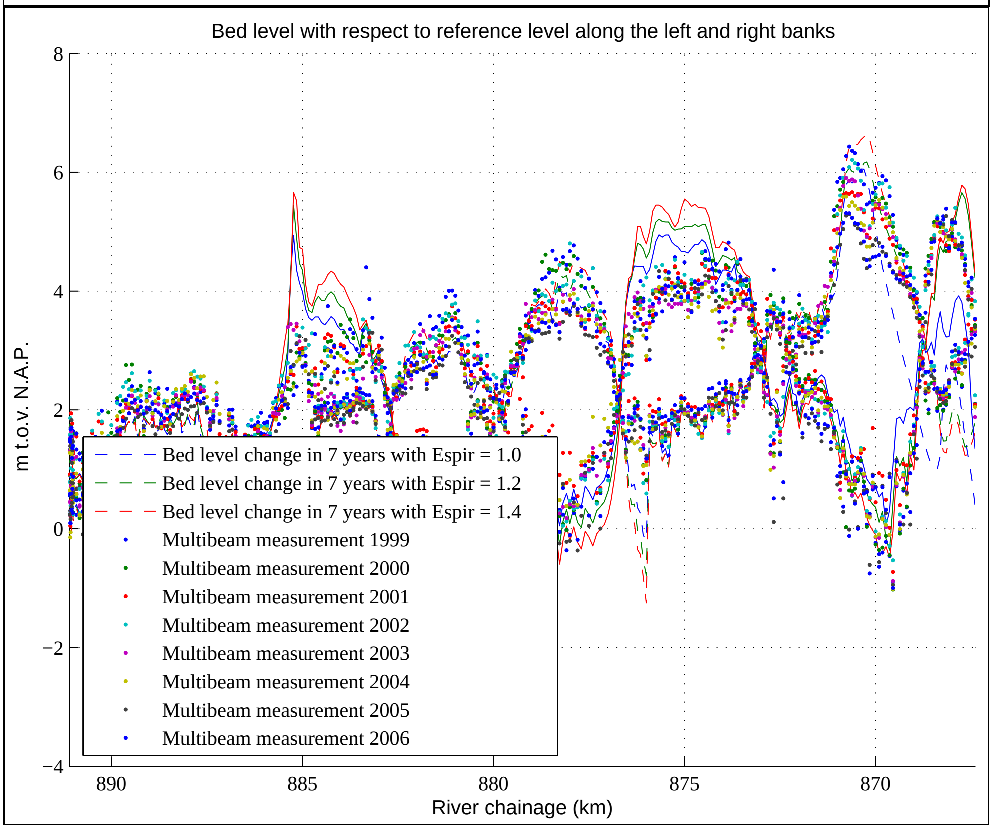

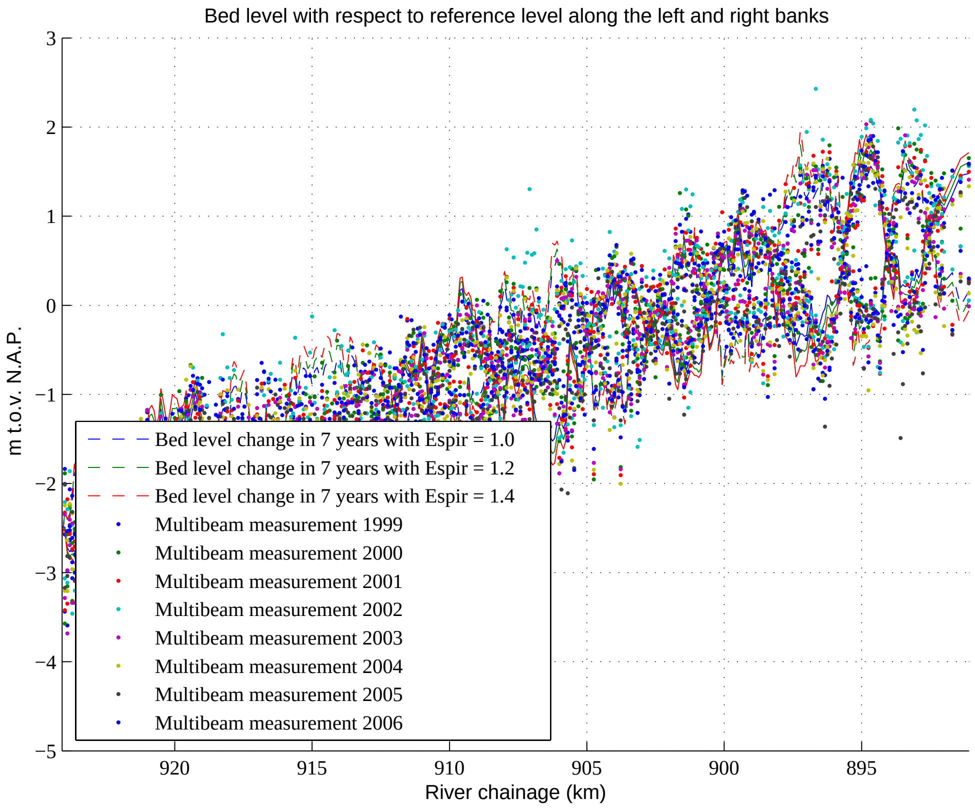
Bed level with respect to reference level along the left and right banks
m t.o.v. N.A.P.
3
2
1
0
−1
−2
−3
−4
−5
920
915
910
905
900
895
River chainage (km)
Bed level change in 7 years with Espir = 1.0
Bed level change in 7 years with Espir = 1.2
Bed level change in 7 years with Espir = 1.4
Multibeam measurement 1999
Multibeam measurement 2000
Multibeam measurement 2001
Multibeam measurement 2002
Multibeam measurement 2003
Multibeam measurement 2004
Multibeam measurement 2005
Multibeam measurement 2006

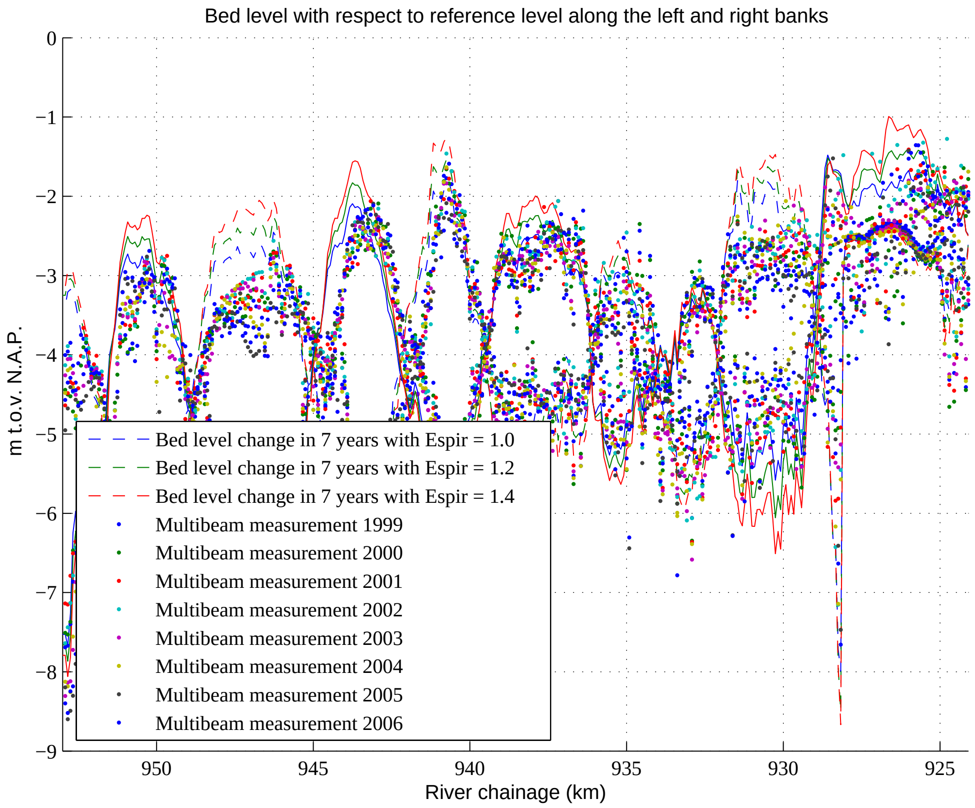
Bed level with respect to reference level along the left and right banks
m t.o.v. N.A.P.
0
−1
−2
−3
−4
−5
−6
−7
−8
−9
950
945
940
935
930
925
River chainage (km)
Bed level change in 7 years with Espir = 1.0
Bed level change in 7 years with Espir = 1.2
Bed level change in 7 years with Espir = 1.4
Multibeam measurement 1999
Multibeam measurement 2000
Multibeam measurement 2001
Multibeam measurement 2002
Multibeam measurement 2003
Multibeam measurement 2004
Multibeam measurement 2005
Multibeam measurement 2006

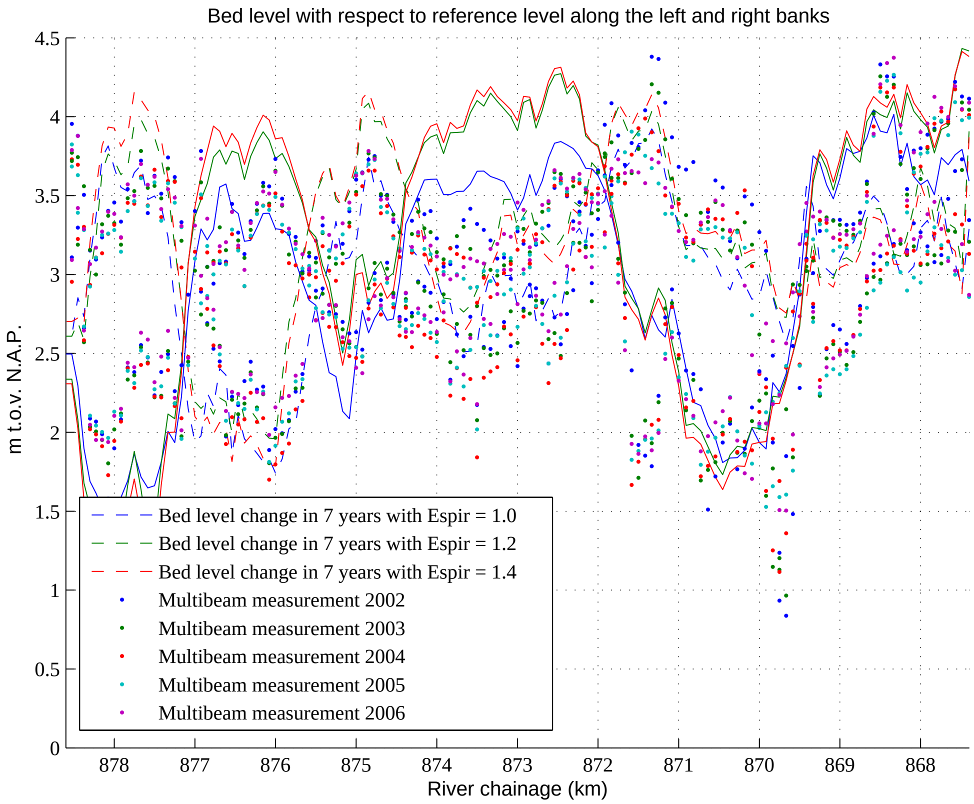
Bed level with respect to reference level along the left and right banks
m t.o.v. N.A.P.
4.5
4
3.5
3
2.5
2
1.5
1
0.5
0
878
877
876
875
874
873
872
871
870
869
868
River chainage (km)
Bed level change in 7 years with Espir = 1.0
Bed level change in 7 years with Espir = 1.2
Bed level change in 7 years with Espir = 1.4
Multibeam measurement 2002
Multibeam measurement 2003
Multibeam measurement 2004
Multibeam measurement 2005
Multibeam measurement 2006

B.4 Effect of parameter Espir on the bar pattern

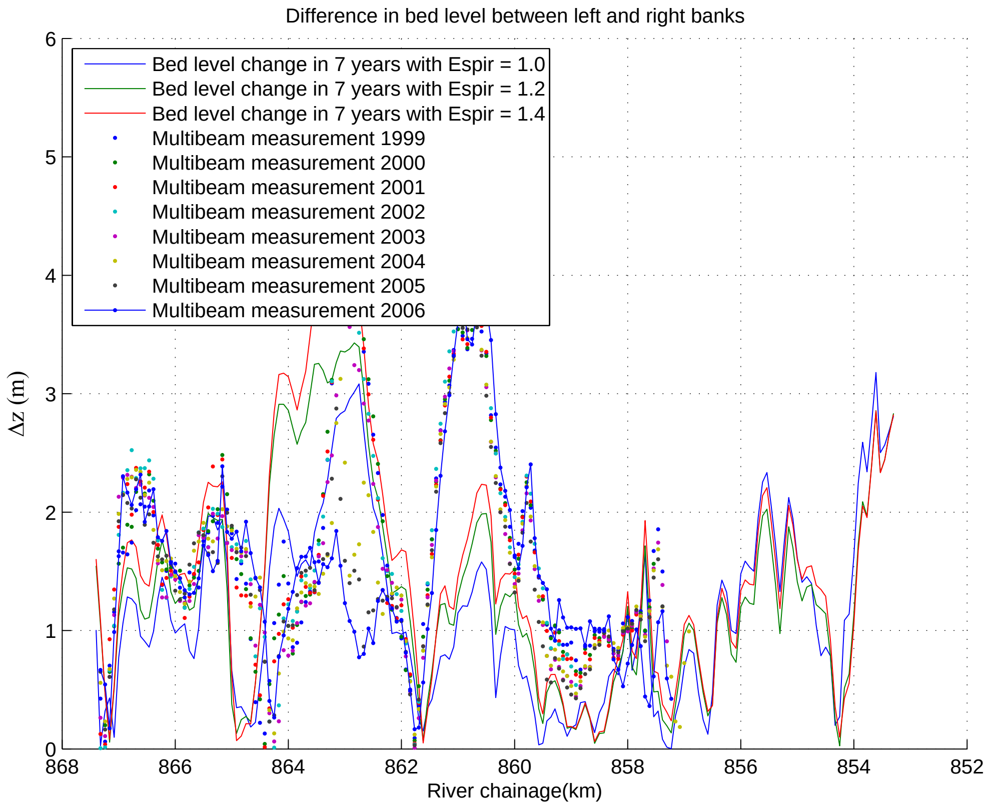

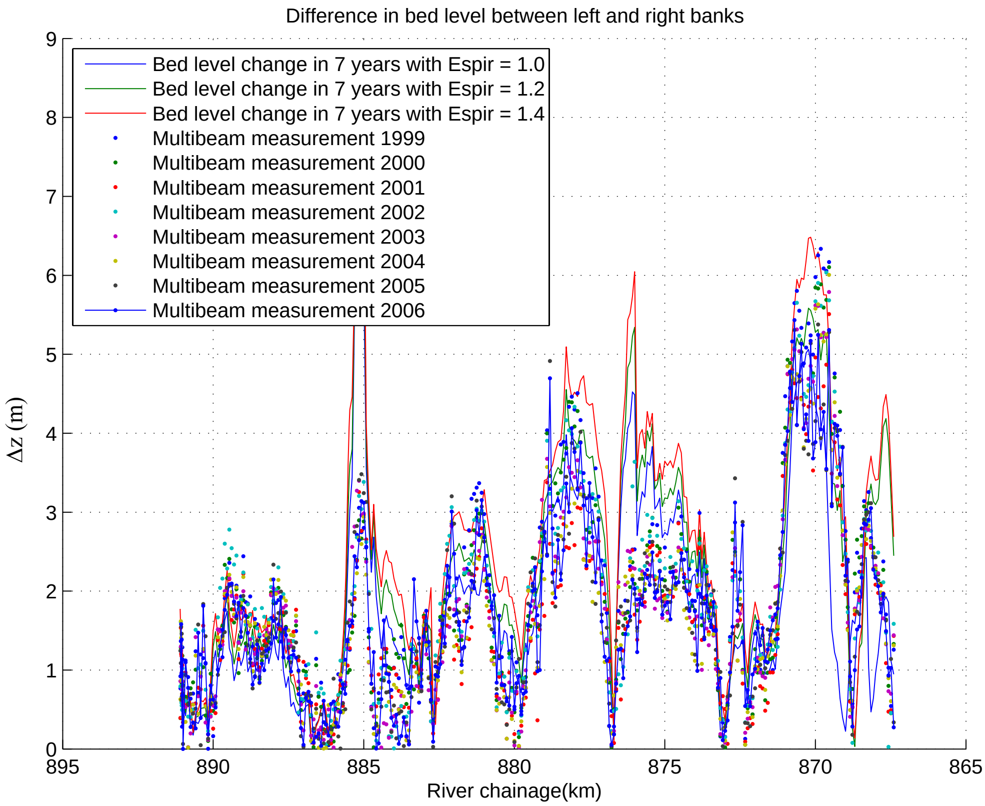

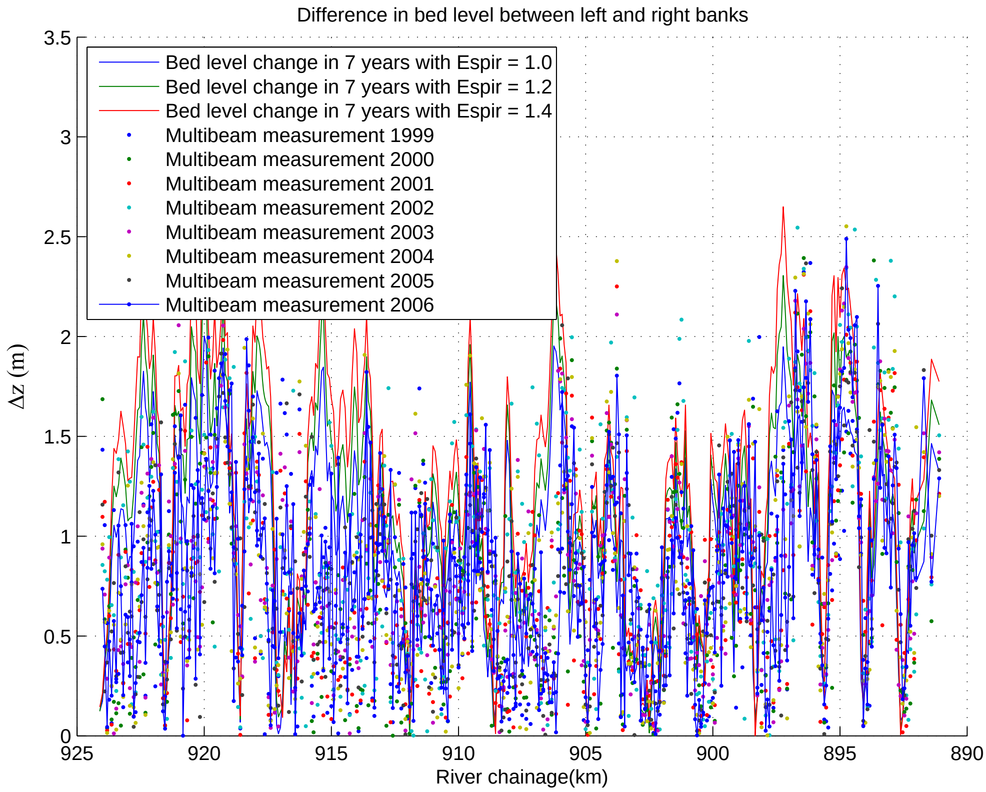
Difference in bed level between left and right banks
Bed level change in 7 years with Espir = 1.0
Bed level change in 7 years with Espir = 1.2
Bed level change in 7 years with Espir = 1.4
Multibeam measurement 1999
Multibeam measurement 2000
Multibeam measurement 2001
Multibeam measurement 2002
Multibeam measurement 2003
Multibeam measurement 2004
Multibeam measurement 2005
Multibeam measurement 2006
Δz (m)
River chainage(km)
0
0.5
1
1.5
2
2.5
3
3.5
925
920
915
910
905
900
895
890

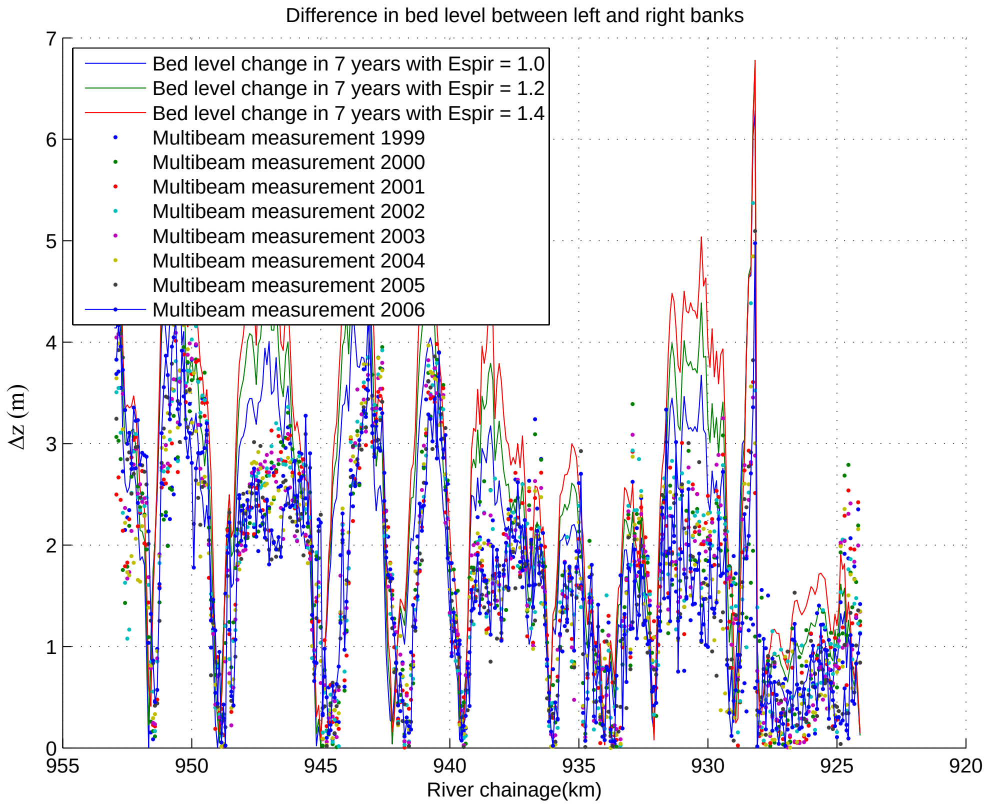
Difference in bed level between left and right banks
Bed level change in 7 years with Espir = 1.0
Bed level change in 7 years with Espir = 1.2
Bed level change in 7 years with Espir = 1.4
Multibeam measurement 1999
Multibeam measurement 2000
Multibeam measurement 2001
Multibeam measurement 2002
Multibeam measurement 2003
Multibeam measurement 2004
Multibeam measurement 2005
Multibeam measurement 2006
Δz (m)
River chainage(km)
0
1
2
3
4
5
6
7
955
950
945
940
935
930
925
920

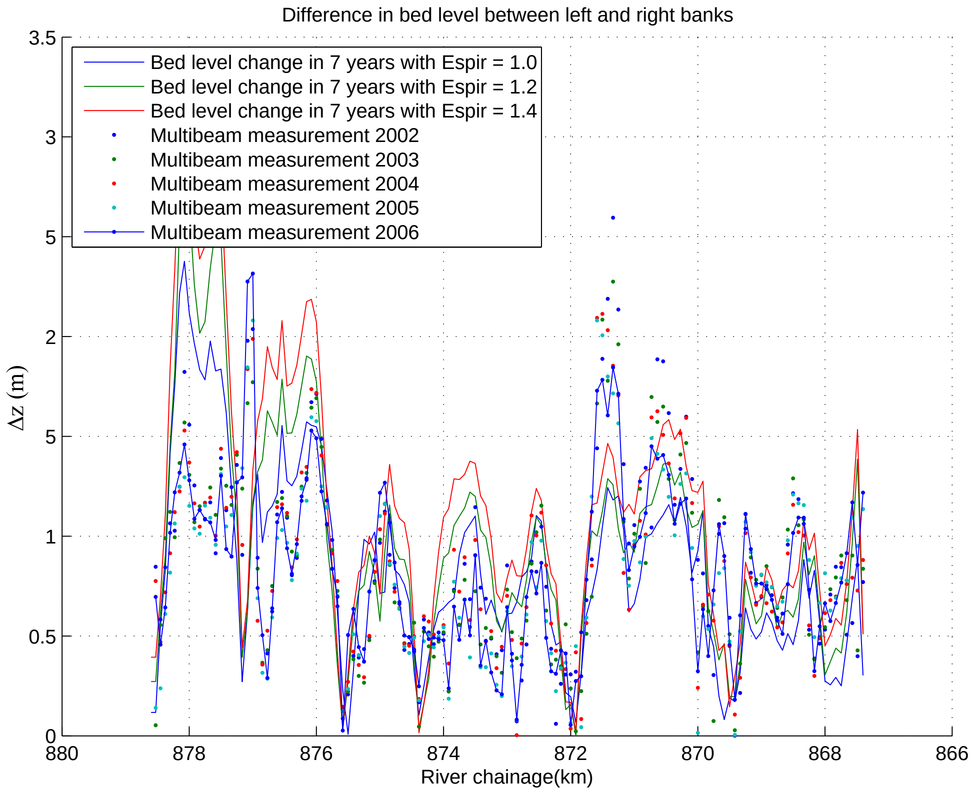
Difference in bed level between left and right banks
Bed level change in 7 years with Espir = 1.0
Bed level change in 7 years with Espir = 1.2
Bed level change in 7 years with Espir = 1.4
Multibeam measurement 2002
Multibeam measurement 2003
Multibeam measurement 2004
Multibeam measurement 2005
Multibeam measurement 2006
Δz (m)
3.5
3
5
2
5
1
0.5
0
880
878
876
874
872
870
868
866
River chainage(km)

B.5 Additional results from the calibrated model

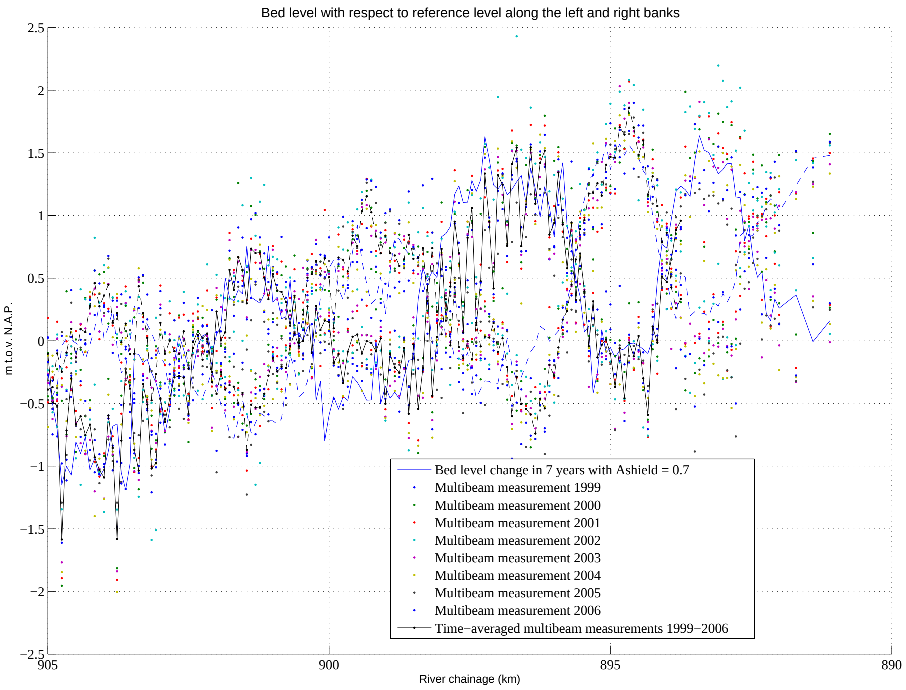

Figure 7.1 Bed changes with respect to the reference level along the left and right bank of the Waal section-2

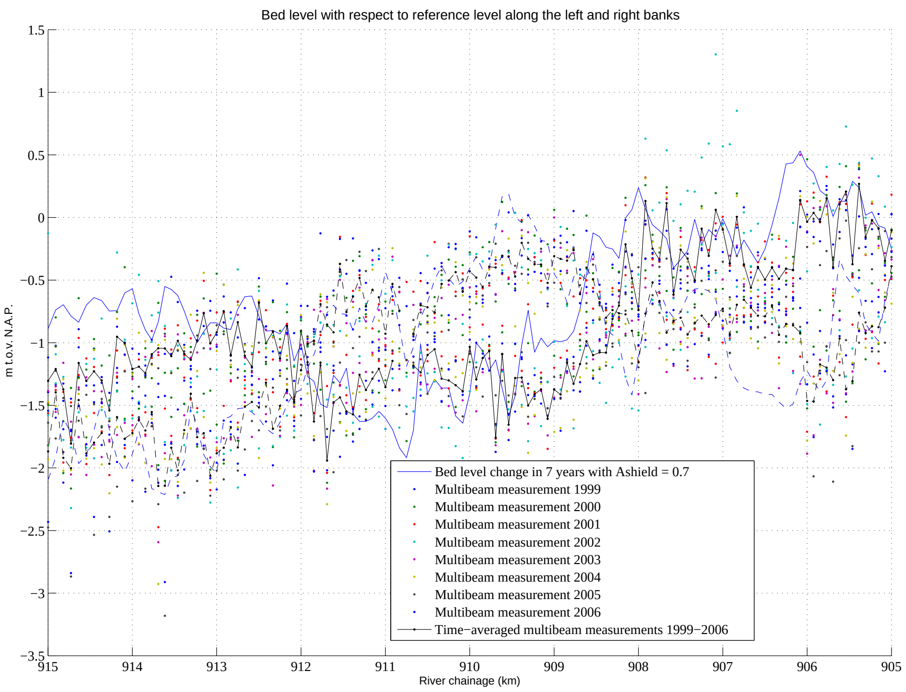

Figure 7.2 Bed changes with respect to the reference level along the left and right bank of the Waal section-3

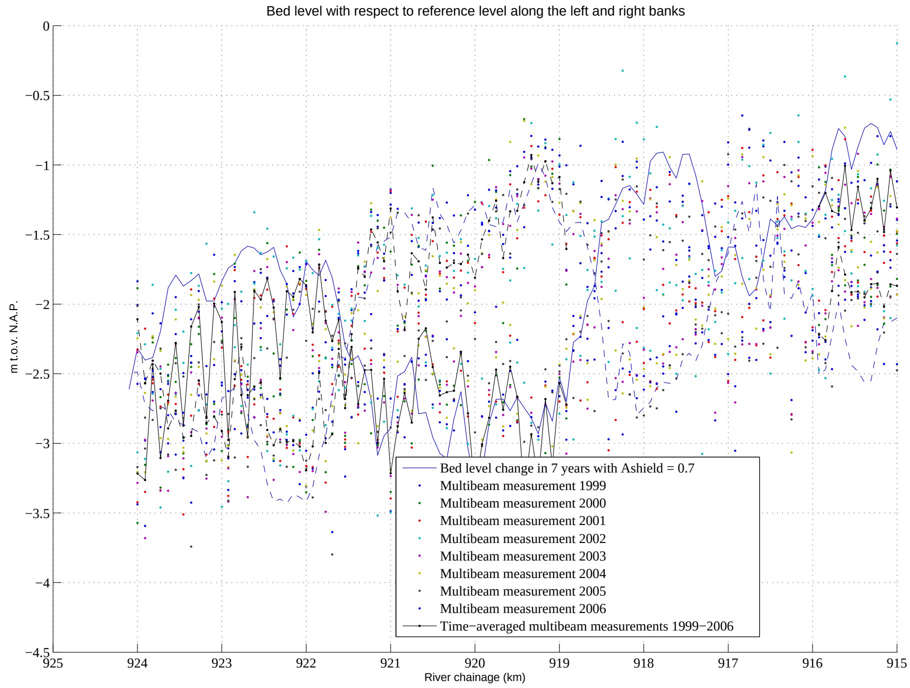

Figure 7.3 Bed changes with respect to the reference level along the left and right bank of the Waal section-4

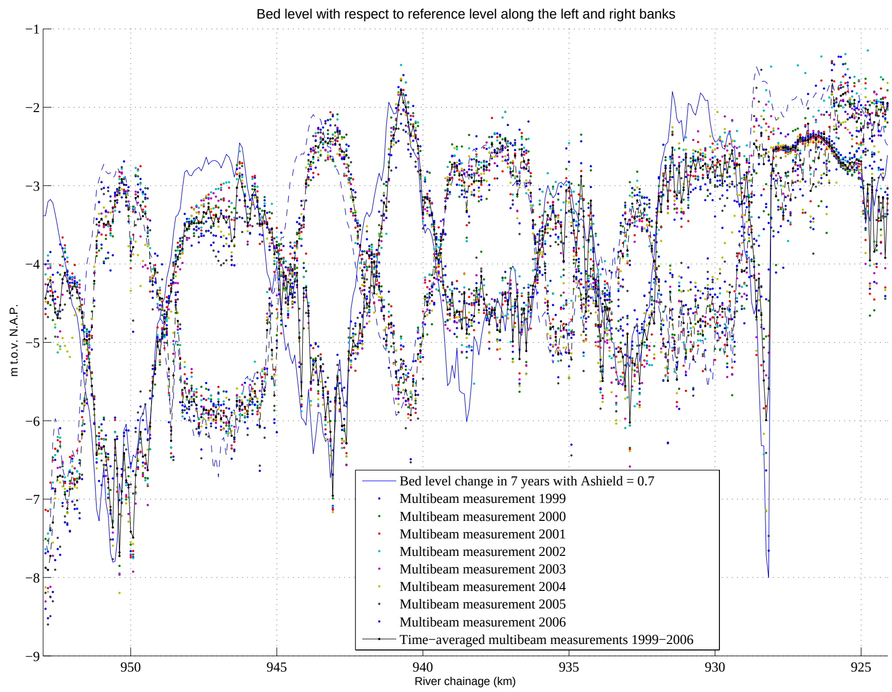

Figure 7.4 Bed changes with respect to the reference level along the left and right bank of the Waal section-5

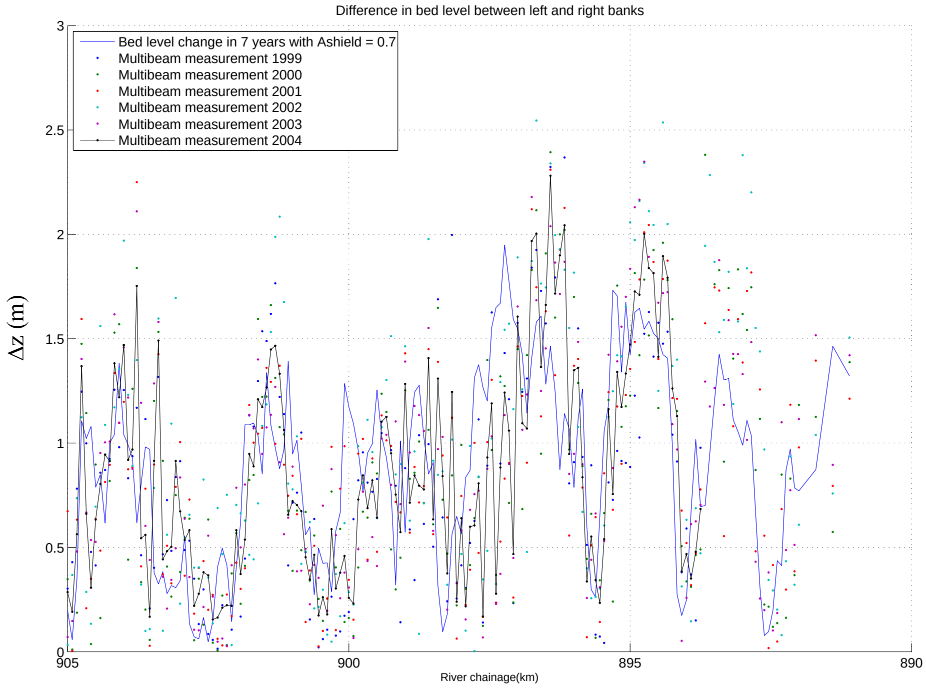

Figure 7.5 Difference in bed level between left and right bank of the Waal section-2

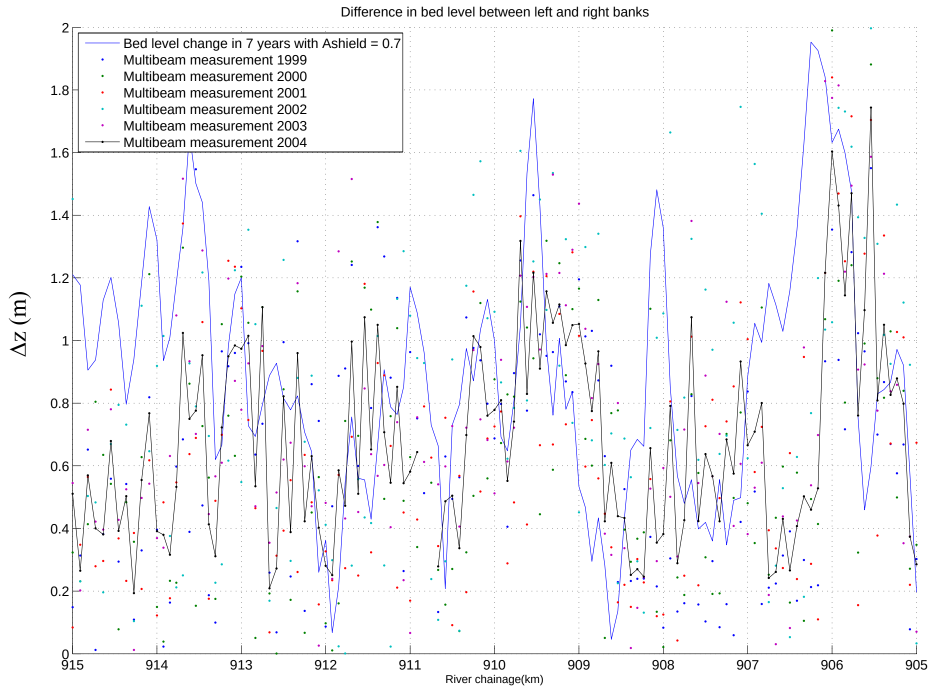

Figure 7.6 Difference in bed level between left and right bank of the Waal section-3

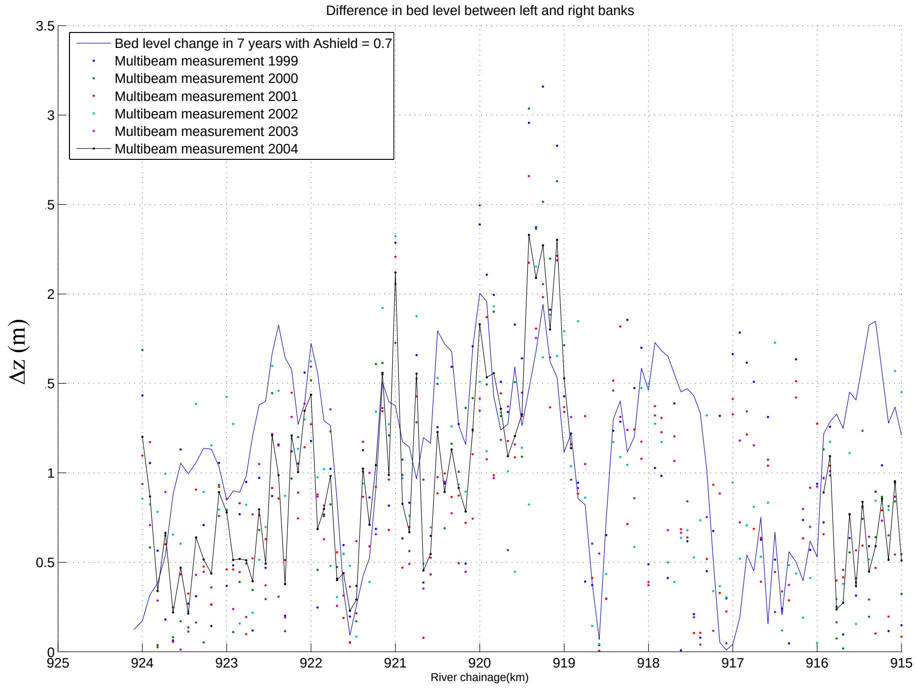

Figure 7.7 Difference in bed level between left and right bank of the Waal section-4

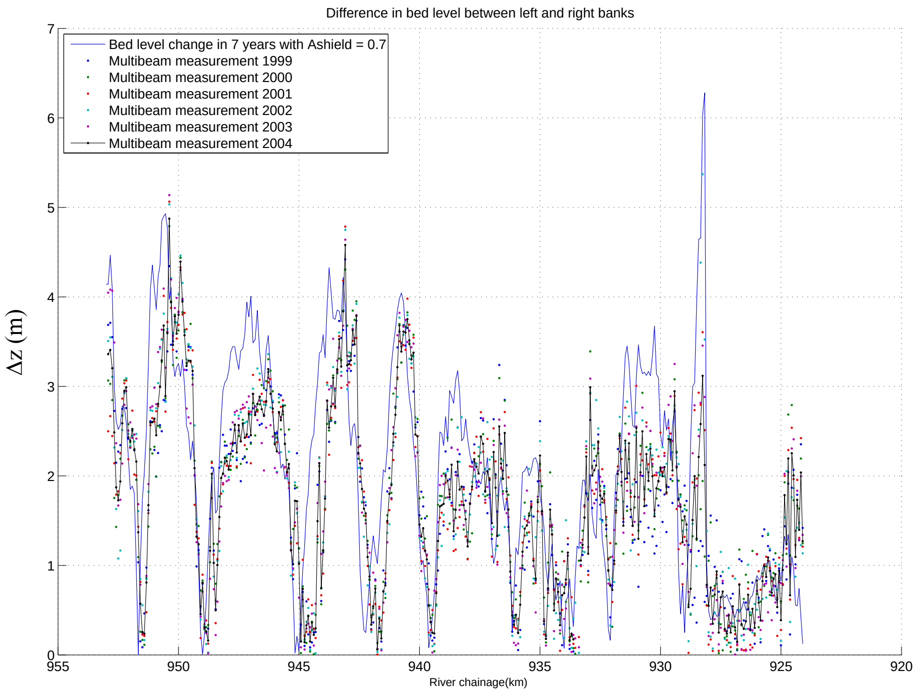

Figure 7.8 Difference in bed level between left and right bank of the Waal section-5

C Impact of dunes, dumping strategy and channel dimensions on dumping volumes

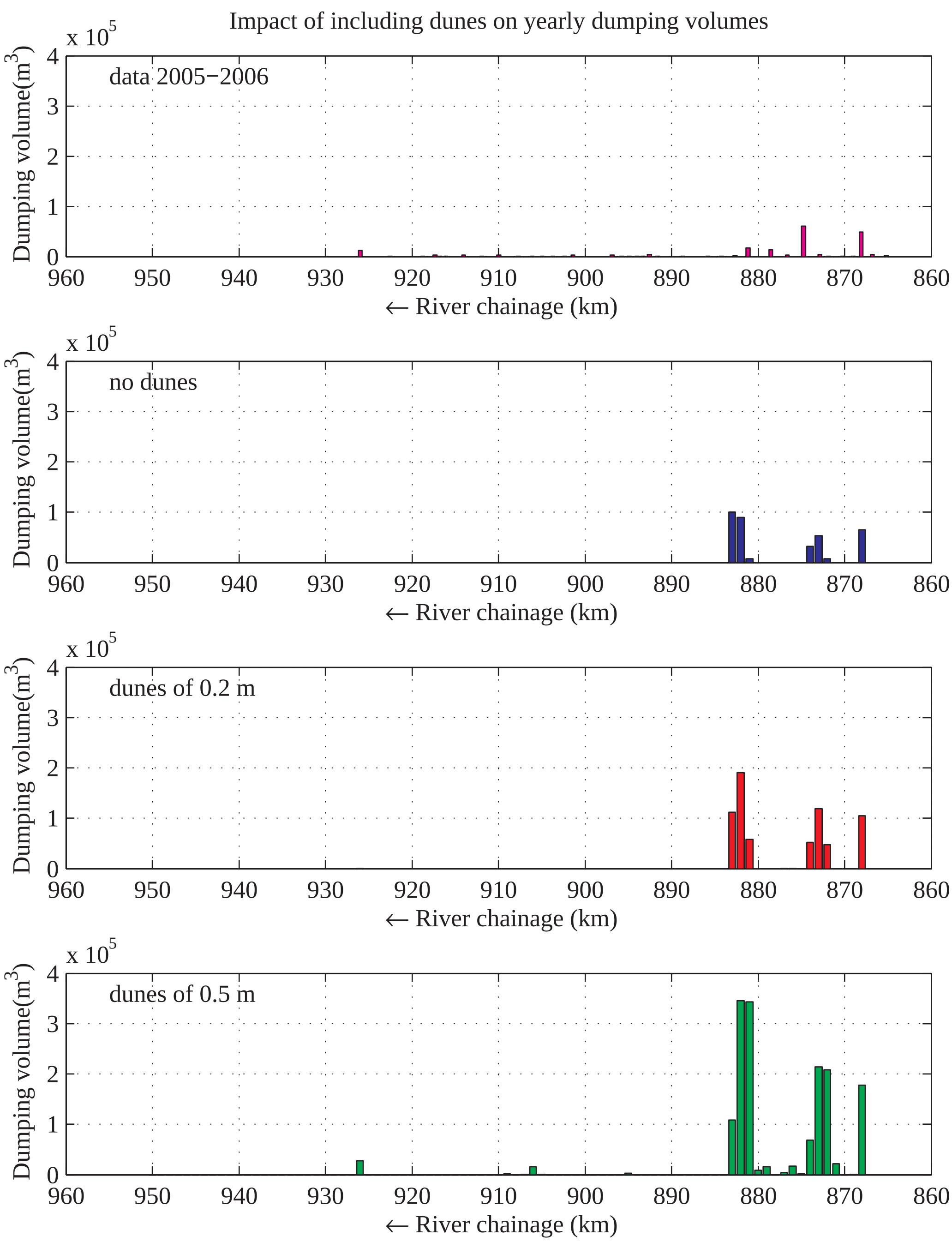

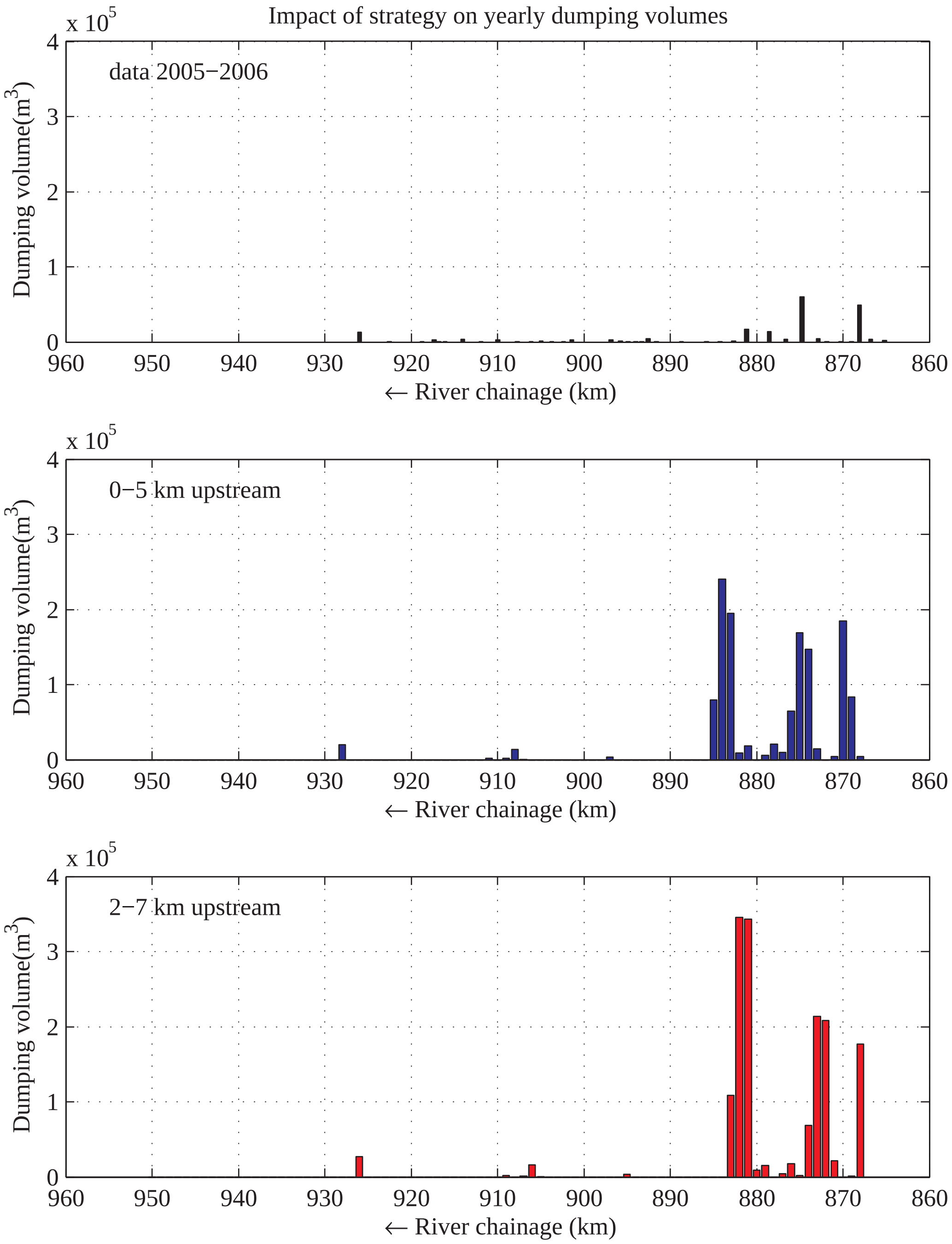
Impact of strategy on yearly dumping volumes
x 10^5
data 2005−2006
0−5 km upstream
2−7 km upstream
Dumping volume(m^3)
0
1
2
3
4
960
950
940
930
920
910
900
890
880
870
860
← River chainage (km)

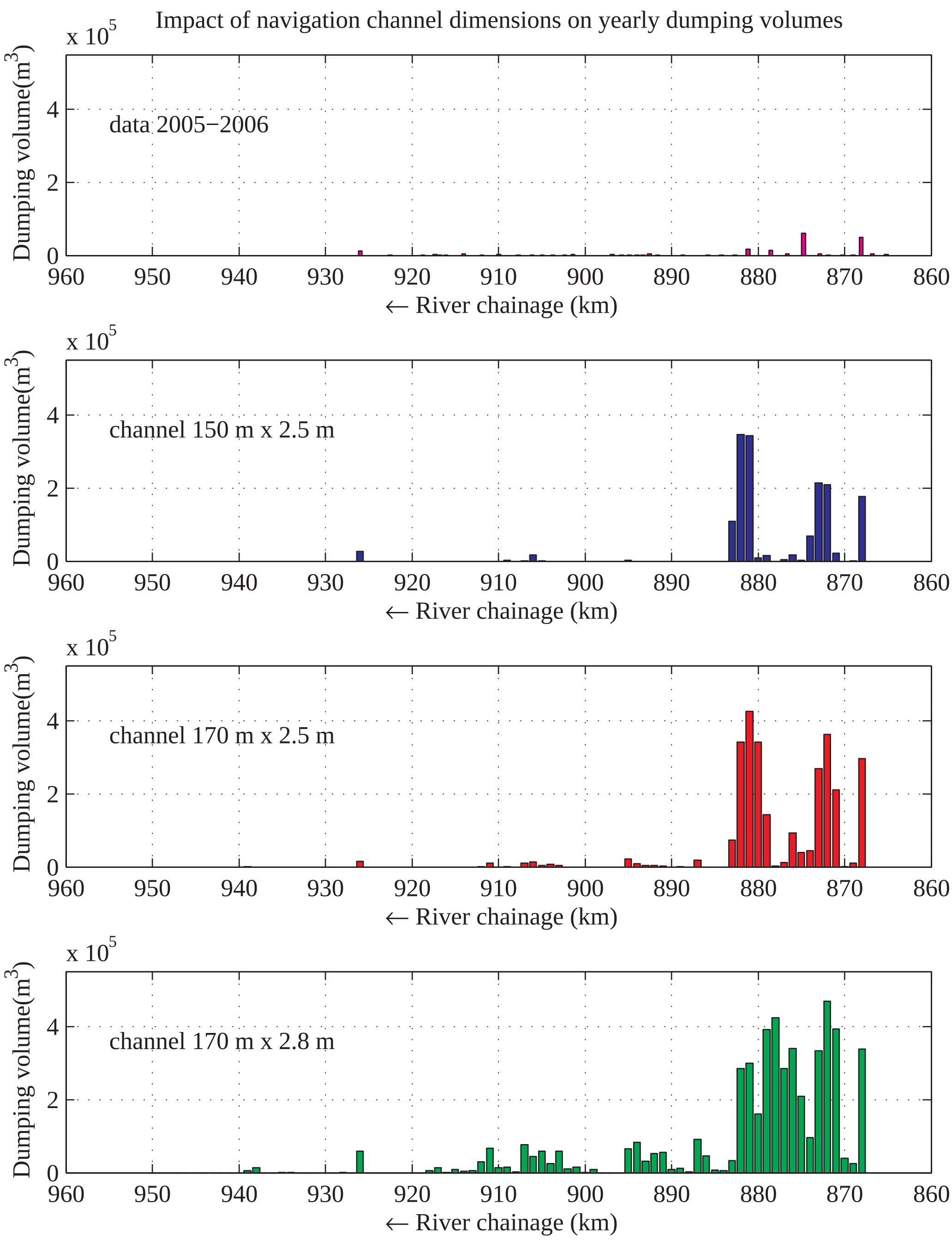
Impact of navigation channel dimensions on yearly dumping volumes
x 10^5
Dumping volume(m^3)
data 2005−2006
channel 150 m x 2.5 m
channel 170 m x 2.5 m
channel 170 m x 2.8 m
0
2
4
960
950
940
930
920
910
900
890
880
870
860
← River chainage (km)